HOMING AND DIFFERENTIATION OF MESENCHYMAL STEM CELLS IN 3D *IN VITRO* MODELS

Tracee Lynn Popielarczyk

Dissertation submitted to the faculty of the Virginia Polytechnic Institute and State University in partial fulfillment of the requirements for the degree of

Doctor of Philosophy
In
Biomedical and Veterinary Sciences

Jennifer G. Barrett, Chair
Amrinder S. Nain
William R. Huckle
Willard H. Eyestone

June 23, 2017
Blacksburg, Virginia

Key Words: mesenchymal stem cells, differentiation, tendon, scaffolds, stem cell homing, regenerative medicine

HOMING AND DIFFERENTIATION OF MESENCHYMAL STEM CELLS IN 3D *IN VITRO* MODELS

Tracee Lynn Popielarczyk

Abstract

Mesenchymal stem cells (MSCs) have great potential to improve clinical outcomes for many inflammatory and degenerative diseases through delivery of exogenous MSCs via injection or cell-laden scaffolds and through mobilization and migration of endogenous MSCs to injury sites. MSC fate and function is determined by microenvironmental cues, specifically dimensionality, topography, and cell-cell interactions. MSC responses of migration and differentiation are the focus of this dissertation. Cell migration occurs in several physiological and pathological processes; migration mode and cell signaling are determined by the environment and type of confinement in three-dimensional (3D) models.

Tendon injury is a common musculoskeletal disorder that occurs through cumulative damage to the extracellular matrix (ECM). Studies combining nanofibrous scaffolds and MSCs to determine an optimal topographical environment have promoted tenogenic differentiation under various conditions. We investigated cellular response of MSCs on specifically designed nanofiber matrices fabricated using a novel spinneret-based tunable engineered parameters production method (STEP). We designed suspended and aligned nanofiber scaffolds to study cellular morphology, tendon marker gene expression, and matrix deposition as determinants for tendon differentiation.

The delivery and maintenance of MSCs at sites of inflammation or injury are major challenges in stem cell therapies. Enhancing stem cell homing could improve their therapeutic effects. Homing is a process that involves cell migration through the vasculature to target organs. This process is defined in leukocyte transendothelial migration (TEM); however, far less is known about MSC homing. We investigated two population subsets of MSCs in a Transwell system mimicking the vasculature; migrated cells that initiated transmigration on the endothelium and nonmigrated cells in the apical chamber that failed to transmigrate. Gene and protein expression changes were observed between these subsets and evidence suggests that multiple signaling pathways regulate TEM.

The results of these experiments have demonstrated that microenvironmental cues are critical to understanding the cellular and molecular mechanisms of MSC response, specifically in homing and differentiation. This knowledge has identified scaffold parameters required to stimulate tenogenesis and signaling pathways controlling MSC homing. These findings will allow us to target key regulatory molecules and cell signaling pathways involved in MSC response towards development of regenerative therapies.

HOMING AND DIFFERENTIATION OF MESENCHYMAL STEM CELLS IN 3D *IN VITRO* MODELS

Tracee Lynn Popielarczyk

General Audience Abstract

Stem cell therapy is one way to improve tissue injury and inflammatory conditions, but to optimize such therapy, we need to study how the environment around cells influence turning them into the injured tissue and how to control their movement to these sites in order for mesenchymal stem cells (MSCs) to exert their therapeutic functions. MSCs move through and detect their environment through the material around them, including organization of the fibers they attach to and neighboring cells. Cell migration is an important cell behavior that occurs in normal and diseased processes. MSCs have great potential to improve clinical outcomes for many inflammatory and degenerative diseases whether through delivery of exogenous MSCs or through mobilization and migration of endogenous MSCs to injury sites.

Tendon damage can occur slowly over time and optimal treatment for normal function after injury remains unknown. Equine MSCs were harvested from bone marrow and subjected to scaffolds of different fiber orientation to study whether cells develop characteristics of tendon cells. Cellular responses were similar between scaffolds of aligned fiber orientation. Manipulation of equine bone marrow MSCs through the use of specifically designed nanofiber scaffolds aid in understanding the mechanisms by which the cells respond and function in tendon development, injury, and repair.

Inflammation is a necessary process after tissue injury; however, it must progress in a controlled manner and be resolved before it leads to tissue damage and dysfunction. MSCs function in regulating the effects of inflammation and immune cells; however, getting them to these sites and keeping them there remains challenging. MSCs adhere to and migrate through capillaries towards these sites, known as stem cell homing. Human bone marrow MSCs were loaded onto human synovial microvascular endothelial cells to study migration towards an inflammatory stimulus. This stimulus acted on the endothelial cells to produce another stimulus that attracted MSCs to the endothelial cells. These actions resulted in complete MSC migration through the endothelial cells and activated intracellular signals that can be used to increase the number of MSCs that reach the inflammatory sites and stimulate tissue-healing effects.

Dedication

To my parents, Richard and Wanda Popielarczyk, for their endless love, support, and encouragement.

Acknowledgments

I would like to thank my PhD advisor, Jennifer G. Barrett for her guidance in this process and support over the years. I am grateful to have had the opportunity to learn from an advisor with such enthusiasm for science and strong work ethic. Thank you to my committee members: Amrinder S. Nain, William R. Huckle, and Willard H. Eyestone for your helpful discussions, insight, and feedback on my projects as my committee members, as well as your advice and support along the way. Thank you Amrinder S. Nain for the opportunities to train in the STEP Laboratory my first year and to collaborate on the tenogenesis study. Thank you William R. Huckle for your feedback and suggestions on the vascular biology of the stem cell homing study. Thank you to Roger J. Avery, Becky Jones, S. Ansar Ahmed, and Susan Rosebrough in the Program of Biomedical and Veterinary Sciences. Thank you to Bethany A. Kerr for serving as the external examiner for my defense.

A special thank you to Mr. E. Roe Stamps and Mrs. Penny Stamps, founders of the Stamps Family Charitable Foundation, for their fellowship support and for all of the opportunities that the funding has allowed me to experience. It has been an honor to be a part of the Stamps Scholars community.

I am happy to have worked with fellow past and present PhD students at the EMC: Daniel W. Youngstrom, Jade E. LaDow, Ibtesam Rajpar, and Sophie H. Bogers. Many thanks to the research and regenerative medicine services staff for your assistance and support: Elaine Meilahn, Xiaojing Guan, Andrew Hogan, and Hannah Dawson. I would like to thank the undergraduate students I had the opportunity to work with, especially Megan Barlow and Lashana Ali, for their assistance and enthusiasm in the lab.

I would also like to thank the past graduate students in the STEP Laboratory for taking the time to train me on the STEP technique and welcoming me into the lab, especially Puja Sharma and Kevin Sheets. Thank you to Kristopher Kubow for all of his help and training on the confocal microscope at James Madison University's Light Microscopy and Imaging Facility.

I would especially like to thank my amazing family and friends for their support and encouragement over the years. I could not have done this without you.

Table of Contents

List of Figures

List of Tables

Overview of Dissertation

Chapter 1 is an introductory chapter on the topics of stem cell research in regenerative medicine. It covers topics in tendon biology, stem cells and their microenvironment, and studies that have used fibrous scaffolds as models to study cell behaviors, specifically differentiation. Understanding these factors individually and in combination will further our advances in cell-based therapies.

Chapter 2 is a study investigating MSC response to topographical cues in their microenvironment. STEP manufactured nanofiber scaffolds were used as a model for studying tenogenic differentiation into tenocytes on scaffolds that mimic native tendon alignment specifically scaffolds of three-dimensional (3D) suspended and aligned nanofibers. This data highlights specific cellular responses to alignment that adds to our understanding of stem cells in development and repair.

Chapter 3 is an introductory chapter that discusses the foundation for the study of MSC homing towards inflammation. It covers topics of exogenous and endogenous stem cell homing and includes a comparison to leukocytes and cancer cells through the stages of transendothelial migration (TEM). The chapter concludes with current models and the findings that contribute to elucidating the mechanisms of MSC homing.

Chapter 4 is a study investigating the underlying mechanisms involved in transmigration of MSCs towards inflammation. Modified Transwell systems were used to mimic the vasculature and inflammatory environment. This vascular model could be used to study MSC transmigration for use in strategies to inhibit inflammation while promoting regeneration, as well as for small molecule screening to identify molecules that attract endogenous stem cells to areas of injury or inflammation.

Chapter 5 summarizes the key findings and conclusions of this dissertation and future directions of MSC tendon differentiation and stem cell homing.

Appendices include additional data for Chapters 2 and 4. Appendix A to Chapter 2 includes optimization data on MSC seeding density and fiber coatings. Appendix B to Chapter 4 includes optimization data from various experiments including monolayer integrity of different endothelial cell types, MSC collections methods and isolation, additional data from transmigration assays, and gene and protein expression changes for the cytoskeletal regulators, PI3K-Akt, and Jak/Stat signaling pathways.

Chapter 1: Mesenchymal Stem Cell-seeded Fibrous Scaffolds for Tenogenesis

I. Tendon Biology

Tendon is a dense connective tissue, attaching muscle to bone that transmits force for locomotion. It is comprised mainly of extracellular matrix (ECM) and has low cellularity and vascularity, likely related to its poor regenerative capacity. This results in prolonged and incomplete healing with a high risk of re-injury [1]. Musculoskeletal conditions cost healthcare systems approximately $1.7 billion worldwide annually; [2] 30 million of these cases are tendon and ligament-related [3]. The number of cases increases yearly due to an increase in athletic activity and an aging population. Estimates of prevalence are challenging and are likely underestimated due to misdiagnosis, [4] injuries diagnosed along with systemic disease, [5] or are accounted for as soft tissue injuries [6]. Tendon injuries and conditions are collectively known as tendinopathies; tendinitis is associated with inflammation while tendinosis does not have an inflammatory component [6]. The most commonly affected tendons in humans include the flexor tendon, patellar tendons, Achilles tendon, tibialis posterior tendon, and supraspinatus tendon [6]. Patients may suffer from long-term pain, disability, decreased quality of life, and loss of productivity. Tendinopathies are common and are becoming an increasing challenge to treat with the rising number of individuals affected and the associated healthcare costs.

Tendon Development

The process of tendon development during embryogenesis has been studied to attempt to apply the principles of tendon formation to the development of therapeutic

treatments in regenerative medicine. During embryogenesis, somites form the compartments of dermomyotome, myotome, and sclerotome towards limb development and are influenced by cell signaling pathways. The main pathways identified in the development of tendon include the transforming growth factor beta (TGF-β), fibroblast growth factor (FGF), and Wnt signaling pathways.

Development of musculoskeletal tissues begins with the dermomyotome and the sclerotome layers; the syndetome forms from the sclerotome as the myotome forms from the dermomyotome. FGF signaling is involved in formation of tissue boundaries of tendon and muscle. Tendon progenitors are induced from the edge of the sclerotome in response to FGF signaling from the myotome, promoting scleraxis expression (*scx*) in adjacent cells, and dividing the sclerotome into muscle progenitor cells that express *pax1* and tendon progenitor cells that express *scx*, FGF4, and FGF8 determine tissue boundaries in the developing limb; specifically FGFR1 in tendon [7]. The sclerotome and myotome form a fourth somatic compartment, a *scx*-positive compartment, known as the syndetome. *Scx* is expressed in axial and ventrolateral tendons, in tendon progenitors in somites, and in tissue maturation. The use of a chick-quail chimera with *scx* has allowed for the tracking of cells during tenogenesis and the visualization of somites [8]. Cross talk between pathway signaling promotes tendon formation and suppresses development of other tissue types.

Berge *et al.* studied the interactions of signaling molecules of Wnt and FGF signaling on cell fate in the developing limb bud. Ectodermal Wnt signaling to the mesenchyme inhibits chondrogenesis and promotes soft tissue differentiation. The ectoderm also induces proliferation and re-directs progenitor fate from chondrogenesis

towards differentiation of soft tissue after exposure to Wnt3a. Progenitors originate from the subridge region where they are exposed to FGF from the apical ectodermal ridge (AER) and Wnt from the ectoderm. The authors concluded that the combination of Fgf8 and Wnt3a inhibited chondrogenesis, promoted progenitor growth, and maintained an undifferentiated state [9].

The TGF-β signaling pathway and its TGF-β isoforms are a critical regulator of tendon development and maturation. Kuo *et al.* studied the spatiotemporal distribution of TGF-β1, TGF-β2, and TGF-β3 and their receptors TGF-βRI and TGF-βRII in intermediate tendon development in chick embryos. Findings showed no detection of TGF-β1; however, TGF-β2, and TGF-β3 showed localization specific for each protein. These findings suggested correlation to the same matrix molecules involved in tendon maturation. The authors concluded that the TGF-βs each have a distinct roles and are regulated by matrix molecules in development [10].

Structure and Function in Health and Disease

Tendon hierarchical structure and mechanical properties vary across the organization of the tissue, including where tendon attaches to muscle (myotendinous junction) and to bone (enthesis). The size of various tendon components and whole tendons varies by several factors including genetics, age, level of conditioning, health, and species. The collagen molecule (~1 nm), consists of procollagen; a triple helix with alternating Gly-Pro-X (glycine, proline, X is any amino acid) amino acid residues. Collagen molecules align and self-assemble in a staggered pattern forming a fibril of ~100 nm. This creates overlapping and non-overlapping regions and formation of fiber crimping. Tenocytes are found at this level. Fibrils are aggregated to form a collagen

fiber of ~1 – 300 um and is encased in an outer layer known as the endotenon. Fibers bundle to form primary, secondary, and tertiary bundles of ~20 – 200 um and are surrounded by an outer layer known as epitenon. These components make up the tendon unit of ~500 um [11].

Tendon ECM consists primarily of two fibrillar collagens; type I collagen (Col I) and type III collagen (Col III). A healthy, adult, conditioned tendon has a higher ratio of Col I to Col III. Col I has larger fibril diameters that provides the tissue with strength; Col III has smaller diameter fibrils in comparison and provides the tissue with its elastic properties. Huang *et al.* summarized tendon matrix associated markers and their functions. Non-fibrillar collagens II, V, XI, XII, and XIV are important in homeostasis and inadequate expression can lead to pathological conditions [12]. Collagen V regulates fibrillogenesis in Col I-rich connective tissues. Its deletion results in structural abnormalities, decreased tissue stiffness, and joint alterations characteristic of Ehlers-Danlos syndrome [13]. The deleterious effects of other non-fibrillar collagens have not been as extensively studied.

The main cell type found in tendon is the tenocyte, also referred to as tendon fibroblast or mature tendon cell. Tenocytes are spindle-like cells that can be found sparsely distributed along tendon fibrils. Tendon cells function in the synthesis, maintenance, and degradation of extracellular matrix proteins [14]. They are arranged in a parallel orientation to each other; however, they are connected laterally through cell processes. Tenoblasts are immature tendon cells with rounded morphology, found in large numbers in younger tendon [15]. Additionally, Bi *et al.* discovered a tendon progenitor/stem cell (TPSC) population and identified components of the tendon niche.

Human and mouse tendon cells showed heterogeneity, clonogenicity, self-renewal, and differentiation characteristic of stem cells. Tendon cells express *scx*, a basic helix-loop-helix transcription factor, is specific to tendon and ligament tissues [16]. The role of scleraxis was discovered though developmental studies of *scx* $^{-/-}$ mice that showed severe tendon defects [17]. *Scx* functions through regulation of the expression and production of Col I [18]. Mohawk (*mkx*) is a homeobox transcription factor expressed in tendon development. *Mkx* $^{-/-}$ mice exhibited hypoplasticity of tendons, decreased diameter of collagen fibers, and a reduction of Col I. This study suggests that *mkx* regulates production of Col I, contributing to tendon development [19]. Biglycan (*bgn*) and fibromodulin are key components in TPSC fate in tendon and regulate bone morphogenic protein (BMP) signaling, specifically BMP-2 and BMP-7 [20]. TGF-β regulates the production of collagen and matrix-associated proteins as evidenced by mouse embryonic development; the use of double mutants of TGF-β2 and TGF-β3 resulted in tendon and ligament loss [21]. Other cell types found in tendon include endothelial cells, osteocytes, and myocytes [22].

In addition to collagens and tendon cell populations, glycosaminoglycans (GAGs) and carbohydrates bind to proteoglycans and glycoproteins in tendon matrix. GAGs are long, non-branched mucopolysaccharides with disaccharide repeat regions. GAGs are differentiated from each other by degree of sulfation. Tendon-related GAGs are chondroitin sulfate (CS), dermatan sulfate (DS), heparin sulfate (HS), and keratin sulfate (KS). Specifically, CS is bound with versican and is found in high proportions in tendon. It functions in ECM organization, aggregation of protein ligands, and resistance to compressional forces. Hyaluronic acid is the only non-sulfated GAG and functions in

joint lubrication and inflammatory responses. Ryan *et al.* provides an extensive review of these tendon GAGs in physiology and pathology [23].

Decorin (*dcn*) is an important proteoglycan in the extracellular matrix and is prominent in collagen fibrillogenesis. Structurally, it has one chondroitin sulfate GAG chain. A *dcn* $^{-/-}$ mouse model showed altered fibril formation including irregular fibrils with varying thickness along the length of the fibril and a large variability in fibril size [24,25]. *Dcn* is critical for proper tendon development, repair, and function. *Bgn* is a class I small leucine rich proteoglycan (SLRP) and has two chondroitin sulfate GAG chains. A *bgn* $^{-/-}$ mouse model was developed for studying biglycan-associated musculoskeletal disease. This study observed bone development in the absence of *Bgn*; however, results showed lower production of marrow stromal cells, reduced response to growth factors, reduced collagen synthesis, and increased apoptosis that can also be related to tenogenesis [24,26]. Other proteoglycans including fibromodulin and lumican and several tendon glycoproteins including fibronectin, tenomodulin (Tnmd), and tenascin C (Tnc) also interact with collagen. For example, *tnmd* regulates fibrillogenesis and tenocyte proliferation. *Tnmd* $^{-/-}$ mice have shown reduced cell density and extreme fibril diameters [27]. Other components of tendon ECM include glycoproteins, elastin, water, ions, and water. The interactions between cell populations and ECM components are key to understanding tendon development, injury, and repair mechanisms.

Tendon Mechanical Properties in Maintenance and Repair

Tendon is primarily subjected to uniaxial tension and displays non-linear, viscoelastic biomechanics. The stress-strain curve illustrates the mechanical properties of the tissue as strain increases and tendon collagen fibrils crimp (Fig. 1.1) [28]. The

relationship between stress and strain is not constant and depends on the time of displacement or load. Fibrils exhibit a crimping pattern when at rest or subjected to low strain. At strains 0-2%, the fibers stretch and the extent of crimping is decreased. This is identified as the toe region. This results from a stretching of the triple helices of the collagen molecules. As the collagen fibril backbone is stretched, the crimping straightens, resulting in increased stiffness. As strain increases, behavior becomes linear. Collagen under 2-4% strains is in the physiological or linear region and deformation occurs in a linear pattern. Young's modulus, or elasticity, can be determined by calculating the slope of this line. Intramolecular sliding of collagen triple helicases occurs at this point and the tissue exhibits elastic behavior and can revert to its original state. Beyond 4% strain, microscopic damage occurs to the fibrils and induces a catabolic response. This is the yield point at which collagen fibers cannot return after deformation. Macroscopic failure occurs by intrafibril damage by molecular slippage at strains 8-10%. The maximum stress for tendon is ~40-50 MPa. As individual fibrils begin to fail damage accumulates, stiffness is reduced and the ligament/tendons begins to fail. Excessive tension causes fibrils to go beyond the yield point which can result in rupture of the tissue at the ultimate failure point of ~12% strain.

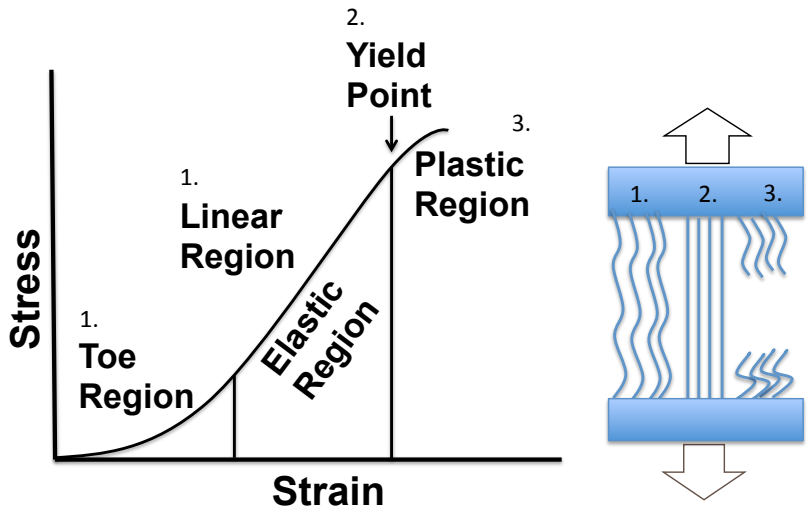

Figure 1.1: A stress-strain curve of the physical properties of tendon. The stress-strain curve shows the Young's modulus through the physiological and non-physiological regions of tendon and the associated fibril crimping, 1.) toe and linear regions, 2.) plastic region, and 3.) rupture.

Cells can adapt to mechanical loading until the point at which mechanical loading overwhelms cellular repair mechanisms, resulting in damage that is reversible up to this point. There are two main causes of tendon injury; 1) a cumulative effect of damage over time due to overuse, including frequency and duration of activity that changes the biomechanics of the tissue and 2) when the impact exceeds the structural and viscoelastic properties of the tissue and results in rupture [29-31]. Irreversible damage due to inadequate repair is caused by insufficient time between exercise, high frequency, long duration, the magnitude of overuse, individual susceptibility, matrix composition, and cellular activity [14]. This results in cell death, matrix degradation, and an increase in production of Col III that lead to tendon degeneration [1,32]. Direct damage to cells and matrix initiates alterations in gene expression and protein production and similarly, results in progression of degeneration and disease. A competing hypothesis is that tendon degeneration is a catabolic response of tenocytes to under-stimulation. Arnoczky *et al.* presented evidence

that *in vitro* studies lack the physiological relevance of mechanical over stimulation. An *in situ* rat-tail tendon model was used to demonstrate that altered cell-matrix interactions result in under stimulation of tenocytes and tissue degeneration. The tenocyte catabolic response was stimulated, producing an upregulation in collagenase mRNA and protein synthesis, degeneration of pericellular matrix, and decreased material properties [33].

Natural healing occurs through the three overlapping phases of inflammation, proliferation, and remodeling. The first phase of inflammation involves the vessels of the injured area; initiating fibrin clots and activating vasodilators, platelets, leukocytes, red blood cells, tenocytes, and pro-inflammatory molecules. This phase typically lasts a few days to two weeks. The proliferative phase begins approximately three days after injury and is characterized by disorganized matrix, large numbers of fibroblasts, tenocytes, macrophages, increased proteoglycan content, and neovascularization. Matrix synthesis, specifically Col III, peaks at this phase. Lastly, in the remodeling phase of tendon healing, Col I synthesis dominates, tissue alignment returns, and cell density decreases. This phase begins 1-2 months after injury and completion can take one year or longer. The resulting scar formation prevents the tissue from regaining full biomechanical properties [34-36].

The impacts of mechanical loading on tendon healing include increased tendon size and improved mechanical properties for tendon healing [37]. Several studies have investigated the molecular mechanisms of loading on maintenance and healing. Actin-associated adherens junctions connect the cell cytoskeleton with strain and increase adhesions and stress fiber formation under loading to aid in recovery [38]. Loaded tendon showed several-fold greater production of TGF-β compared to unloaded tendon that

correlated to synthesis of proteoglycans [39]. Loading promoted gene expression of *scx*, *tnmd*, and growth stimulators [40]. Cyclic loading has been shown to induce tenocyte activated stress-activated protein kinase (SAPKs) and JNK signaling that changed with magnitude. JNK signaling was mediated through a calcium-dependent pathway and continued JNK signaling may lead to tendon degeneration [41]. Mechanical stimulation without growth factors induced Akt signaling and tenogenic differentiation of tendon stem cells [42]. Mechanical loading with macromolecular crowding (MMC) increased cell and ECM alignment and ECM production [43]. Eccentric and concentric training was compared in an untrained rat model and showed improved mechanical properties after training, specifically eccentric training [44].

Tendon Treatments

Conservative options for tendon injury include rest, immobilization, eccentric training, and injections that can reduce pain and inflammation. Surgical intervention may be more beneficial in reducing symptoms and stabilizing function than the more limited nonsurgical options, depending on the tendon type, severity, and injury progression. Surgical options include the use of allografts, xenografts, and autografts with the latter being the gold standard for treatment. However, disadvantages of autografts include donor-site morbidity, decreased function, and decreased long-term outcomes to the tissue. Nillson-Helander *et al.* investigated the outcome of acute Achilles tendon ruptures with surgical versus nonsurgical treatment, both with immobilization. There was no significant difference between treatments; however, the authors concluded that immobilization was a key component of the treatment to prevent re-rupture and that function in both groups

was decreased compared to the uninjured leg in this one year study [45]. The rate of re-injury is still high after surgery.

Tendon biologics including matrices/scaffolds, stem cells, growth factors, and gene therapy are alternatives that may provide improved long term results [27,46]. Tissue engineering and regenerative medicine have studied the use of implantation of acellular and cellular scaffolds in replacing or healing injured tissue. Natural and synthetic biomaterials mimicking the structure and organization to replace damaged tendon are commonly manufactured by electrospinning. Commonly studied stem cell sources include bone marrow-derived MSCs, adipose-derived MSCs, tendon-derived MSCs, placental-derived stem cells, embryonic stem cells, and induced pluripotent stem cells. The use of cells or cell-laden matrices may have immunomodulatory and regenerative effects to return structural and biomechanical function of the tissue [27,46]. Stem cell therapy has shown great promise and improved healing compared to conservative management. However, cell therapies need further study and optimization; the underlying molecular mechanisms are poorly understood. Specific cellular and molecular changes have been observed in tendon processes of development and degeneration that will be critical in developing models and therapeutic applications [47].

II. Mesenchymal Stem Cell Behavior

Friedenstein *et al.* first isolated fibroblast colony forming cells from bone marrow [48,49] and these cells were later named mesenchymal stem cells (MSCs) [50]. Since then, efforts have been made to define, isolate, and understand the immunomodulatory and regenerative effects of MSCs. MSCs are commonly used in *in vivo* and *in vitro* studies

and the effects of expansion, maintenance of phenotype and function in cell culture are still being investigated. Components of the microenvironment influence cell response, specifically topography, stiffness, mechanical stimulation, oxygen tension, and density as well as spatiotemporal control over biochemical and biomechanical stimuli. Engineering microenvironments incorporating these factors is driving cell based therapies and drug discovery applications [51].

MSCs have been studied extensively in regenerative medicine. They are defined by criteria stated by the International Society for Cell Therapy as 1) plastic adherent in standard cell culture conditions, 2) express CD105, CD73, CD90, and negative for expression of CD45, CD34, CD14, or CD11b, CD79alpha or CD19, and HLA-DR surface molecules, and 3) differentiate into osteoblasts, adipocytes, and chondrocytes *in vitro* [52]. MSCs have been successfully isolated from several tissues in the body including bone marrow, [49] tendon, [20] skeletal muscle, [53] heart, [54] and brain, [55] among others. Other types of stem cells not discussed in this review include embryonic stem cells, placental stem cells, and induced pluripotent stem cells that are categorized by the extent of their differentiation capabilities.

MSC fate is regulated by a complex and intertwined system of signals from the cellular microenvironment (Figure 1.2); biochemical and biophysical cues provided by the ECM and surrounding tissue influence cell-matrix interactions and cell-cell signaling [56]. A study using stiffness and cell-cell contact showed that cells with direct contact to a stiff matrix produced alkaline phosphatase and calcium deposition in osteogenesis [57]. Shear stress influences cell contractility, gene expression, and determination of cell lineage. Higher fluid shear stress increased contractility and promoted osteogenesis while

lower forces maintained multipotency [58]. In another study, mechanical loading induced BMP-12 triggered Smad8 and increased *scx* expression and tenomodulin, resulting in tenogenesis and loss of plasticity [59]. Manipulating components in the MSC microenvironment influence cell behavior and ultimate cell fate and function.

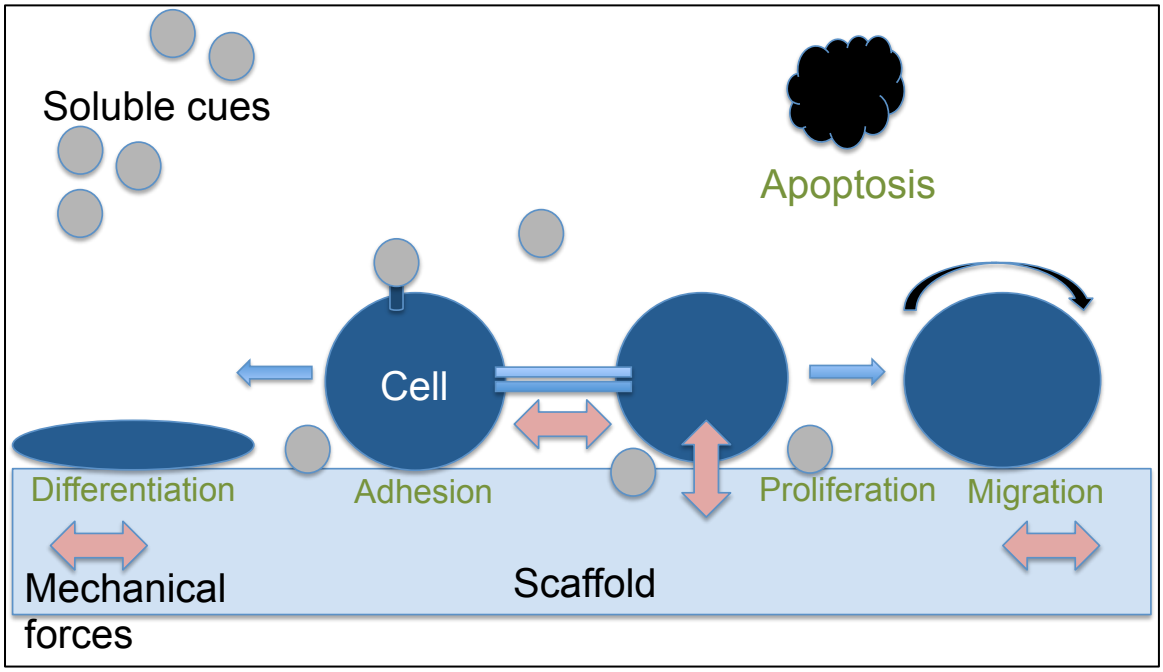

Figure 1.2: Stem cell fate is determined via a combination of microenvironmental cues. The major cues are from 1) cell interactions with other stem cells, native cell populations, and the matrix, 2) scaffolds mimicking native extracellular matrix (ECM), 3) molecule cues may be soluble, immobilized, or embedded within the ECM, and 4) mechanical forces. These cues promote specific cellular responses and ultimate cell fate and function.

MSCs are capable of a vast array of functions of either regenerative or trophic effects and are promising for treating tissue injury/disease [56]. L. da Silva Meirelles *et al.* described MSC factor secretion of cytokines, growth factors, and ECM proteins that contributed to their therapeutic properties. Regenerative effects of MSCs include proliferation, growth, and differentiation that have a direct impact on tissue remodeling and repair. MSCs contribute indirectly through trophic effects that create a more

favorable environment for healing including immunomodulation, inhibiting apoptosis, angiogenesis, inhibiting fibrosis, and chemoattraction [60].

The immunomodulatory effects of MSC have been shown to act upon both the innate and adaptive immune systems. These effects broadly include immunosuppressive effects during inflammation or disease conditions and in immunologically quiescent conditions. These effects are a result of complex interactions between MSC and immune cells through indirect cell contact via secreted factors and direct MSC contact with immune cells. Immunomodulation capabilities include inhibition of T cell proliferation, inhibition or promotion of B cell proliferation, inhibition of NK cell activation, and the regulation of cytokine secretions of dendritic cells and macrophages. MSCs have been shown to reduce cell death, reduce fibrosis, and establish blood supply to promote healing and secretion of chemokines. Secreted factors include a large number of chemokines, cytokines and prostaglandins. Additional molecules that may play a role include transforming growth factor-beta (TGF-β), hepatocyte growth factor (HGF), nitric oxide (NO), human leukocyte antigen G (HLA-G), indoleamine 2,3 dioxygenase (IDO) and Toll-like receptor (TLR) expression. MSC immunosuppressive effects include inhibition of T lymphocyte proliferation, inhibition of pro-inflammatory molecules, inhibition of B cell antibody production and inhibition of antigen presenting cells [61]. Specific examples include promoting the shift of T helper type 1 cells to T-helper type 2 cells, down-regulation of interferon gamma (IFNγ) by NK cells. A number of *in vitro* and *in vivo* studies provide evidence to support MSC capacity immunomodulation. *In vivo* disease models including sepsis, allograft rejection and several others have shown induced immune modulation and decreased disease progression. They examine treatment

or exposure of MSC with chemokines, cytokines and prostaglandin molecules that have the potential to induce MSC immunomodulation. These models provide insight into the mechanisms involved in activation of MSC immunomodulation in inflammatory and diseased states.

The Mesenchymal Stem Cell Niche and Extracellular Matrix

The ECM is constantly being remodeled; structural components, function, and mechanical properties i.e. rigidity promote cell responses of proliferation, migration, differentiation, apoptosis, or senescence through biochemical and mechanical stimulation [62]. These microenvironmental cues control stem cell activities and function in homeostasis, repair and pathological conditions, including aging and cancer. MSCs have been studied through lineage tracing, single-cell transplantation, genetic manipulation including gain and loss of function studies, and real time imaging in vivo [63]. MSCs reside in the bone marrow that controls their behavior and migration. The niche includes hematopoietic stem cells, perivascular MSCs, sinusoidal endothelial cells, sympathetic nerve fibers, and osteoblastic cells. Stem cell niches aid in tissue maintenance and repair [64] and hypoxia enhanced proliferation and plasticity [65]. MSCs in the bone marrow are *nestin*$^{+}$, self-renewing, and exhibit multilineage differentiation during transplantations [66]. MSCs originate from perivascular space, possibly as pericytes. However, a recent study investigating pericyte function showed that pericytes from various organs did not function in the same manner as MSCs *in vivo*, without *in vitro* manipulations [67]. The tendon niche, similarly to the bone marrow niche maintains stemness of these cells until conditions change and promote migration and differentiation.

Cell Mechanotransduction

Tendon experiences a mechanical environment, primarily tensile loading, as it functions to transmit the load from muscle to bone. Tendon not only requires mechanical stimulation for proper function, but mechanical stimulus also promotes development and repair [68]. Mechanical stimulation influences cell signaling from surrounding tissues. Cell mechanotransduction is the process in which a cell converts a mechanical or biochemical signal to a physical cell behavior through a cascade of intracellular signaling that leads to gene transcription in the nucleus and cell response (Figure 1.3) [22,69]. It contributes to collagen alignment and progenitor differentiation to tenocytes. Force is determined by the loading history of the tissue and the condition of the ECM. Factors affecting force are regional variation along the tissue from anterior and posterior fibrils, [70] variation in GAG composition, [71] and strain and pre-stress of the cytoskeleton exists due to matrix stiffness, cell-cell interactions, cell-matrix interactions, and contractility. Tenocytes can detect this mechanical environment and "sense" their environment through cell-cell interactions, cell-matrix interactions, and primary cilia. Tensile load is transferred to cells by matrix components and intracellular signaling [22].

Components of the ECM function in cell adhesion and signaling. Tensile loading can also stretch ECM molecules, such as collagen, exposing new binding sites. In the case of collagen, GFOGER binding sites allow for further α1β1 integrin interaction and environmental sensing [72]. Integrins are transmembrane proteins, connecting the ECM to the inside of the cell and actin cytoskeleton. They are α/β heterodimers that extend from the ECM and across the membrane to extend their short cytoplasmic tail into the cell. Integrins function to transmit the extracellular signal, chemical or mechanical to an

intracellular biochemical signal. Actin binding proteins bind to the cytoplasmic β tail and induce conformation changes in the extracellular portion that is exposed to ECM. Some actin binding proteins also function as mechanosensors, including FAK and p130Cas. When the integrin is activated, it, in turn, activates signaling cascades involving protein kinases and phosphatases that lead to phosphorylation and/or dephosphorylation, resulting in translocation of a transcription factor to the nucleus and transcription of the target DNA and eventual cell response. This is known as "outside – in" signaling. Elosegui-Artola *et al.* provide evidence for an actin-talin-integrin-fibronectin clutch, the clutch bond strengthens as it is stretched. A threshold for talin unfolding exists that is based on surface stiffness. If the stiffness is above the talin threshold, it will unfold and allow vinculin to bind, resulting in a strengthened bond. If stiffness is below the threshold, talin does not unfold and further binding does not occur [73].

Integrins also function in "inside-out" signaling. Cell surface receptors can be activated by intracellular signaling, initiating binding of the receptor and further cell signaling. The cytoskeleton can rearrange itself to cluster integrins, recruit actin binding proteins, and form focal adhesions. As focal adhesions mature, the cell forms stronger adhesion to its matrix. The number of active receptors on the cell surface and their affinity for a ligand will determine signaling response [22].

Tenocyte mechanotransduction is influenced by primary cilia that deflect in the direction of stimuli. This deflection at the cell surface causes a cascade of intracellular signaling events to occur, leading to transcription factor translocation to the nucleus and transcription of genes that result in cell response [22]. Gardner *et al.* showed that primary

cilia under stress deprivation caused a lengthening of the cilia that was restored to a shorter length after 24 hours of mechanical stimulus [74].

Cells sensing a rigid environment will form stress fibers that cells use to exert force back on the substrate and sense the resistance. Actomyosin activity provides the cell with its own contractility that also influences its ability to sense the environment. Cell-cell interactions occur through gap junctions. For example, tenocytes communicate through connexins 26, 43, and 32 aid in mechanosensing; signals can travel 4-7 cell diameters deep. Mechanical stimulation can also activate ion channels; an increase in intracellular calcium can lead to activation of Rho/ROCK that increases phosphorylation of MLC (myosin light chain) and myosin II. Transient receptor potentials (TRPs), specifically PIEZOS have recently been identified in tendon inflammation and mechanotransduction. Mechanical stimuli can also interfere with ATP production leading to temporary desensitization of cells when over-stimulated. Hippo signaling pathway, specifically YAP has recently been shown to play a role in mechanotransduction [22]. Several cell signaling pathways are activated, specifically Smad2/3 signaling has been identified in tendon mechanotransduction in collagen-GAG scaffolds [75].

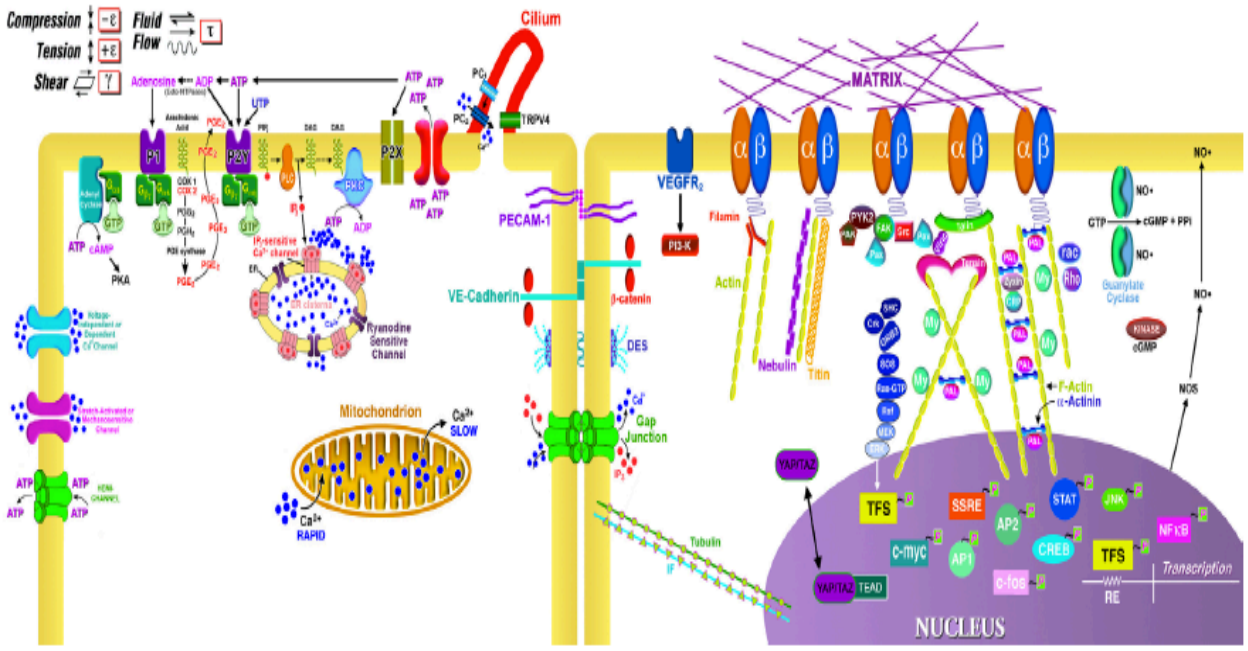

Figure 1.3: Mechanisms of tendon mechanotransduction. Several factors influence how a cell can sense and response to mechanical cues in the microenvironment; ion channels, gap junctions, intracellular Ca2+ levels, primary cilia, and integrin-ECM interactions induce various intracellular signaling pathways that result in different cell responses. Journal of Orthopaedic Research 2015; 33(6):813-822 22.

III. Factors in Cell Migration

Cells migrate in physiological and pathological contexts in response to various stimuli including chemotaxis, haptotaxis, and durotaxis. Migration occurs as single cells, in groups as chains, and sheets or clusters and can switch between single-cell and collective cell migration. This decision is dependent on cell type, environmental conditions, and stimuli [76,77]. An example of individual cell migration is the macrophage as it progresses through diapedesis in response to proinflammatory cytokines. Collective cell migration occurs in development during various embryonic stages. Adherens junctions in addition to desmosomes, tight junctions, gap junctions, and matrix

metalloproteinases (MMPs) all contribute to collective cell migration. The leading edge has a loosely packed cell structure with the protrusive lamellipodia in two-dimensional (2D) environments and filopodia or pseudopodia in three-dimensional (3D) environments. The trailing edge is more tightly packed with cells and propels non-protruding cells. Disruption of cell-cell or cell-matrix adhesions can lead to a change in migration from collection to individual [76].

Migration modes include mesenchymal migration, used primarily by fibroblasts and amoeboid migration, used primarily by leukocytes. Mesenchymal migration is observed in slow moving cells that have highly organized cytoskeletons and complex adhesions. Mesenchymal cell motility involves cyclic lamellipodia-driven cell migration characteristic of fibroblasts and other mesenchymal cells. This cell migration cycle consists of polarization, protrusion, translocation, and detachment. The leading and lagging edges of the cell both contribute to the stages; similarities and differences in activated signaling pathways are observed at both edges [76,78]. Polarization in 2D environments leads to a dorsal and ventral orientation that does not exist in 3D environments. Proteolysis is critical in this mode of migration for matrix degradation and integrins for cell-matrix adhesions. Amoeboid migration is observed in fast moving cells that do not have highly organized actin cytoskeletons and therefore show weak adhesions. Amoeboid migration exhibits cell morphology that is rounded, less dendritic, and exhibits less clustering of MTI-MMP (membrane type I metalloprotease) and β1 integrins [76]. Cancer cells have been shown to switch between both modes depending on their environment and additionally, exhibit nonapoptotic membrane blebbing that occurs without a highly organized cytoskeleton [79]. Cancer cells can migrate as individual cells or

collectively protecting them from the immune system or increasing the cell entrapment in the blood vessels [80]. Blebbing and contractility through the matrix have also been observed in embryonic cell migration [79].

Dimensional Effects

Cells migrate in both 2D and 3D environments *in vivo;* however, 3D environments are more common and cell migration is limited by several confinement factors not observed in 2D environments (Fig. 1.4) [81]. The nucleus is the stiffest part of the cell and limits migration to the nuclear threshold, or size of the cell nucleus. Migration does not occur at pore sizes less than the nuclear limit without proteolysis [82]. MMPs are secreted to degrade the ECM surrounding the cell and cancer cells migrate in mesenchymal mode of migration to create migration tracks for other cells to follow in [83]. Cells can then migrate in a MMP-dependent amoeboid mode. MTLn3E breast cancer cells migrated in a ROCK-dependent pathway [84]. Fibroblasts migrate through lobopodial migration on substrates with a linear elastic behavior. This mode is dependent on RhoA-ROCK-myosin II, vinculin, and paxillin and produces a blunt protrusion with blebbing. Blebbing is generally caused by limited cell adhesion and increased cell contractility. In contrast, protrusions are observed in low adhesion and low contractility cells. [81] Lastly, migration via osmotic engine model is described as water uptake and expulsion through the cell membrane at the leading and trailing edge of the cell body [85].

Cellular Adhesion and Speed

Integrin-ECM interactions decrease cell migration on 2D substrates, whereas increasing ECM concentration in one-dimensional (1D) fibrillar substrates promotes increased cell migration. Migration speed is more complex to understand in 3D substrates

and include factors of stiffness, [86] pore size, [87] confinement, [88] and crosslinking [89] that influence speed, persistence, velocity, and force. Focal adhesions are more stable in a 2D environment than in a 3D environment and migration decreases with stiffness [62].

Cell adhesions are categorized in to four groups; nascent adhesions, focal complexes, focal adhesions, and fibrillar adhesions (stress fibers). Rigidity and high forces promote focal adhesions and soft substrates with inhibition of contractility promote nascent adhesions and focal complexes [90]. Integrin clusters constitute nascent adhesions, requiring actin and talin, that mature through cell contractility [91]. Adhesion size and duration is regulated by vinculin-tension and adhesion complex area. A positive correlation between the two was observed for medium sized adhesions and a negative correlation was observed for small and large adhesions [92]. Stress fiber and fibrillar adhesions development through inverted formin 2 (INF2) regulate actin structures for remodeling of ECM [93]. Force-activated activation induces binding proteins, dissociation, and localization [90]. Cells on 1D printed lines show a distribution of α_5 integrin, FAK, vinculin, and paxillin. Vinculin distribution is similar in vertical confinement. Cells migrating from narrow to wide lines or groves show increased focal adhesions [94]. Kulangara *et al.* used 350 nm grated topographies to investigate focal adhesion composition and dynamics, specifically zyxin. Zyxin expression was dowregulated, resulting in smaller adhesions, higher adhesion turnover, and thus faster migration. These findings suggest that nanofibers decrease mechanical stimulation on adhesions and exert force-dependent changes in zyxin expression [95]. Talin is another critical adaptor protein in cell adhesion, stretching talin rods exposes binding sites for vinculin binding and reorganization of the cytoskeleton [96]. Talin phosphorylation induces cell migration.

Smurf1-mediated ubiquitination degrades the talin head after phosphorylation by Cdk5, controlling talin head turnover, cell adhesion, and migration [97]. Bachir *et al.* studied how the molecule ratio determines nascent and mature adhesion formation. Results showed that integrins bind with α-actinin clusters and kindlin during the formation of nascent adhesion and integrin-talin complexes in response to myosin II in mature adhesions [98].

Assembly of nascent adhesions and formation of protrusions leads to cell spreading and increased substrate attachment. Nascent adhesion proteins, including FAK, talin, vinculin and tensin, bind to each other and actin filaments. Traction is low at this stage. Protrusions form as actin monomers are added to the barbed ends of the F-actin filaments. This actin polymerization drives actin retrograde flow. Actin retrograde flow is the movement of actin from the leading edge of the cell towards the cell body and it exhibits a biphasic relationship with traction force. Over time, integrins and actin binding proteins increase in number, forming more stable adhesions [99].

Focal adhesion size and migration are regulated by stiffness. Focal adhesions connect to actin stress fibers that grow and are maintained through mechanical stress or substrate rigidity. Activation of myosin increases contractility of the cytoskeleton and increases focal adhesion size. Stiffer substrates promote larger focal adhesions and slower/no migration and soft substrates promote smaller or no adhesions and faster migration [99].

Myosin drives the flow of actin as protrusions elongate and retrograde movement decreases as traction force increase. Mature adhesion proteins are recruited to form focal complexes. Stress fibers formation occurs with the activation of myosin in response to the rigidity of the substrate. The area of cell-matrix interaction continues to increase as the

number of integrins become clustered and activated to form mature focal adhesions. Mature adhesion proteins function to stabilize actin filaments, including α-actinin and the addition of a number of other actin binding proteins that results in increased focal adhesion size. The larger/mature focal adhesions are found in the lamella while the smaller/nascent complexes are found in the lamellipodia. Actin retrograde flow continues and stress fibers persist at this stage. Traction is at a steady state until adhesion size reaches its threshold. Signaling from the clustering of integrins and the recruitment of actin binding proteins results in additional stabilization of actin provided by microtubules. GTPase Rap1 increases integrin affinity for ligands, resulting in integrin clustering and adhesion formation. Adhesion turnover is required at both the leading and trailing edges. The role of Rho GTPases in retraction and disassembly is the activation of Rac-GEFs that leads to activation of the MAPK ERK pathway and adhesion turnover [99].

Cellular Morphology

Cell morphology and Rho GTPase signaling differ in 1D, 2D, and 3D environments. Mechanosensing in 3D non-linear elastic environments promotes lamellipodia versus linear elastic substrates that promote lobopodial formation. Rho GTPase signaling for cells on 1D and 3D matrices share similarities in migration including cell protrusions, polarization and persistence. Cell morphology on a 1D line and in 3D matrix environments exhibit spindle-shape morphology with a single lamellipodia. These cells cannot extend protrusions laterally; they experience a confined environment. Cdc42-regulated retrograde actomyosin flow positions the nucleus to the rear of the cell. In polarization, the Par complex regulates Rho GTPases Cdc42, Rac1, and RhoA activity. Rac1 and Cdc42 promote RhoA activity at the trailing edge of the cell

for formation of both the leading and trailing edges. Their activity at the leading edge of the cell functions in adhesion, protrusion, and retraction. While signaling is regulated between Rac1 and RhoA signaling, they can suppress each other's activity. Stabilization of microtubules occurs through Cdc42 activation of the Par complex and activation of CLASP2. The Par complex activation of Rac1 and RhoA promote persistent migration. RhoA can activate ROCK and inhibit the Par complex. Rac1 also interacts with PI3K at the leading edge to promote cell polarization [99].

On a 2D surface, protrusions can expand laterally resulting in multiple lamellae and random migration; induced by high levels of Rac activity. Cells in 3D environments express less Rac1 activity, resulting in a single lamellipodia and chemotaxis. Similar signaling pathways are activated in lamellipodia of cells in 1-3D environments. Rac1 triggers actin polymerization at the leading edge through WAVE and the Arp2/3 complex and Cdc42 acts similarly through WASP and the Arp2/3 complex. LIMK acts as a cofilin severing protein that interrupts actin polymerization. When cofilin activity is decreased, random migration increases and vice versa. RhoA contributes to polymerization and the indirect regulation of cofilin [99].

A 3D microenvironment induces cytoskeletal reorganization in cell migration. Microchannels have shown an increase in actin, reduced stress fibers, and phosphorylation of MLCK (myosin light chain kinase) along the cell body. Tubulin arranges similarly on fibronectin printed parallel lines. Stress fibers are reduced in vertical confinement and myosin II is concentrated at the trailing edge. Microtubule polymerization plays a critical role in confined cell migration [94].

Studies have begun to elucidate the effect of nucleus morphology on cell response. Cell shape determines nucleus morphology, effecting gene expression and cell signaling. Cylindrical nuclei were observed in confinement, in comparison to elongated nuclei on 1D lines or grooves. Microgrooves stimulate gene expression changes involved in Rho GTPase signaling and microtubules while microcontact islands promoted elongated nuclei and increased collagen I production and osteocalcin mRNA [94].

Cell Contractility

Myosin II regulates morphological changes and mechanical response. Myosin II is regulated by phosphorylation of MLC that is phosphorylated by MLCK, through intracellular calcium and kinase activation or ROCK, through Rho GTPases. Myosin II and actin are concentration at the trailing edge of the cell in vertical confinement. Manipulation via micropipette aspiration has shown an accumulation of actin at the cortical region [100]. Rac1 and RhoA both regulate myosin activity, resulting in contraction that increases protrusion and adhesion formation. Traction occurs through integrin signaling and is partially regulated by Rho GTPases. RhoA signaling leads to actomyosin contraction. [99]

Cell Signal Transduction

Evidence suggests that confinement sensing occurs through PIEZO1/PKA and myosin II pathways [101]. Calcium release activates calcium-stretch cation channels, PIEZO1, and decreased PKA signaling. Increases in myosin II can function via Rac1, independently of PIEZO1/Ca^{2+}/PDE1/PKA. Rigidity and elastic behavior of the ECM greatly affects migration and cell lineage determination [102]. Microenvironmental factors of dimensionality and length scales influence intrinsic cell signaling to regulate cell

behavior at intersections. Cell migration was affected independently of pore size, using contact guidance and was enhanced by Cdc42 inhibition. Inhibition of myosin IIA/IIB and RhoA/MLCK inhibitor combinations prevented contact guidance [103]. Molecular clutches are involved in ligand-integrin-actin interactions [104]. The stages of clutch activation are partial-, local-, long term-engagement and disengagement, optical imaging showed that multi-level clutch involvement varied by cell type and protrusion [105].

Cell migration is influenced by matrix properties; pore size, crosslinking, organization, and stiffness. Increasing collagen density resulted in biphasic changes of protrusion rate, orientation, migration speed, invasion, and MMP activity with fiber alignment being most influential [106].

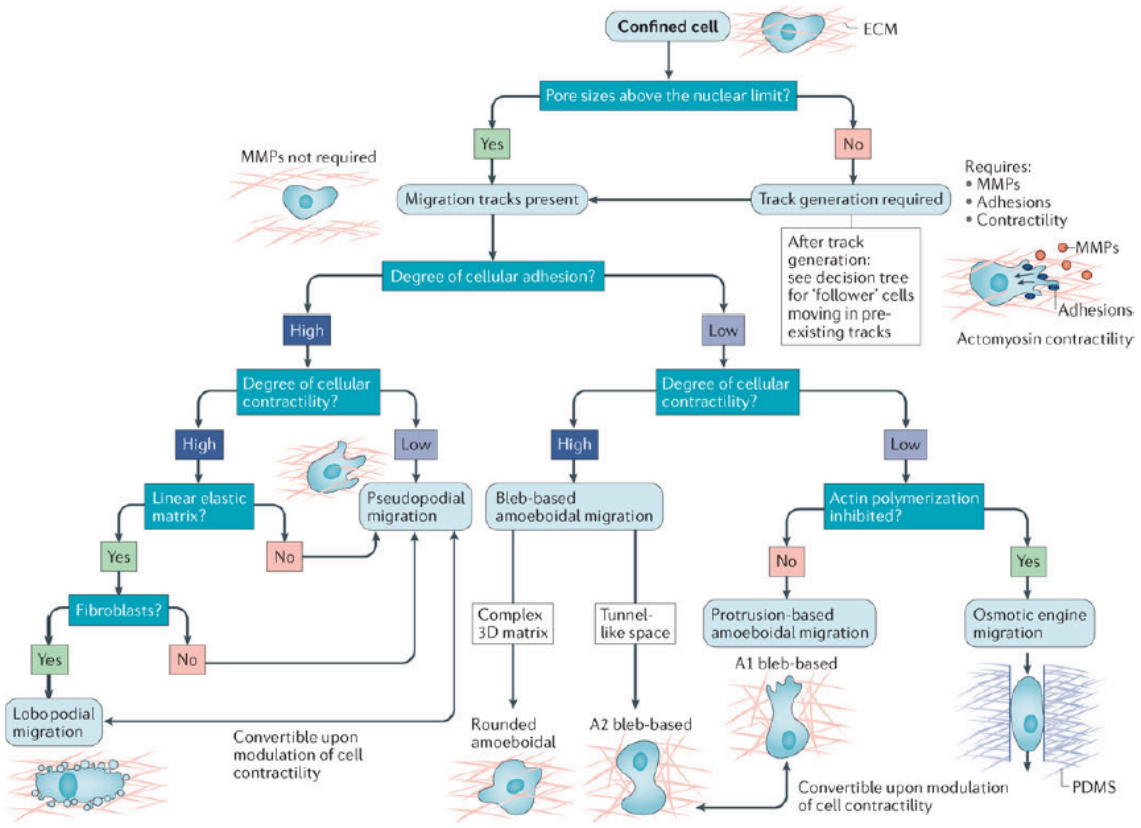

Figure 1.4: Cell migration adaptations in confined environments. Cell mode of migration and protrusions are influenced by the characteristics of the

microenvironment; pore size, crosslinking density, stiffness, structural organization, and other cell types. Nature Reviews Cancer 2016 81.

IV. Regenerative Medicine Applications of Fibrous Scaffolds

Regenerative medicine as defined by the NIH is "the process of creating living functional tissues to repair or replace tissue or organ function lost due to age, disease, damage, or congenital defects". Regenerative medicine is a multidisciplinary field, incorporating knowledge from the fields of biology, engineering, and medicine. Tissue engineering is defined as an "interdisciplinary field that applies the principles of engineering and the life sciences towards the development of biological substitutes that restore, maintain, or improve tissue function" [107]. The classical approach of tissue engineering has been incorporated in regenerative medicine and uses three main components towards development of a construct. Cells, scaffolds, and signaling molecules are studied individually or in combination [108]. MSCs and their signaling molecules including production of growth factors and hormones have been discussed previously. Briefly, stem cells recognize and respond to cues in their environment to determine their behavior. Multiple cell types and sources have been studied for application in tendon repair [109,110]. MSCs are widely used to study musculoskeletal differentiation and studies have provided evidence for tenogenic differentiation of stem cells for tendon repair [111]. Scaffolds provide support for cell adhesion and growth and are typically designed to mimic the structure of the native tissue. They also provide extracellular signals and environmental cues such as biochemical and mechanical properties for directing cell processes [108]. Various scaffold constructs have been

developed to mimic the tendon environment for studying stem cell behavior; [112] however, no standard has been established.

Important characteristics to manufacture a tendon scaffold include dimensionality, fiber density, diameter size, and fiber orientation. Such features influence the structural cues that cells receive and influence cell response and cell fate [113]. Using 3D scaffolds, we can more closely mimic physiology *in vivo* and improve our understanding of cell function [114]. Density of fibrous scaffolds of high, medium, and low fiber density have been studied for their influence on osteogenesis [115]. Additionally, fibrous scaffolds can vary in diameter distribution; [116] however, there is evidence that the use of submicron sized fibers promotes tenogenic differentiation [117]. Many studies have also used engineered fibrous scaffolds to compare scaffolds of aligned fiber orientations and randomly aligned fibers to study cell behavior [118-121]. Researchers in regenerative medicine have adapted this classical approach to include mechanical stimuli as a fourth component. Studies investigate these factors individually and in combination.

Animal Tendon Injury Models

The most commonly injured tendon in humans is the Achilles tendon [122] and is comparable to injury of the superficial digital flexor tendon in the horse [123], providing a relevant model for studying tendon injury and repair. In addition, the horse is a preferred model due to its clinical relevance; tendon injury naturally occurs in the horse and does not need to be induced as with small animal models, the pathology is similar to that of humans, and tissue is readily available [14]. Horses suffer similar injuries that similarly result in pain, decreased function, and increased veterinary costs. Small animal models are less clinically relevant due to their small size and tendon injury is not naturally

occurring; collagenase-induced tendon injury is a common method used in rodent, [124] rabbit, [125] and sheep [126] injury models. Additionally, MSCs have been collected for use in *in vitro* studies from various species including, but not limited to rodents, [127] rabbits, [128] horses, [129] and humans [130].

Fibrous Scaffolds for Basic Research

ECM composition and orientation *in vivo* differs by tissue type and function. Cells can sense and respond to their microenvironment through topographical cues; controlling cell adhesion, growth, migration, maintenance, and differentiation. Tissues that consist of random features for example promote osteoblasts to increase spreading and adhesion or promote MSC differentiation towards an osteogenic lineage. Tissues with anisotrophic features promote maintenance of tenocyte phenotype or MSC differentiation towards tenogenesis. Lastly, isotrophic tissues including bone marrow maintain "stemness" or multipotency characteristic of MSCs [51].

The most commonly used scaffolds are decellularized matrices, organ printing, and biomimetic scaffolds. Decellularized matrices are tissues or organs that have been collected and treated with chemical, biological, or physical agents for cell removal. They are advantageous because they maintain the chemical composition, topography, and mechanical integrity of the native tissue *in vivo*. Organ printing and biofabrication uses computer-aided technology that layers biologically relevant materials; molecules, cells, tissues, and biomaterials to produce 3D vascularized organs. Hydrogels are 3D polymer networks designed to mimic tissue ECM. They allow for biocompatibility and modifications of chemical and mechanical properties. Lastly, biomimetic scaffolds are designed to mimic the structure, composition, and function of native tissue ECM to

optimize cell function. Fibrous scaffolds manufactured by electrospinning use polymers spun into fibers of a specific diameter, length, and orientation to mimic collagen organization in ECM [108]. Ahn *et al.* studied the effects of spatial control and the influence of topographical variations on directing cell lineage [131]. Another study investigated the effects of topography on cytoskeleton organization and cell response. Scaffolds of nano- and microtopography were used to modulate the actin cytoskeleton towards various cell responses [132]. Hydrogels and fibers are commonly combined to further tune the capabilities of the scaffold, specifically mechanical properties and alignment.

Electrospinning produces fibers on the nano- and microscale that control topographical cues and cell contact guidance for regeneration. This technique uses different polymers, polymer blends, and coaxial spinning of two polymers simultaneously [133]. A rotating mandrel is common for manufacturing aligned scaffolds and maintaining cell alignment, ECM production, cell phenotype, differentiation, and anisotrophic mechanical properties [46]. Yuan *et al.* used stable jet electrospinning to manufacture aligned micro- and nanofibers utilizing electrostatic force and high molecular weight polyethylene glycol (PEO) with various polymers. This technique, along with the combination of polymers, was shown to remove the bending instability found in other spinning systems [134]. Zhang *et al.* also used this novel spinning technique to develop a topographic strategy for hiPSC differentiation. This was a three-step study; reprograming of fibroblasts to MSCs, tenocyte differentiation of stem cells on topographic fibers, and implantation into rats as an Achilles tendon repair model. Topographical cues were determined for induced pluripotent stem cell (iPSC) differentiation and as potential use for tissue engineered tendons [135]. STEP (Spinneret based Tunable Engineered

Parameters) is a non-electrospinning method that uses a continuous polymer that winds around a spinning substrate to produce multilayered highly aligned nano- and microfibers [136] that regulate cellular responses [137]. Electrohydrodynamic jet spinning (E-jetting) was used previously with thermal stretching for tendon regeneration. E-jetting promoted aligned cell morphology and increased tendon-associated gene expression when compared to electrospun fibers and demonstrates degenerative impacts on geometric cues and mechanical properties [138]. Solid phase extrusion of co-continuous PCL/PEO (polycaprolactone/polyethylene oxide) blends with phase removal of PEO to produce 3D porous interconnected scaffolds for cell attachment and proliferation. These scaffolds introduce a scalable scaffold with interconnected alignment of pores [139].

Natural and Synthetic Polymers

Scaffolds are manufactured from biomaterials of natural and synthetic polymers, ceramics, metals, and composites that are a blend of these materials. Important characteristic are the mechanical properties of the material, adhesion of cells to the material, scaffold design, porosity that allows for infiltration and viability, biocompatibility, and a degradation rate comparable to the rate of tissue repair [108]. Polymers of natural and synthetic biomaterials have been used to manufacture fibrous scaffolds, including blends and coaxial spinning. For example, Zheng *et al.* developed a 3D collagen/silk scaffold for rotator cuff repair. Tendon stem/progenitor cells showed elongated morphology, alignment, intercellular contact, and ECM deposition on these scaffolds *in vitro*. Implanted scaffolds showed increased fiber diameter, collagen alignment, and mechanical integrity at 12 weeks. These scaffolds can be used in studies of regeneration and tissue engineering approaches [140]. Nowotny *et al.* designed a chitosan

scaffold for tendon repair. A wet spinning method was used to manufacture braided fibers into a 3D tendon scaffold. A higher ultimate stress was measured for large fiber yarns compared to smaller fiber yarns. These 3D scaffolds supported cell growth and mechanical properties for tendon augmentation [141]. Moffat *et al.* demonstrated the use of electrospun PLGA fibers in rotator cuff repair. Attachment, alignment, gene expression, and matrix on aligned and unaligned scaffolds were studied. Polygonal cell morphology was observed on fibers of random organization and expressed distinct integrin expression and lower mechanical properties. In conclusion, PLGA and nanofiber organization influenced cell behavior and matrix properties [142].

Alignment of Fibers

Due to the importance of microenvironmental cues on cell behavior, constructs are designed to mimic the alignment found in native tissue for physiological relevance. Most methods focus on topographical cues because of a phenomenon known as contact guidance. Contact guidance means that the cell will elongate and migrate along the axis of the ECM. Techniques of aligning cells include collagen gels, electromagnetic fields, electrospinning and its alternatives, microstructured culture plates, and mechanical strain. Collagen is the major component of ECM, making it a relevant protein for constructs. Collagen gels take advantage of the self-assembly properties of collagen and cells can be easily added and uniformly distributed. Cells adhere to the collagen fibers and elongate, resulting in gel compaction. If the gel is anchored at one end, the cells contract the gel in both axes, resulting in fiber and cell alignment in the constrained axis.

The negative diamagnetic anisotropy of collagen molecules results in perpendicular orientation and polymerization of collagen when exposed to a strong

electromagnetic field. Electrospinning uses a polymer solution that is pumped through a charged needle and polymerizes into fibers onto a collector. This technique is commonly used to manufacture aligned fibers of micro- and nanoscale. Microfabrication is a process that controls the type and structure of "guiding" structures including features that match ECM proteins. Many cell types undergo mechanical stress during development and normal function. It has also been used to induce cell and matrix alignment for cell maturation [143]. Lastly, electrochemical alignment produces aligned collagen bundles by utilizing a pH gradient between parallel electrodes [46]. Zheng developed a 3D aligned collagen silk scaffold (ACS) for a rabbit rotator cuff injury model TPSCs exhibited elongated morphology, alignment, matrix production and increased alignment and mechanical properties after implantation [144]. Alignment of nanofibers has been identified as the predominant cue in inducing tenogenic morphology, gene expression, and protein production [145].

Fiber Diameter, Length, and Boundary Effects

The effects of different fiber diameters have been studied to understand various cell responses. Erisken *et al.* studied the effects of fiber diameter on fibroblast growth and differentiation. Fiber diameters of 320 nm, 680 nm, and 1.8 μm were used to determine cell responses of cell proliferation, differentiation, and matrix production. Nanofibers promoted increased cell proliferation and matrix production to simulate injury and microfibers promoted differentiation to simulate healthy tendon. This study emphasizes fiber diameter as a key component in design and healing [146].

Studies rarely combine different diameter fibers into a single scaffold; however, this technique more closely mimics physiological conditions where multiple collagen

types are observed. Kim *et al.* used a hybrid spinning technique, incorporating solution and melt electrospinning to manufacture poly (lactic co-glycolic acid) (PLGA) scaffolds of nano-/microfibers and scaffolds of microfibers. Scaffolds were manufactured with nanofibers averaging 530 nm and microfibers averaging 28 um. Characterization of these scaffolds showed similar fiber porosity between scaffold groups. Cell to fiber interaction showed increased cell adhesion, spreading, and infiltration on scaffolds of mixed fiber diameters compared to those of microfiber scaffolds [147].

Another study investigated different fiber lengths and their effects on neo-tissue development. Gilchrist *et al.* studied diameter, length, and boundaries of micropatterned scaffolds of aligned and grid orientation at two scale lengths, micro-scale and meso-scale. Both architectures promoted cell alignment and when combined, meso-scale cues dominated. Differences were observed in collagen content; however no gene expression changes were observed. The authors concluded that multiple length scales could improve tissue organization [148].

Fiber Density and Architecture

Fiber density is another factor that is used to mimic native tissue structures for studying cell response. Chang *et al.* studied MSC adhesion, morphology, proliferation, cell communication, and differentiation in response to electrospun fibers of varying densities and orientations. PCL fibers were spun at low, medium, and high densities as 1D or 2D microfibers. Vinculin staining was concentrated at both ends of the cells grown on 1D fibers and at fiber intersections of cells grown on 2D fibers. MSCs grew along the direction of the 1D fibers regardless of fiber density; however, MSC arrangement on 2D fibers was only observed on high-density fibers. Cell to cell communication was

increased in MSCs on 1D fibers, compared to PCL film and decreased on 2D fibers, compared to PCL film. An increase in osteogenic genes expression was observed in the 1D group in comparison to 2D and TCP (tissue culture plate) groups. The 2D group only showed an increase in RUNX2 compared to TCP controls. Alignment of MSCs was controlled by fiber density and orientation. The greatest cell alignment was observed on low-density 1D and high-density 2D fibers. This study showed that cell to cell communication and osteogenesis were influenced by MSC alignment and fiber orientation; osteogenesis was increased in MSCs on 1D fibers [115].

There are an increasing number of scaffolds being manufactured to mimic native tendon structure and mechanical properties using a multi-layered, braided, or weaving approach. Omi *et al.* manufactured a multilayered scaffold in a rat tendon model. The three experimental groups were no augmentation, scaffold only implantation, and seeded-scaffold implantation. Results showed increased healing strength and stiffness after 6 weeks of the MSC-seeded scaffold after rotator cuff injury [149]. Rothrauff *et al.* compared scaffolds that were stacked or braided to promote tenogenesis. Braided scaffolds showed enhanced tensile and suture retention, but a reduction in moduli. Both scaffolds showed expression of tendon-related markers; however, braided scaffolds showed a greater increase. Stacked scaffolds were superior in cell infiltration, cell number, collagen and GAG production. This study highlights the importance of macroarchitecture in scaffold development [150]. Younesi *et al.* used electrophoretic compaction with macromolecular alignment to manufacture collagen threads for the study of MSCs towards tenogenesis. Aligned fibers promoted MSC gene expression and matrix production of tendon-related proteins compared to fibers of random orientation. MSC-seeded woven scaffolds may

potentially be used for functional repair [151]. Lastly, electrospinning and cell sheet technologies combined low density PCL fibers with sheep MSCs organization into a sheet of cells and were braided (3) for a tissue engineered ligament construct (TELC) [152].

Fiber Modifications

Additional modifications including ECM coating, micropatterning, and bioprinting can be incorporated onto fibers to promote cell responses. Chainani *et al.* manufactured multilayered PCL electrospun scaffolds to compare adipose stem cell (ASC) response of fibers treated with tendon-derived ECM (TDM), fibronectin, and PBS. Protein production, marker expression, and mechanical properties were analyzed. Results showed that TDM scaffolds promoted the greatest collagen content. Gene expression, s-GAG (sulfated-GAG), and cell proliferation increased over time, but was not effected by fiber coating. Young's modulus did not increase over time, but yield strain increased. The authors concluded that multilayered fibrous scaffolds enhanced tenogenic differentiation of ASCs and that TDM may contribute to differentiation in specific ways [153]. Alshomer *et al.* manufactured scaffolds of micropatterned POSS-PCU (polyhedral oligomeric silsesquioxane poly (carbonate-urea) urethane with a phosphate glass fiber template. The scaffolds supported tenocyte growth, alignment, and increased levels of tendon ECM proteins compared to flat substrates [154]. Ker *et al.* used growth factor bioprinting to promote cell alignment and differentiation of mouse myoblasts and mesenchymal fibroblasts. Submicron fibers patterned with FGF2 promoted tendon differentiation, BMP-2 promoted osteogenic differentiation, and unpatterned fibers promoted myogenic differentiation [155].

Biomechanical Functions and Crosslinking

Scaffolds have been designed to mimic not only the native organization of tendon, but also the specific structural characteristics. Scaffolds have been fabricated to mimic collagen fiber behavior and ECM proteoglycans necessary in development and repair *in vivo* [156]. Chen *et al.* manufactured an electrospun poly (L-lactide-co-acryloyl carbonate) scaffold with post-processing tensile modulus and crimp stability compared to non cross-linked polymer and supported fibroblast growth [157]. In another study, Banik *et al.* manufactured a multilayered PLA scaffold in a "chinese-fingertrap" design mimicking the non-linear behavior of tendon. These crisscrossed fibers showed a toe and linear elastic region characteristic of tendon mechanical properties and preliminary data with cell adhesion and growth [158]. Mimetic collagen and collagen/nano-carbon fibers were gel-spun and tested under dry and wet state ensile testing with properties comparable to native tendon [159]. Bansal *et al.* developed a PCL scaffold of aligned fibers with interspersed non-aligned patches to mimic meniscus architecture and study fiber response to strain. The tensile properties changed as the ratio of aligned to non-aligned fibers were adjusted. Mechanical function loss was less in "torn" scaffolds with a higher ratio of nonaligned fibers compared to those comprised of aligned fibers. Composite scaffolds showed an increase in strain in areas surrounding the defect. The authors concluded that non-aligned organization can improve mechanical properties by strain distribution [160].

Crosslinking or fusion of fibers has been used to strengthen mechanical properties of the scaffolds. Zhong *et al.* designed aligned nanofiber collagen scaffolds cross-linked with glutaraldehyde vapor to compare to randomly oriented scaffolds. Fibroblasts showed lower cell adhesion and higher proliferation, cell orientation, and cell interaction on

aligned fibers compared to random fibers [161]. In another study, Yang *et al.* developed a biomimetic scaffold of PCL and mGLT (methacrylated gelatin) to mimic physical and biochemical properties of native tendon. Photocrosslinking maintained mechanical strength, construction of multilayered scaffolds, and cells responded to topographical and biochemical cues. This scaffold could potentially be used as a tendon graft due to its architecture and cell phenotype [162]. Nordihydroguaiaretic acid in another method used for crosslinking collagen fibers that supported cell adhesion, spreading, and migration even after an initial decrease [163].

Combinatorial Effects

Several studies have investigated MSC differentiation on fibers in combination with environmental factors including growth factors, oxygen tension, and mechanical stimulation. Leung at al. investigated MSC differentiation an aligned, chitosan-PCL fibrous scaffold in media supplemented with TGF-β3. MSCs showed an elongated morphology along nanofibers, upregulated gene expression by day 5, and increased production of collagen by day 10 compared to controls. Combining these factors resulted in increased efficiency of MSC differentiation [164]. Subramony *et al.* investigated the combination of alignment and mechanical stimulation on MSC differentiation. Loaded aligned and loaded unaligned fibers promoted an increase in MSC production of collagen compared to MSCs on unloaded fibers at day 28. Increased gene expression of *scx*, *tnc*, *col III*, and fibronectin were increased in MSCs on aligned loaded fibers compared to aligned unloaded fibers. These two factors alone resulted in MSC differentiation [120]. Studies rarely compare a 2D model to a 3D model. In an electrospinning studies, chitosan-PCL coated fibers were compared to MSC behavior on chitosan-PCL film and

TCPS (tissue culture polystyrene). Results showed increased adhesion, gene expression, and collagen production on fibers, particularly aligned fibers, versus the coated film and TCPS [119]. Knowing the combination of factors that are most influential to tenogenesis will contribute to the development of new treatments.

Composite, Hybrid, and Functional Fibrous Scaffolds

Studies have examined the effects of incorporating spun nanofibers with composite hydrogels. Park *et al.* manufactured a hybrid scaffold of aligned and random fibers for *in vitro* and *in vivo* applications. The upper aligned fiber layers provided topographic guidance and the lower random fiber layers functioned in mechanical support. The density of the upper aligned fibers determined cell alignment and differentiation. High-density fibers promoted aligned myotubules more efficiently than low-density aligned fibers. Characterization showed high porosity and stability for manipulation and modification to a multilayered scaffold [165].

Functional scaffolds have been manufactured to incorporate alternatives including magnetic particles (MNPs) and growth factors. Gonclaves *et al.* developed aligned magnetic polymer scaffolds. Iron oxide was incorporated in MNPs into starch and PCL fibers by rapid prototyping. ASCs synthesized tendon-associated matrix proteins. The scaffolds showed biocompatibility and integration upon implantation in a rat model and used magnetic stimulation for regeneration [166]. Cheng *et al.* developed a collagen-nanoparticle scaffold that released PDGF to promote tenogenesis. The scaffold functioned to control ASCs via topographical cues and release of PDGF from nanoparticles. Alignment induced increased gene expression of *tnmd* and *scx*. Evidence suggests that this technique may be useful in tissue engineering and regeneration [167].

Sahoo *et al.* developed a bioactive scaffold for MSC differentiation. A blend, with bFGF coating, released over a week induced proliferation, gene expression, and matrix production associated with tendon repair. Results provided evidence of decreased multipotency and increased tenogenesis [168].

Webb *et al.* developed a synthetic polymer for tendon repair in a rat model. Poly (3-hydroxybutyrate-co-3-hydroxyhexanoate) (PHBHHx) tubes and fibers were tested for biomechanical properties. Collagen gels were reinforced with fibers and inserted into the tubes to for completion of the scaffold. Mechanical properties of the scaffolds were comparable to rat tendon and implantation of PHBHHx-collagen-tenocyte scaffolds showed increased function compared to the control, PHBHHx, and PHBHHx-collagen groups. These scaffolds promoted tissue remodeling and cellular alignment [169]. Deepthi *et al.* developed a scaffold combining a collagen-chitosan hydrogel with PLLA fibers, rolled the membrane, and coated it with and without alginate. Both scaffolds showed cell proliferation, adhesion, and spreading [170]. Manning *et al.* developed a construct of heparin/fibrin hydrogel containing PDGF and electrospun PLGA fibers for tendon repair. The layered (11alternating layers) scaffold maintained cell viability and PDGF release *in vitro* and maintained ASCs at the repair site 9 days post-operatively in a flexor tendon canine model [171]. Combining materials may provide the optimal conditions for biocompatibility and mechanical properties.

Implantable Scaffolds

Many scaffolds have been designed for *in vivo* implantation. Bhaskar *et al.* developed an implantable construct of electrospun PCL fibers for use as a tendon graft in tissue regeneration. The authors compared gamma irradiation sterilization and ethanol for

sterilization and small-scale and large-scale production of scaffolds. Large-scale production of electrospun scaffolds, sterilized in ethanol, may be a potential alternative to autografts [172]. As an alternative, engineered niche matrices were used to mimic the native tendon microenvironment for cell delivery [173]. Implantation of the niche matrix into a rat rotator cuff injury model showed improved mechanical properties and tissue morphology. Electrospun PCL grafts for tendon repair showed that ethanol submersion can be used for scaffold sterilization and large scale manufacturing of scaffolds, producing similar results of small-scale scaffolds and autografts. This study provides evidence of a potential alternative to autografts in tendon healing [172].

Future Research Directions

Cellular fibrous scaffolds have been studied extensively *in vitro* and *in vivo* for studying cell behaviors; cell adhesion, migration, proliferation, differentiation, and maintenance of phenotype. Scaffold properties include cell infiltration and biocompatible implantation including scale-up, mechanical properties, functionality, and long-term effects. Scaffolds of various manufacturing techniques, polymers, orientations, diameters, lengths, densities, architectural manipulations, modifications, composites, and hybrids have successfully demonstrated the cell behaviors listed above. The addition of biochemical and biomechanical stimulation has also provided insight into cell behavior and tissue healing. While many factors have been considered in such studies, limitations in our depth of understanding and translation of these findings still exist. Studies that utilize and characterize engineered scaffolds often fail to delve into the underlying molecular mechanisms of MSC-matrix interactions and long-term MSC response *in vivo*. In addition, studies that aim to understand the complex, underlying mechanisms of MSCs

often focus on one or two parameters of design and characterization of scaffolds towards mimicry of native tissue. The next chapter introduces a study that used a novel spinning technique for manufacturing nanofibers to study MSC response to topographical cues towards tenogenesis. Studies incorporating the aspects of engineered scaffolds, molecular biology, and medicine will be most effective in development of cellular scaffolds for understanding tendon repair and development of stem cell therapies.

References

1. Patterson-Kane JC, Firth EC. The pathobiology of exercise-induced superficial digital flexor tendon injury in Thoroughbred racehorses. The Veterinary Journal 2009;181(2):79-89.
2. Weinstein SI, Yelin, Edward H., and Watkins-Castillo, Sylvia I. Bone and Joint Burden. The Burden of Musculoskeletal Diseases in the United States; 2013-2017.
3. Maffulli N, Wong J, Almekinders LC. Types and epidemiology of tendinopathy. Clinics in sports medicine 2003;22(4):675-692.
4. Guly H. Diagnostic errors in an accident and emergency department. Emergency Medicine Journal 2001;18(4):263-269.
5. Kricun R, Kricun M, Arangio G, Salzman G, Berman A. Patellar tendon rupture with underlying systemic disease. American Journal of Roentgenology 1980;135(4):803-807.
6. Rees J, Wilson A, Wolman R. Current concepts in the management of tendon disorders. Rheumatology 2006;45(5):508-521.
7. Eloy‐Trinquet S, Wang H, Edom‐Vovard F, Duprez D. Fgf signaling components are associated with muscles and tendons during limb development. Developmental Dynamics 2009;238(5):1195-1206.
8. Brent AE, Schweitzer R, Tabin CJ. A somitic compartment of tendon progenitors. Cell 2003;113(2):235-248.
9. ten Berge D, Brugmann SA, Helms JA, Nusse R. Wnt and FGF signals interact to coordinate growth with cell fate specification during limb development. Development 2008;135(19):3247-3257.
10. Kuo CK, Petersen BC, Tuan RS. Spatiotemporal protein distribution of TGF‐βs, their receptors, and extracellular matrix molecules during embryonic tendon development. Developmental Dynamics 2008;237(5):1477-1489.
11. Silver FH, Freeman JW, Seehra GP. Collagen self-assembly and the development of tendon mechanical properties. Journal of biomechanics 2003;36(10):1529-1553.
12. Huang AH, Lu HH, Schweitzer R. Molecular regulation of tendon cell fate during development. Journal of Orthopaedic Research 2015;33(6):800-812.
13. Johnston JM, Connizzo BK, Shetye SS, Robinson KA, Huegel J, Rodriguez AB, Sun M, Adams SM, Birk DE, Soslowsky LJ. Collagen V haploinsufficiency in a murine model of classic Ehlers–Danlos syndrome is associated with deficient structural and mechanical healing in tendons. Journal of Orthopaedic Research 2017.
14. Patterson-Kane J, Becker D, Rich T. The pathogenesis of tendon microdamage in athletes: the horse as a natural model for basic cellular research. Journal of comparative pathology 2012;147(2):227-247.
15. Ippolito E, Natali PG, Postacchini F, Accinni L, De Martino C. Morphological, immunochemical, and biochemical study of rabbit achilles tendon at various ages. J Bone Joint Surg Am 1980;62(4):583-598.

16. Schweitzer R, Chyung JH, Murtaugh LC, Brent AE, Rosen V, Olson EN, Lassar A, Tabin CJ. Analysis of the tendon cell fate using Scleraxis, a specific marker for tendons and ligaments. Development 2001;128(19):3855-3866.
17. Murchison ND, Price BA, Conner DA, Keene DR, Olson EN, Tabin CJ, Schweitzer R. Regulation of tendon differentiation by scleraxis distinguishes force-transmitting tendons from muscle-anchoring tendons. Development 2007;134(14):2697-2708.
18. Espira L, Lamoureux L, Jones SC, Gerard RD, Dixon IMC, Czubryt MP. The basic helix–loop–helix transcription factor scleraxis regulates fibroblast collagen synthesis. Journal of Molecular and Cellular Cardiology 2009;47(2):188-195.
19. Ito Y, Toriuchi N, Yoshitaka T, Ueno-Kudoh H, Sato T, Yokoyama S, Nishida K, Akimoto T, Takahashi M, Miyaki S and others. The Mohawk homeobox gene is a critical regulator of tendon differentiation. Proceedings of the National Academy of Sciences of the United States of America 2010;107(23):10538-10542.
20. Bi Y, Ehirchiou D, Kilts TM, Inkson CA, Embree MC, Sonoyama W, Li L, Leet AI, Seo B-M, Zhang L. Identification of tendon stem/progenitor cells and the role of the extracellular matrix in their niche. Nature medicine 2007;13(10):1219-1227.
21. Pryce BA, Watson SS, Murchison ND, Staverosky JA, Dünker N, Schweitzer R. Recruitment and maintenance of tendon progenitors by TGFβ signaling are essential for tendon formation. Development 2009;136(8):1351-1361.
22. Lavagnino M, Wall ME, Little D, Banes AJ, Guilak F, Arnoczky SP. Tendon mechanobiology: Current knowledge and future research opportunities. Journal of Orthopaedic Research 2015;33(6):813-822.
23. Ryan CN, Sorushanova A, Lomas AJ, Mullen AM, Pandit A, Zeugolis DI. Glycosaminoglycans in tendon physiology, pathophysiology, and therapy. Bioconjugate chemistry 2015;26(7):1237-1251.
24. Kazam E, Iozzo RV, Birk DE, Soslowsky LJ. Influence of decorin and biglycan on mechanical properties of multiple tendons in knockout mice. 2005.
25. Reed CC, Iozzo RV. The role of decorin in collagen fibrillogenesis and skin homeostasis. Glycoconjugate journal 2002;19(4):249-255.
26. Young MF, Bi Y, Ameye L, Chen X-D. Biglycan knockout mice: new models for musculoskeletal diseases. Glycoconjugate journal 2002;19(4):257-262.
27. Docheva D, Hunziker EB, Fässler R, Brandau O. Tenomodulin is necessary for tenocyte proliferation and tendon maturation. Molecular and cellular biology 2005;25(2):699-705.
28. Hauser RA, Dolan EE. Ligament injury and healing: an overview of current clinical concepts. Journal of Prolotherapy 2011;3(4):836-846.
29. Sharma P, Maffulli N. Tendon injury and tendinopathy: healing and repair. The Journal of Bone & Joint Surgery 2005;87(1):187-202.
30. Sharma P, Maffulli N. Basic biology of tendon injury and healing. The surgeon 2005;3(5):309-316.
31. Selvanetti A, Cipolla M, Puddu G. Overuse tendon injuries: basic science and classification. Operative Techniques in Sports Medicine 1997;5(3):110-117.

32. Birch HL, Bailey A, Goodship A. Macroscopic 'degeneration'of equine superficial digital flexor tendon is accompanied by a change in extracellular matrix composition. Equine veterinary journal 1998;30(6):534-539.
33. Arnoczky SP, Lavagnino M, Egerbacher M. The mechanobiological aetiopathogenesis of tendinopathy: is it the over‐stimulation or the under‐stimulation of tendon cells? International journal of experimental pathology 2007;88(4):217-226.
34. Lin TW, Cardenas L, Soslowsky LJ. Biomechanics of tendon injury and repair. Journal of biomechanics 2004;37(6):865-877.
35. Voleti PB, Buckley MR, Soslowsky LJ. Tendon healing: repair and regeneration. Annual review of biomedical engineering 2012;14:47-71.
36. Yang G, Rothrauff BB, Tuan RS. Tendon and ligament regeneration and repair: clinical relevance and developmental paradigm. Birth Defects Research Part C: Embryo Today: Reviews 2013;99(3):203-222.
37. Goh K, Holmes D, Lu H-Y, Richardson S, Kadler K, Purslow P, Wess TJ. Ageing changes in the tensile properties of tendons: influence of collagen fibril volume fraction. Journal of biomechanical engineering 2008;130(2):021011.
38. Ralphs J, Waggett A, Benjamin M. Actin stress fibres and cell–cell adhesion molecules in tendons: organisation in vivo and response to mechanical loading of tendon cells in vitro. Matrix Biology 2002;21(1):67-74.
39. Robbins JR, Evanko SP, Vogel KG. Mechanical loading and TGF-β regulate proteoglycan synthesis in tendon. Archives of biochemistry and biophysics 1997;342(2):203-211.
40. Eliasson P, Andersson T, Aspenberg P. Rat Achilles tendon healing: mechanical loading and gene expression. Journal of applied physiology 2009;107(2):399-407.
41. Arnoczky SP, Tian T, Lavagnino M, Gardner K, Schuler P, Morse P. Activation of stress‐activated protein kinases (SAPK) in tendon cells following cyclic strain: the effects of strain frequency, strain magnitude, and cytosolic calcium. Journal of orthopaedic research 2002;20(5):947-952.
42. Wang T, Ni M, Thien C, Wang A, Zheng M. Induction of tendon stem cells toward tenogenic differentiation and tendon formation by uniaxial mechanical loadings without growth factors. Journal of Science and Medicine in Sport 2017;20:e114.
43. Gaspar D, Pandit A, Zeugolis D. Tenogenic phenotype maintenance and differentiation using macromolecular crowding and mechanical loading. Bone Joint J 2017;99(SUPP 1):39-39.
44. Kaux JF, Drion P, Libertiaux V, Colige A, Hoffmann A, Nusgens B, Besançon B, Forthomme B, Le Goff C, Franzen R. Eccentric training improves tendon biomechanical properties: a rat model. Journal of Orthopaedic Research 2013;31(1):119-124.
45. Nilsson-Helander K, Silbernagel KG, Thomeé R, Faxén E, Olsson N, Eriksson BI, Karlsson J. Acute Achilles tendon rupture: a randomized, controlled study comparing surgical and nonsurgical treatments using validated outcome measures. The American journal of sports medicine 2010;38(11):2186-2193.

46. Santos ML, Rodrigues MT, Domingues RM, Reis RL, Gomes ME. Biomaterials as Tendon and Ligament Substitutes: Current Developments. Regenerative Strategies for the Treatment of Knee Joint Disabilities: Springer; 2017. p 349-371.
47. Kohler J, Popov C, Klotz B, Alberton P, Prall WC, Haasters F, Müller‐Deubert S, Ebert R, Klein‐Hitpass L, Jakob F. Uncovering the cellular and molecular changes in tendon stem/progenitor cells attributed to tendon aging and degeneration. Aging cell 2013;12(6):988-999.
48. Friedenstein A, Latzinik N, Gorskaya U, Sidorovich S. Radiosensitivity and postirradiation changes of bone marrow clonogenic stromal mechanocytes. International Journal of Radiation Biology and Related Studies in Physics, Chemistry and Medicine 1981;39(5):537-546.
49. Friedenstein A, Latzinik N, Grosheva A, Gorskaya U. Marrow microenvironment transfer by heterotopic transplantation of freshly isolated and cultured cells in porous sponges. Experimental hematology 1982;10(2):217-227.
50. Caplan AI. Mesenchymal stem cells. Journal of orthopaedic research 1991;9(5):641-650.
51. Cigognini D, Lomas A, Kumar P, Satyam A, English A, Azeem A, Pandit A, Zeugolis D. Engineering in vitro microenvironments for cell based therapies and drug discovery. Drug discovery today 2013;18(21):1099-1108.
52. Dominici M, Le Blanc K, Mueller I, Slaper-Cortenbach I, Marini F, Krause D, Deans R, Keating A, Prockop D, Horwitz E. Minimal criteria for defining multipotent mesenchymal stromal cells. The International Society for Cellular Therapy position statement. cytotherapy 2006;8(4):315-317.
53. Goldring K, Partridge T, Watt D. Muscle stem cells. The Journal of pathology 2002;197(4):457-467.
54. Messina E, De Angelis L, Frati G, Morrone S, Chimenti S, Fiordaliso F, Salio M, Battaglia M, Latronico MV, Coletta M. Isolation and expansion of adult cardiac stem cells from human and murine heart. Circulation research 2004.
55. Thored P, Arvidsson A, Cacci E, Ahlenius H, Kallur T, Darsalia V, Ekdahl CT, Kokaia Z, Lindvall O. Persistent production of neurons from adult brain stem cells during recovery after stroke. Stem cells 2006;24(3):739-747.
56. Metallo CM, Mohr JC, Detzel CJ, de Pablo JJ, Van Wie BJ, Palecek SP. Engineering the stem cell microenvironment. Biotechnology Progress 2007;23(1):18-23.
57. Mao AS, Shin J-W, Mooney DJ. Effects of substrate stiffness and cell-cell contact on mesenchymal stem cell differentiation. Biomaterials 2016;98:184-191.
58. Sonam S, Sathe SR, Yim EK, Sheetz MP, Lim CT. Cell contractility arising from topography and shear flow determines human mesenchymal stem cell fate. Scientific reports 2016;6.
59. Li Y, Ramcharan M, Zhou Z, Leong DJ, Akinbiyi T, Majeska RJ, Sun HB. The role of scleraxis in fate determination of mesenchymal stem cells for tenocyte differentiation. Scientific reports 2015;5:13149.

60. Caplan A. Why are MSCs therapeutic? New data: new insight. The Journal of pathology 2009;217(2):318-324.
61. Hoogduijn MJ, Popp F, Verbeek R, Masoodi M, Nicolaou A, Baan C, Dahlke M-H. The immunomodulatory properties of mesenchymal stem cells and their use for immunotherapy. International immunopharmacology 2010;10(12):1496-1500.
62. Harjanto D, Zaman MH. Modeling extracellular matrix reorganization in 3D environments. PloS one 2013;8(1):e52509.
63. Voog J, Jones DL. Stem cells and the niche: a dynamic duo. Cell stem cell 2010;6(2):103-115.
64. Scadden DT. The stem-cell niche as an entity of action. Nature 2006;441(7097):1075.
65. Grayson WL, Zhao F, Izadpanah R, Bunnell B, Ma T. Effects of hypoxia on human mesenchymal stem cell expansion and plasticity in 3D constructs. Journal of cellular physiology 2006;207(2):331-339.
66. Méndez-Ferrer S, Michurina TV, Ferraro F, Mazloom AR, MacArthur BD, Lira SA, Scadden DT, Ma'ayan A, Enikolopov GN, Frenette PS. Mesenchymal and haematopoietic stem cells form a unique bone marrow niche. nature 2010;466(7308):829-834.
67. Rockenstein E, Masliah E, Peterson KL, Stallcup WB, Chen J, Evans SM. Pericytes of Multiple Organs Do Not Behave as Mesenchymal Stem Cells In Vivo. Cell Stem Cell 2017;20:1-15.
68. Marturano JE, Arena JD, Schiller ZA, Georgakoudi I, Kuo CK. Characterization of mechanical and biochemical properties of developing embryonic tendon. Proceedings of the National Academy of Sciences of the United States of America 2013;110(16):6370-6375.
69. Miranti CK, Brugge JS. Sensing the environment: a historical perspective on integrin signal transduction. Nature cell biology 2002;4(4):E83-E90.
70. Haraldsson BT, Aagaard P, Krogsgaard M, Alkjaer T, Kjaer M, Magnusson SP. Region-specific mechanical properties of the human patella tendon. Journal of applied physiology 2005;98(3):1006-1012.
71. Rigozzi S, Müller R, Snedeker J. Local strain measurement reveals a varied regional dependence of tensile tendon mechanics on glycosaminoglycan content. Journal of biomechanics 2009;42(10):1547-1552.
72. Docheva D, Popov C, Alberton P, Aszodi A. Integrin signaling in skeletal development and function. Birth Defects Research Part C: Embryo Today: Reviews 2014;102(1):13-36.
73. Elosegui-Artola A, Oria R, Chen Y, Kosmalska A, Pérez-González C, Castro N, Zhu C, Trepat X, Roca-Cusachs P. Mechanical regulation of a molecular clutch defines force transmission and transduction in response to matrix rigidity. Nature cell biology 2016;18(5):540-548.
74. Gardner K, Arnoczky SP, Lavagnino M. Effect of in vitro stress‐deprivation and cyclic loading on the length of tendon cell cilia in situ. Journal of Orthopaedic Research 2011;29(4):582-587.

75. Grier W, Moy A, Harley B. Cyclic tensile strain enhances human mesenchymal stem cell Smad 2/3 activation and tenogenic differentiation in anisotropic collagen-glycosaminoglycan scaffolds. European cells & materials 2017;33:227-239.
76. Harjanto D, Zaman M. 7.7 Biophysics of Three-Dimensional Cell Motility.
77. Friedl P, Wolf K. Plasticity of cell migration: a multiscale tuning model. The Journal of cell biology 2009:jcb. 200909003.
78. Ridley AJ, Schwartz MA, Burridge K, Firtel RA, Ginsberg MH, Borisy G, Parsons JT, Horwitz AR. Cell migration: integrating signals from front to back. Science 2003;302(5651):1704-1709.
79. Fackler OT, Grosse R. Cell motility through plasma membrane blebbing. The Journal of cell biology 2008;181(6):879-884.
80. Reymond N, d'Agua BB, Ridley AJ. Crossing the endothelial barrier during metastasis. Nature Reviews Cancer 2013;13(12):858-870.
81. Paul CD, Mistriotis P, Konstantopoulos K. Cancer cell motility: lessons from migration in confined spaces. Nature Reviews Cancer 2016.
82. Wolf K, Te Lindert M, Krause M, Alexander S, Te Riet J, Willis AL, Hoffman RM, Figdor CG, Weiss SJ, Friedl P. Physical limits of cell migration: control by ECM space and nuclear deformation and tuning by proteolysis and traction force. J Cell Biol 2013;201(7):1069-1084.
83. Page-McCaw A, Ewald AJ, Werb Z. Matrix metalloproteinases and the regulation of tissue remodelling. Nature reviews Molecular cell biology 2007;8(3):221-233.
84. Wyckoff JB, Pinner SE, Gschmeissner S, Condeelis JS, Sahai E. ROCK-and myosin-dependent matrix deformation enables protease-independent tumor-cell invasion in vivo. Current Biology 2006;16(15):1515-1523.
85. Stroka KM, Jiang H, Chen S-H, Tong Z, Wirtz D, Sun SX, Konstantopoulos K. Water permeation drives tumor cell migration in confined microenvironments. Cell 2014;157(3):611-623.
86. Justin RT, Engler AJ. Stiffness gradients mimicking in vivo tissue variation regulate mesenchymal stem cell fate. PloS one 2011;6(1):e15978.
87. Murphy CM, O'Brien FJ. Understanding the effect of mean pore size on cell activity in collagen-glycosaminoglycan scaffolds. Cell adhesion & migration 2010;4(3):377-381.
88. Junkin M, Wong PK. Probing cell migration in confined environments by plasma lithography. Biomaterials 2011;32(7):1848-1855.
89. Doyle AD, Petrie RJ, Kutys ML, Yamada KM. Dimensions in cell migration. Current opinion in cell biology 2013;25(5):642-649.
90. Hanein D, Horwitz AR. The structure of cell–matrix adhesions: the new frontier. Current opinion in cell biology 2012;24(1):134-140.
91. Changede R, Xu X, Margadant F, Sheetz MP. Nascent integrin adhesions form on all matrix rigidities after integrin activation. Developmental cell 2015;35(5):614-621.
92. Hernández-Varas P, Berge U, Lock JG, Strömblad S. A plastic relationship between vinculin-mediated tension and adhesion complex area defines adhesion size and lifetime. Nature communications 2015;6.

93. Skau CT, Plotnikov SV, Doyle AD, Waterman CM. Inverted formin 2 in focal adhesions promotes dorsal stress fiber and fibrillar adhesion formation to drive extracellular matrix assembly. Proceedings of the National Academy of Sciences 2015;112(19):E2447-E2456.
94. He L, Chen W, Wu P-H, Jimenez A, Wong BS, San A, Konstantopoulos K, Wirtz D. Local 3D matrix confinement determines division axis through cell shape. Oncotarget 2016;7(6):6994.
95. Kulangara K, Yang Y, Yang J, Leong KW. Nanotopography as modulator of human mesenchymal stem cell function. Biomaterials 2012;33(20):4998-5003.
96. del Rio A, Perez-Jimenez R, Liu R, Roca-Cusachs P, Fernandez JM, Sheetz MP. Stretching single talin rod molecules activates vinculin binding. Science 2009;323(5914):638-641.
97. Huang C, Rajfur Z, Yousefi N, Chen Z, Jacobson K, Ginsberg MH. Talin Phosphorylation by Cdk5 regulates Smurf1-mediated talin head ubiquitination and cell migration. Nature cell biology 2009;11(5):624.
98. Bachir AI, Zareno J, Moissoglu K, Plow EF, Gratton E, Horwitz AR. Integrin-associated complexes form hierarchically with variable stoichiometry in nascent adhesions. Current Biology 2014;24(16):1845-1853.
99. Tojkander S, Gateva G, Lappalainen P. Actin stress fibers–assembly, dynamics and biological roles. J Cell Sci 2012;125(8):1855-1864.
100. Kubow KE, Conrad SK, Horwitz AR. Matrix microarchitecture and myosin II determine adhesion in 3D matrices. Current Biology 2013;23(17):1607-1619.
101. Hung W-C, Yang JR, Yankaskas CL, Wong BS, Wu P-H, Pardo-Pastor C, Serra SA, Chiang M-J, Gu Z, Wirtz D. Confinement sensing and signal optimization via Piezo1/PKA and Myosin II pathways. Cell reports 2016;15(7):1430-1441.
102. Engler AJ, Sen S, Sweeney HL, Discher DE. Matrix elasticity directs stem cell lineage specification. Cell 2006;126(4):677-689.
103. Paul CD, Shea DJ, Mahoney MR, Chai A, Laney V, Hung W-C, Konstantopoulos K. Interplay of the physical microenvironment, contact guidance, and intracellular signaling in cell decision making. The FASEB Journal 2016;30(6):2161-2170.
104. Chen L, Vicente-Manzanares M, Potvin-Trottier L, Wiseman PW, Horwitz AR. The integrin-ligand interaction regulates adhesion and migration through a molecular clutch. PLoS One 2012;7(7):e40202.
105. Giannone G, Mège R-M, Thoumine O. Multi-level molecular clutches in motile cell processes. Trends in cell biology 2009;19(9):475-486.
106. Fraley SI, Wu P-h, He L, Feng Y, Krisnamurthy R, Longmore GD, Wirtz D. Three-dimensional matrix fiber alignment modulates cell migration and MT1-MMP utility by spatially and temporally directing protrusions. Scientific reports 2015;5:14580.
107. Langer R. I ARTICLES. Science 1993;260:5110.
108. Carvalho JL, de Goes AM, Gomes DA, de Carvalho PH. Innovative Strategies for Tissue Engineering: INTECH Open Access Publisher; 2013.

109. Stewart AA, Barrett JG, Byron CR, Yates AC, Durgarn SS, Evans RB, Stewart MC. Comparison of equine tendon-, muscle-, and bone marrow-derived cells cultured on tendon matrix. American Journal of Veterinary Research 2009;70(6):750-757.
110. Uysal AC, Mizuno H. Differentiation of adipose-derived stem cells for tendon repair. Adipose-derived stem cells: Methods and Protocols 2011:443-451.
111. Lui P, Rui Y, Ni M, Chan K. Tenogenic differentiation of stem cells for tendon repair—what is the current evidence? Journal of tissue engineering and regenerative medicine 2011;5(8).
112. Hortensius RA, Harley BA. The use of bioinspired alterations in the glycosaminoglycan content of collagen–GAG scaffolds to regulate cell activity. Biomaterials 2013;34(31):7645-7652.
113. Caliari S, Weisgerber D, Hortensius R, Mozdzen L, Kelkhoff D, Harley B. Patterning biochemical and structural cues in collagen-GAG scaffolds to drive mesenchymal stem cell differentiation for tendon insertion regeneration. 2012. WILEY-BLACKWELL 111 RIVER ST, HOBOKEN 07030-5774, NJ USA. p 50-51.
114. Baker SC, Atkin N, Gunning PA, Granville N, Wilson K, Wilson D, Southgate J. Characterisation of electrospun polystyrene scaffolds for three-dimensional in vitro biological studies. Biomaterials 2006;27(16):3136-3146.
115. Chang J-C, Fujita S, Tonami H, Kato K, Iwata H, Hsu S-h. Cell orientation and regulation of cell–cell communication in human mesenchymal stem cells on different patterns of electrospun fibers. Biomedical Materials 2013;8(5):055002.
116. Kahn CJ, Dumas D, Arab-Tehrany E, Marie V, Tran N, Wang X, Cleymand F. Structural and mechanical multi-scale characterization of white New-Zealand rabbit Achilles tendon. Journal of the mechanical behavior of biomedical materials 2013;26:81-89.
117. Czaplewski SK, Tsai T-L, Duenwald-Kuehl SE, Vanderby R, Li W-J. Tenogenic differentiation of human induced pluripotent stem cell-derived mesenchymal stem cells dictated by properties of braided submicron fibrous scaffolds. Biomaterials 2014;35(25):6907-6917.
118. Andalib MN, Lee JS, Ha L, Dzenis Y, Lim JY. The role of RhoA kinase (ROCK) in cell alignment on nanofibers. Acta biomaterialia 2013;9(8):7737-7745.
119. Leung M, Jana S, Tsao C-T, Zhang M. Tenogenic differentiation of human bone marrow stem cells via a combinatory effect of aligned chitosan–poly-caprolactone nanofibers and TGF-β3. Journal of Materials Chemistry B 2013;1(47):6516-6524.
120. Subramony SD, Dargis BR, Castillo M, Azeloglu EU, Tracey MS, Su A, Lu HH. The guidance of stem cell differentiation by substrate alignment and mechanical stimulation. Biomaterials 2013;34(8):1942-1953.
121. Yin Z, Chen X, Chen JL, Shen WL, Nguyen TMH, Gao L, Ouyang HW. The regulation of tendon stem cell differentiation by the alignment of nanofibers. Biomaterials 2010;31(8):2163-2175.
122. Järvinen TA, Kannus P, Paavola M, Järvinen TL, Józsa L, Järvinen M. Achilles tendon injuries. Current opinion in rheumatology 2001;13(2):150-155.

123. Dowling B, Dart A, Hodgson D, Smith R. Superficial digital flexor tendonitis in the horse. Equine veterinary journal 2000;32(5):369-378.
124. Durgam SS, Stewart AA, Sivaguru M, Wagoner Johnson AJ, Stewart MC. Tendon‐derived progenitor cells improve healing of collagenase‐induced flexor tendinitis. Journal of Orthopaedic Research 2016;34(12):2162-2171.
125. González JC, López C, Álvarez ME, Pérez JE, Carmona JU. Autologous leukocyte-reduced platelet-rich plasma therapy for Achilles tendinopathy induced by collagenase in a rabbit model. Scientific reports 2016;6.
126. Luan T, Liu X, Easley JT, Ravishankar B, Puttlitz C, Feeley BT. Muscle atrophy and fatty infiltration after an acute rotator cuff repair in a sheep model. Muscles, ligaments and tendons journal 2015;5(2):106.
127. Shou K, Huang Y, Qi B, Hu X, Ma Z, Lu A, Jian C, Zhang L, Yu A. Induction of mesenchymal stem cell differentiation in the absence of soluble inducer for cutaneous wound regeneration by a chitin nanofibers‐based hydrogel. Journal of Tissue Engineering and Regenerative Medicine 2017.
128. Prosecká E, Rampichová M, Litvinec A, Tonar Z, Králíčková M, Vojtova L, Kochova P, Plencner M, Buzgo M, Míčková A. Collagen/hydroxyapatite scaffold enriched with polycaprolactone nanofibers, thrombocyte‐rich solution and mesenchymal stem cells promotes regeneration in large bone defect in vivo. Journal of Biomedical Materials Research Part A 2015;103(2):671-682.
129. Venugopal J, Rajeswari R, Shayanti M, Low S, Bongso A, R. Giri Dev V, Deepika G, Choon AT, Ramakrishna S. Electrosprayed hydroxyapatite on polymer nanofibers to differentiate mesenchymal stem cells to osteogenesis. Journal of Biomaterials Science, Polymer Edition 2013;24(2):170-184.
130. Lai G-J, Shalumon K, Chen S-H, Chen J-P. Composite chitosan/silk fibroin nanofibers for modulation of osteogenic differentiation and proliferation of human mesenchymal stem cells. Carbohydrate polymers 2014;111:288-297.
131. Ahn EH, Kim Y, Kshitiz, An SS, Afzal J, Lee S, Kwak M, Suh KY, Kim DH, Levchenko A. Spatial control of adult stem cell fate using nanotopographic cues. Biomaterials 2014;35(8):2401-2410.
132. Miyoshi H, Adachi T. Topography design concept of a tissue engineering scaffold for controlling cell function and fate through actin cytoskeletal modulation. Tissue Engineering 2014(ja).
133. Chen R, Huang C, Ke QF, He CL, Wang HS, Mo XM. Preparation and characterization of coaxial electrospun thermoplastic polyurethane/collagen compound nanofibers for tissue engineering applications. Colloids and Surfaces B-Biointerfaces 2010;79(2):315-325.
134. Yuan H, Zhao S, Tu H, Li B, Li Q, Feng B, Peng H, Zhang Y. Stable jet electrospinning for easy fabrication of aligned ultrafine fibers. Journal of Materials Chemistry 2012;22(37):19634-19638.
135. Zhang C, Yuan H, Liu H, Chen X, Lu P, Zhu T, Yang L, Yin Z, Heng BC, Zhang Y. Well-aligned chitosan-based ultrafine fibers committed teno-lineage differentiation of human induced pluripotent stem cells for Achilles tendon regeneration. Biomaterials 2015;53:716-730.

136. Nain AS, Sitti M, Jacobson A, Kowalewski T, Amon C. Dry spinning based spinneret based tunable engineered parameters (STEP) technique for controlled and aligned deposition of polymeric nanofibers. Macromolecular rapid communications 2009;30(16):1406-1412.
137. Nain AS, Phillippi JA, Sitti M, MacKrell J, Campbell PG, Amon C. Control of Cell Behavior by Aligned Micro/Nanofibrous Biomaterial Scaffolds Fabricated by Spinneret‐Based Tunable Engineered Parameters (STEP) Technique. Small 2008;4(8):1153-1159.
138. Wu Y, Wong YS, Fuh JYH. Degradation behaviors of geometric cues and mechanical properties in a 3D scaffold for tendon repair. Journal of Biomedical Materials Research Part A 2017;105(4):1138-1149.
139. Yin H-M, Li X, Xu J-Z, Zhao B, Li J-H, Li Z-M. Highly aligned and interconnected porous poly (ε-caprolactone) scaffolds derived from co-continuous polymer blends. Materials & Design 2017.
140. Zheng Z, Ran J, Chen W, Hu Y, Zhu T, Chen X, Yin Z, Heng BC, Feng G, Le H. Alignment of collagen fiber in knitted silk scaffold for functional massive rotator cuff repair. Acta Biomaterialia 2017.
141. Nowotny J, Aibibu D, Farack J, Nimtschke U, Hild M, Gelinsky M, Kasten P, Cherif C. Novel fiber-based pure chitosan scaffold for tendon augmentation: biomechanical and cell biological evaluation. Journal of Biomaterials Science, Polymer Edition 2016;27(10):917-936.
142. Moffat KL, Kwei AS-P, Spalazzi JP, Doty SB, Levine WN, Lu HH. Novel nanofiber-based scaffold for rotator cuff repair and augmentation. Tissue Engineering Part A 2008;15(1):115-126.
143. Bourget J-M, Auger FA, Germain L, Guillemette M, Veres T. Alignment of cells and extracellular matrix within tissue-engineered substitutes: INTECH Open Access Publisher; 2013.
144. Zheng Z, Ran J, Chen W, Hu Y, Zhu T, Chen X, Yin Z, Heng BC, Feng G, Le H. Alignment of collagen fiber in knitted silk scaffold for functional massive rotator cuff repair. Acta biomaterialia 2017;51:317-329.
145. Popielarczyk TL, Nain AS, Barrett JG. Aligned Nanofiber Topography Directs the Tenogenic Differentiation of Mesenchymal Stem Cells. Applied Sciences 2017;7(1):59.
146. Erisken C, Zhang X, Moffat KL, Levine WN, Lu HH. Scaffold fiber diameter regulates human tendon fibroblast growth and differentiation. Tissue Engineering Part A 2012;19(3-4):519-528.
147. Kim SJ, Jang DH, Park WH, Min BM. Fabrication and characterization of 3-dimensional PLGA nanofiber/microfiber composite scaffolds. Polymer 2010;51(6):1320-1327.
148. Gilchrist CL, Ruch DS, Little D, Guilak F. Micro-scale and meso-scale architectural cues cooperate and compete to direct aligned tissue formation. Biomaterials 2014;35(38):10015-10024.
149. Omi R, Gingery A, Steinmann SP, Amadio PC, An K-N, Zhao C. Rotator cuff repair augmentation in a rat model that combines a multilayer xenograft

tendon scaffold with bone marrow stromal cells. Journal of Shoulder and Elbow Surgery 2016;25(3):469-477.
150. Rothrauff BB, Lauro BB, Yang G, Debski RE, Musahl V, Tuan R. Braided and Stacked Electrospun Nanofibrous Scaffolds for Tendon and Ligament Tissue Engineering. Tissue Engineering 2017(ja).
151. Younesi M, Islam A, Kishore V, Anderson JM, Akkus O. Tenogenic Induction of Human MSCs by Anisotropically Aligned Collagen Biotextiles. Advanced Functional Materials 2014.
152. Vaquette C, Kumar S, Petcu EB, Ivanovski S. Combining electrospinning and cell sheet technology for the development of a multiscale tissue engineered ligament construct (TELC). Journal of Biomedical Materials Research Part B: Applied Biomaterials 2017.
153. Chainani A, Hippensteel KJ, Kishan A, Garrigues NW, Ruch DS, Guilak F, Little D. Multilayered Electrospun Scaffolds for Tendon Tissue Engineering. Tissue Engineering Part A 2013;19(23-24):2594-2604.
154. Alshomer F, Chaves C, Serra T, Ahmed I, Kalaskar DM. Micropatterning of nanocomposite polymer scaffolds using sacrificial phosphate glass fibers for tendon tissue engineering applications. Nanomedicine: Nanotechnology, Biology and Medicine 2017.
155. Ker ED, Nain AS, Weiss LE, Wang J, Suhan J, Amon CH, Campbell PG. Bioprinting of growth factors onto aligned sub-micron fibrous scaffolds for simultaneous control of cell differentiation and alignment. Biomaterials 2011;32(32):8097-8107.
156. Franchi M, Torricelli P, Giavaresi G, Fini M. Role of moderate exercising on Achilles tendon collagen crimping patterns and proteoglycans. Connective tissue research 2013;54(4-5):267-274.
157. Chen F, Hayami JW, Amsden BG. Electrospun poly (l-lactide-co-acryloyl carbonate) fiber scaffolds with a mechanically stable crimp structure for ligament tissue engineering. Biomacromolecules 2014;15(5):1593-1601.
158. Banik BL, Lewis GS, Brown JL. Multiscale Poly-(ϵ-caprolactone) Scaffold Mimicking Non-linearity in Tendon Tissue Mechanics. Regenerative engineering and translational medicine 2016;2(1):1-9.
159. Green EC, Zhang Y, Li H, Minus ML. Gel-spinning of mimetic collagen and collagen/nano-carbon fibers: Understanding multi-scale influences on molecular ordering and fibril alignment. Journal of the Mechanical Behavior of Biomedical Materials 2017;65:552-564.
160. Bansal S, Mandalapu S, Aeppli C, Qu F, Szczesny SE, Mauck RL, Zgonis MH. Mechanical function near defects in an aligned nanofiber composite is preserved by inclusion of disorganized layers: Insight into meniscus structure and function. Acta Biomaterialia 2017.
161. Zhong SP, Teo WE, Zhu X, Beuerman RW, Ramakrishna S, Yung LYL. An aligned nanofibrous collagen scaffold by electrospinning and its effects on in vitro fibroblast culture. Journal of Biomedical Materials Research Part A 2006;79A(3):456-463.

162. Yang G, Lin H, Rothrauff BB, Yu S, Tuan RS. Multilayered polycaprolactone/gelatin fiber-hydrogel composite for tendon tissue engineering. Acta biomaterialia 2016;35:68-76.
163. Rioja AY, Muniz-Maisonet M, Koob TJ, Gallant ND. Effect of nordihydroguaiaretic acid cross-linking on fibrillar collagen: in vitro evaluation of fibroblast adhesion strength and migration. 2017.
164. Leung M, Jana S, Tsao CT, Zhang MQ. Tenogenic differentiation of human bone marrow stem cells via a combinatory effect of aligned chitosan-polycaprolactone nanofibers and TGF-beta 3. Journal of Materials Chemistry B 2013;1(47):6516-6524.
165. Park S-H, Kim MS, Lee B, Park JH, Lee HJ, Lee NK, Jeon NL, Suh K-Y. Creation of a hybrid scaffold with dual configuration of aligned and random electrospun fibers. ACS applied materials & interfaces 2016;8(4):2826-2832.
166. Gonçalves AI, Rodrigues MT, Carvalho PP, Bañobre‐López M, Paz E, Freitas P, Gomes ME. Exploring the potential of starch/polycaprolactone aligned magnetic responsive scaffolds for tendon regeneration. Advanced healthcare materials 2016;5(2):213-222.
167. Cheng X, Tsao C, Sylvia VL, Cornet D, Nicolella DP, Bredbenner TL, Christy RJ. Platelet-derived growth-factor-releasing aligned collagen–nanoparticle fibers promote the proliferation and tenogenic differentiation of adipose-derived stem cells. Acta biomaterialia 2014;10(3):1360-1369.
168. Sahoo S, Ang LT, Goh JCH, Toh SL. Bioactive nanofibers for fibroblastic differentiation of mesenchymal precursor cells for ligament/tendon tissue engineering applications. Differentiation 2010;79(2):102-110.
169. Webb WR, Dale TP, Lomas AJ, Zeng GD, Wimpenny I, El Haj AJ, Forsyth NR, Chen GQ. The application of poly(3-hydroxybutyrate-co-3-hydroxyhexanoate) scaffolds for tendon repair in the rat model. Biomaterials 2013;34(28):6683-6694.
170. Deepthi S, Sundaram MN, Kadavan JD, Jayakumar R. Layered chitosan-collagen hydrogel/aligned PLLA nanofiber construct for flexor tendon regeneration. Carbohydrate Polymers 2016;153:492-500.
171. Manning C, Schwartz A, Liu W, Xie J, Havlioglu N, Sakiyama-Elbert S, Silva M, Xia Y, Gelberman R, Thomopoulos S. Controlled delivery of mesenchymal stem cells and growth factors using a nanofiber scaffold for tendon repair. Acta biomaterialia 2013;9(6):6905-6914.
172. Bhaskar P, Bosworth LA, Wong R, O'brien MA, Kriel H, Smit E, McGrouther DA, Wong JK, Cartmell SH. Cell response to sterilized electrospun poly (ε‐caprolactone) scaffolds to aid tendon regeneration in vivo. Journal of Biomedical Materials Research Part A 2017;105(2):389-397.
173. Peach MS, Ramos DM, James R, Morozowich NL, Mazzocca AD, Doty SB, Allcock HR, Kumbar SG, Laurencin CT. Engineered stem cell niche matrices for rotator cuff tendon regenerative engineering. PloS one 2017;12(4):e0174789.

Chapter 2: Aligned Nanofiber Topography Directs the Tenogenic Differentiation of Mesenchymal Stem Cells

Published as:

> Popielarczyk, T. L., Nain, A. S., & Barrett, J. G. (2017). Aligned Nanofiber Topography Directs the Tenogenic Differentiation of Mesenchymal Stem Cells. *Applied Sciences*, *7*(1), 59.

Abstract

Tendon is commonly injured, heals slowly and poorly, and often suffers re-injury after healing. This is due to failure of tenocytes to effectively remodel tendon after injury to recapitulate normal architecture, resulting in poor mechanical properties. One strategy for improving the outcome is to use nanofiber scaffolds and mesenchymal stem cells (MSCs) to regenerate tendon. Various scaffold parameters are known to influence tenogenesis. We designed suspended and aligned nanofiber scaffolds with the hypothesis that this would promote tenogenesis when seeded with MSCs. Our aligned nanofibers were manufactured using the previously reported non-electrospinning Spinneret-based Tunable Engineered Parameters (STEP) technique. We compared parallel versus perpendicular nanofiber scaffolds with traditional flat monolayers and used cellular morphology, tendon marker gene expression, and collagen and glycosaminoglycan deposition as determinants for tendon differentiation. We report that compared with traditional control monolayers, MSCs grown on nanofibers were morphologically elongated with higher gene expression of tendon marker scleraxis and type I collagen, along with increased production of extracellular matrix components collagen (p = 0.0293) and glycosaminoglycan (p = 0.0038). Further study of MSCs in

different topographical environments is needed to elucidate the complex molecular mechanisms involved in stem cell differentiation.

Introduction

Tendon injury is a common clinical problem among veterinary and human patients with significant similarities in physiology and tendon pathologies. The inherent regenerative capacity of tendon is poor due to low cellularity and low vascularity of the tissue. These characteristics contribute to prolonged and incomplete healing with a high risk of re-injury [1]. Mesenchymal stem cells (MSCs) are used in tissue engineering and regenerative medicine applications for musculoskeletal tissue repair, particularly for their regenerative capabilities. MSCs can differentiate into tenocytes to promote tendon healing [2-4]. Engineered *in vitro* nanofiber scaffolds mimic the native topography of the extracellular matrix (ECM) microenvironmental cues that influence cell response and function including adhesion, migration, proliferation, and differentiation [5,6]. Scaffold directed MSC differentiation is determined through a combination of morphology, panels of tendon-related markers, collagen production and alignment, and levels of glycosaminoglycan (GAG) content [7,8]. Scleraxis (*scx*), a transcription factor, is a key tendon-related marker which functions in tendon development and differentiation and promotes the expression and production of type I collagen (*Col I*) [9-11]. Col I is the main fibrillar collagen functioning as a structural protein in healthy tendon composition [12]. GAGs aid in collagen fiber growth and function; abnormal levels signify disease or injury [13].

A challenge of designing scaffolds is determining the specific topographical cues of fiber diameter, orientation, and alignment that are most suited for tendon studies.

Techniques used to manufacture fibrous scaffolds vary in their ability to control these parameters and produce various combinations. Fiber alignment influences MSC-fiber interaction and guides cell behavior. Kim *et al.* fabricated a nanofiber/microfiber composite scaffold that enhanced cell adhesion, cell spreading, and scaffold infiltration [14]. In another study, multilayered aligned electrospun scaffolds provided an anisotropic environment that promoted expression of tenomodulin, a marker of tendon maturation, and alignment of collagen throughout the scaffold in comparison to nonaligned scaffolds [15]. Yin *et al.* showed that compared to random electrospun fibers, aligned nanofibers provided microenvironmental cues for differentiation into the teno-lineage [16]. MSCs seeded on aligned nanofibers showed evidence that topography alone promoted changes in cell morphology and orientation. Cell differentiation was only enhanced by addition of TGF-β3 [6] and printing of growth factors on aligned fibers [17]. These studies demonstrate that differentiation is a complex process sensitive to environmental cues, thus necessitating the need to optimize fibrous and growth factor parameters to mimic native environment to achieve specific lineages.

Electrospinning is a common manufacturing technique used to engineer fibrous scaffolds for tissue engineering. Improvements to this technique, including the use of modified collectors and fiber manipulation, have increased the applicability of this technique [18-21]. Besides electrospinning, other approaches including micropatterning, electro-chemically aligned have been used to study differentiation. For example, Gilchrist *et al.* studied the effects of architectural cues on aligned tissue formation using micropatterned aligned scaffolds of varying lengths and orientation and concluded that the combination of cues i.e. fiber length, boundaries, and orientation regulate tissue

formation in a complex manner [22]. Kishore *et al.* investigated the effects of topography on tenogenesis with electro-chemically aligned threads, and showed alignment induced increased expression of *scx* and *tnmd* (tenomodulin) [23]. In the context of fibrous scaffolds, the non-electrospinning Spinneret-based Tunable Engineered Parameters technique (STEP) [24] is a pseudo dry spinning method and a novel alternative to electrospinning, capable of depositing uniform nanofiber arrays. This method allows for the manufacturing of scaffolds with increased control of fiber diameter, spacing, length, alignment, orientation, and hierarchical assembly to influence cell response. The advantage of STEP fibers, in contrast to electrospun fibers, is that the parameter control allows for not only the traditional studies comparing aligned fibers to nonaligned or random fibers, but rather scaffolds of suspended and highly aligned fibers in different orientations [25].

Using STEP fibrous scaffolds, the aim of this study was to understand the biological response of MSCs to topographical cues provided by nanofibers to determine the optimal scaffold design to study tenogenesis. Polystyrene was used strictly for the purpose of studying MSC response to alignment and orientation. We hypothesized that MSCs would differentiate into tenocytes on scaffolds that mimic native tendon alignment specifically scaffolds of three-dimensional (3D) suspended and aligned nanofibers. MSCs from aligned parallel and aligned perpendicular nanofibers were compared to traditional two-dimensional (2D) monolayers with increases in gene expression of tendon-related genes, collagen production, and GAG levels. This data highlights specific cellular responses to alignment that adds to our understanding of stem cells in development and repair.

Materials and Methods

STEP scaffolds were manufactured as 3D suspended and aligned fibers in parallel and perpendicular orientation as described previously [24-26]. Nanofiber diameters were measured using environmental scanning electron microscopy. Equine bone marrow MSCs, passage 3, were seeded at a density of 2×10^5 cells per scaffold on a total of 154 scaffolds. In addition, MSCs were seeded on cell culture treated plastic for monolayer controls. Microscopy, qPCR, and biochemical data are in reference to monolayer. Experiments were performed in triplicate. Gene expression analysis of *scx* and *col I* was assessed on day 7 and day 14 from scaffolds relative to monolayers. Production of soluble collagen and GAG content in the media were assessed on days 1, 7, and 14 and averaged from 6 scaffolds per time point for collagen production and averaged from 8 scaffolds per time point for GAG content.

Scaffold Manufacturing and Characterization

Fibers were spun on scaffolds using the STEP technique (US9029149 B2 patent) to manufacture multi-layered, aligned suspended nanofibers in parallel or perpendicular orientations [24-26]. Briefly, the polymer is pushed through a syringe pump and stretched out into a continuous fiber as the spinneret comes in contact with the rotating frame and the solvent evaporates. Fiber surface area and density are determined by a combination of factors; scaffold frame dimensions, polymer solution, and spinning parameters. Scaffolds were manufactured with dimensions measuring 4 mm in length × 4 mm in width. Standard polystyrene (Mw 1,571,000 and Mw 2,257,000 g/mol, Polymer Scientific Products, Ontario, NY, USA) solutions were prepared with xylene to produce 400 nm diameter fibers. All scaffolds were sterilized with 70% alcohol and plasma-treated with a

high frequency generator (Electro-technic Products Inc., Chicago, IL, USA) before coating with 20 μg/mL of bovine fibronectin protein (Thermo Fisher Scientific, Waltham, MA, USA).

Environmental Scanning Electron Microscopy

Fibers from each batch of scaffolds were sputter-coated in gold/palladium alloy and imaged with a Quanta 600 FEG Environmental Scanning Electron Microscope (FEI, Hillsboro, OR, USA). Scaffolds were randomly selected from each batch and diameters of 25 fibers per scaffold were measured with ImageJ and Fiji plugin (National Institutes of Health [27]) from ESEM images.

Isolation and Characterization of Primary Equine Mesenchymal Stem Cells

MSCs were isolated from bone marrow aspirate harvested from the sternum of a one year old male horse, euthanized for unrelated conditions, following approval of the Institutional Animal Care and Use Committee (IACUC) of the Virginia Polytechnic Institute and State University and assessed via previously described techniques [28]. Briefly, bone marrow was collected, centrifuged to remove the plasma, and cultured in media containing low-glucose GlutaMAX DMEM with 110 mg/mL sodium pyruvate (Thermo Fisher Scientific, Waltham, MA, USA), supplemented with 10% MSCs fetal bovine serum (Thermo Fisher Scientific, Waltham, MA, USA), and 1% sodium penicillin and streptomycin sulfate (Sigma, St. Louis, MO, USA) at 37ºC, 5% CO^2 and 90% humidity. Media was added after two days, cells were fed on day 4, washed in PBS on day 5, and then fed every two days until cells were 80% confluent. Flow cytometry results showed > 99% of cells were positive for both markers of stemness OCT4 and

CD90, 22% positive for CD44, 19% positive for MHC I, and non-detectable for MHC II. Multilineage potential of MSCs was confirmed through adipogenesis, chondrogenesis, and osteogenesis assays.

Cell Culture and Scaffold Seeding

Scaffolds were each seeded with 2×10^5 equine bone marrow MSCs and cultured for 14 days in 12 well plates. Scaffolds were transferred to new 12 well plates with new cell culture media 24 h after seeding. In addition, MSCs were seeded on plasma-treated, fibronectin-coated plastic as previously described for nanofibers for monolayer controls. All MSCs were passage 3. Culture media contained low-glucose GlutaMAX DMEM with 110 mg/mL sodium pyruvate (Thermo Fisher Scientific, Waltham, MA, USA), supplemented with 10% MSCs fetal bovine serum (Thermo Fisher Scientific, Waltham, MA, USA), and 1% sodium penicillin and streptomycin sulfate (Sigma, St. Louis, MO, USA) at 37 °C, 5% CO^2 and 90% humidity.

Phase-Contrast and Time-Lapse Microscopy

Cell morphology was observed for days 0–14 under phase microscopy. Each time-lapse video was recorded for MSCs on scaffolds over a 12-h period. Scaffolds were seeded in 35 mm glass petri dishes and loaded into the on-stage incubator (Okolab, Naples, Italy) at 37 °C, 5% CO^2 and 90% humidity. Microscopy was performed using an AMG EVOS fl digital inverted fluorescence microscope (Thermo Fisher Scientific, Walham, MA, USA).

Fluorescence Microscopy

Seeded parallel and perpendicular oriented fibrous scaffolds were stained with calcein AM on day 14 to assess cell viability on polystyrene fibers. Scaffolds were washed in PBS and stained with calcein AM in low-glucose GlutaMAX DMEM for 30 min and washed in PBS. Seeded scaffolds were fixed in 4% paraformaldehyde, incubated with 0.2% Triton X-100 and stained with rhodamine phalloidin (Thermo Fisher Scientific, Walham, MA, USA), followed by Prolong Gold Antifade Mountant with DAPI (4′, 6-diamidino-2-phenylindole) (Thermo Fisher Scientific, Walham, MA, USA) for F-actin and nuclei staining, respectively. Microscopy was performed using an AMG EVOS fl digital inverted fluorescence microscope (Thermo Fisher Scientific, Waltham, MA, USA).

RNA Isolation, Quantification, and Quantitative PCR

MSCs were harvested from scaffolds, monolayers from tissue culture treated plastic, and tenocytes with TRIzol (Thermo Fisher Scientific, Walham, MA, USA). Parallel and perpendicular scaffolds were pooled into their respective groups on day 7 and day 14. An RNeasy Mini Kit (Qiagen, Hilden, Germany) was used to isolate the RNA. RNA quantification was performed using a Quant-iT Ribogreen RNA Assay Kit (Thermo Fisher Scientific, Walham, MA, USA). RNA was converted to cDNA using a high frequency RNA-to cDNA Kit (Thermo Fisher Scientific, Walham, MA, USA) and Eppendorf Thermal Cycler (Brinkmann Instruments Inc, Westbury, NY, USA). Applied Biosystems Real-Time 7500 PCR System (Thermo Fisher Scientific, Waltham, MA, USA) was used to run quantitative PCR (qPCR) with TaqMan Master Mix (Thermo

Fisher Scientific, Waltham, MA, USA) and 20 ng of cDNA per 50 μL PCR reaction. Relative quantitation was calculated using the Comparative C_T method ($2^{\wedge-\Delta\Delta CT}$). Gene expression was normalized to monolayer controls using Glyceraldehyde 3-phosphate dehydrogenase (GAPDH). Custom equine primer and probe sequences for GAPDH, scleraxis, and type I collagen were purchased (Thermo Fisher Scientific, Waltham, MA, USA).

Biochemical Assay of Media Content

Biochemical analyses of collagen and glycosaminoglycan (GAG) content were used to determine ECM production over 7 and 14 days. Solubilized collagen was measured using the Sircol Soluble Collagen Assay (Biocolor Ltd., Carrickfergus, Ireland, UK). Sulfated glycosaminoglycan content was measured using the 1,9-dimethylmethylene blue (DMMB) assay, referencing bovine chondroitin sulfate A [29]. All absorbance readings were measured at 540 nm with a HIDEX Chameleon V microplate reader (HIDEX, Turku, Finland).

Statistical Analysis

Two-way analysis of variance (ANOVA) was used to determine fiber orientation and temporal effects on gene expression and matrix production, followed by post hoc Tukey HSD (JMP Pro 10 Software, SAS Institute Inc, Rockville, MD, USA, 2015). Mean ± standard error for each statistic was calculated for each scaffold design. p-values ≤ 0.05 were considered significant.

Results

STEP-Manufactured Fibers Exhibit Fibril-Like Organization

STEP scaffolds were manufactured as nanofibers in aligned parallel and aligned perpendicular orientation, suspended from a scaffold frame (Fig. 2.1A). Environmental Scanning Electron Microscopy (ESEM) images of parallel (Fig. 2.1Bi) and perpendicular (Fig. 2.1Bii) oriented fibrous scaffolds show alignment and orientation of fibers. Fiber diameters measured 400 nm ± 128.17 nm standard deviation (Fig. 2.1C). STEP fibers provided a three-dimensional, multilayer, aligned structure with fibers comparable to the diameter range of 50–500 nm of native equine tendon collagen fibrils [30]. The seeding density and fiber coating were determined previously (Fig. A2.1) and enabled complete integration of cells into the scaffolds and provided increased cell to fiber interaction in response to these scaffold designs.

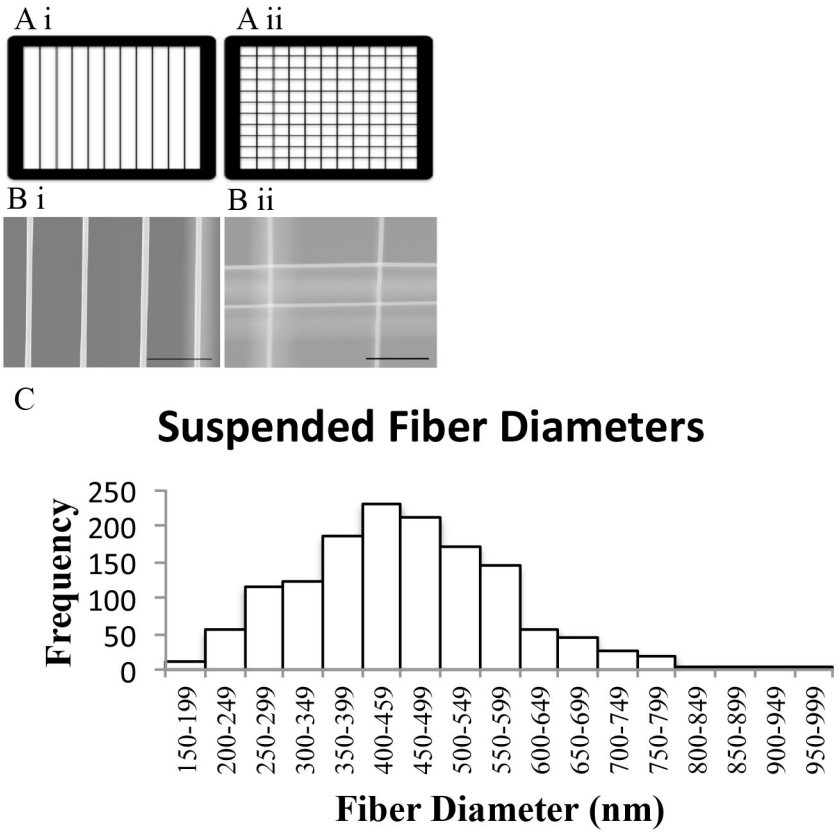

Figure 2.1. STEP scaffold characterization of fiber diameter**.** A schematic of an aligned parallel fibrous scaffold (Ai) and an aligned perpendicular fibrous scaffold (Aii); SEM images of aligned parallel fibrous scaffold (Bi) and aligned perpendicular fibrous scaffold (Bii). Scale bar 5 μm and 3 μm, respectively; Histogram of aligned parallel and aligned perpendicular fiber diameters, measured with ImageJ, n = 1400 (C).

MSCs Exhibit Tenocyte-Like Morphology on Suspended Fibrous Scaffolds

MSCs were guided by the three dimensional structure of the fibers and fiber orientation as assessed by phase-contrast microscopy (Fig. 2.2). MSCs on parallel fibers elongated along the nanofibers in a tenocyte-like morphology within 24 h of seeding (Fig. 2.2A) and maintained by day 7 (Fig. 2.2B). Morphological changes were similar on day 14. Parallel orientation of fibers promoted an elongated tenocyte-like morphology and maintained parallel MSC orientation between adjacent cells. Similar spindle-like MSC morphology was observed on perpendicular fibrous scaffolds. Additional cell

morphologies were observed on perpendicular suspended nanofibers as MSCs spread across multiple fibers at intersections of fibers, on day 1 (Fig. 2.2C) and day 7 (Fig. 2.2D).

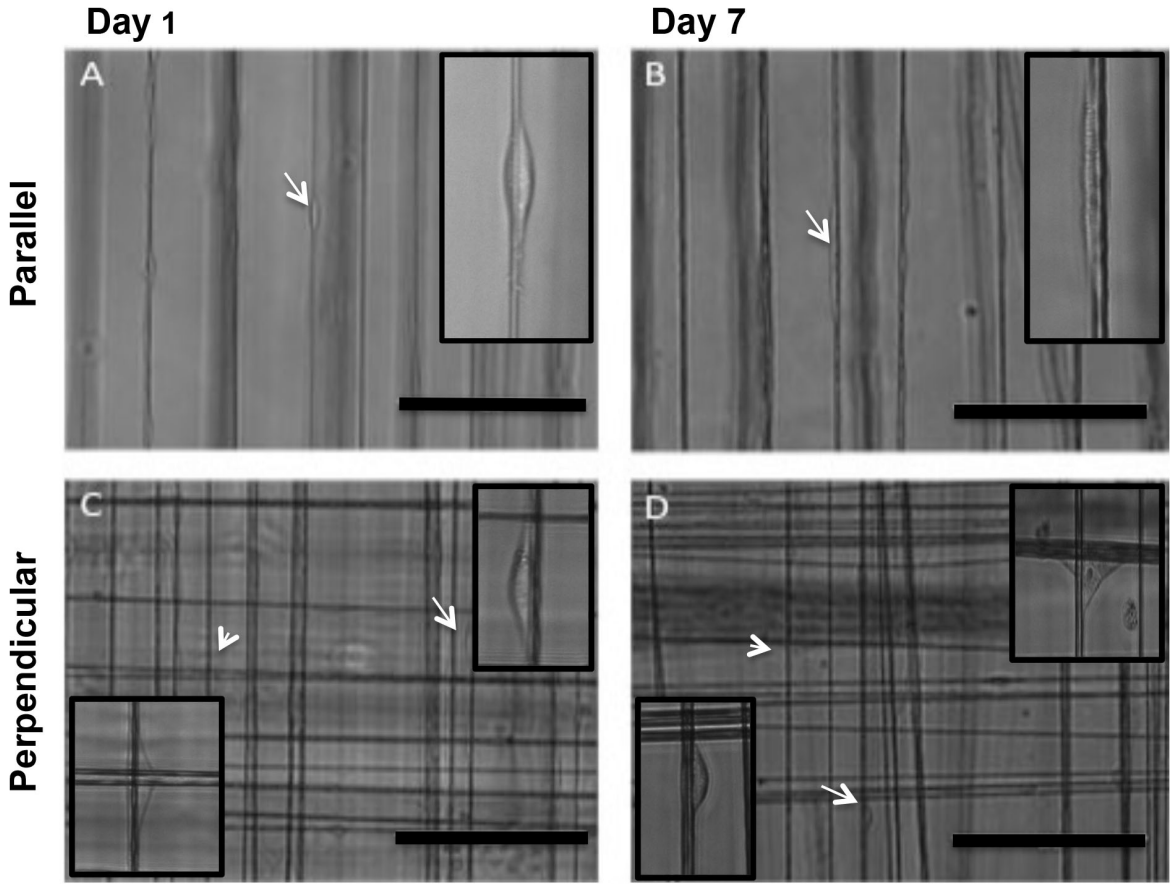

Figure 2.2: MSC morphology on aligned scaffolds. Representative phase-contrast microscopy images of equine bone marrow MSCs (mesenchymal stem cells) on aligned parallel oriented fibrous scaffolds (A,B) and aligned perpendicular fibrous scaffolds (C,D) on day 1 and day 7 of culture. Arrows, elongated cells; arrowheads, cell spreading. Insets show enlarged image of the cell. Scale bar 200 μm.

Cell migration and associated cell shape were better observed under time-lapse microscopy where we could clearly observe the cell-fiber interaction and changes in cell morphology (Fig. 2.3). Time-lapse microscopy recording was started 24 h after seeding for parallel fibers (Video S2.1: Mesenchymal stem cell migration on aligned parallel nanofibers) and perpendicular fibers (Video S2.2: Mesenchymal stem cell migration on

aligned perpendicular nanofibers). At this time, cell elongation was observed as a spindle-like morphology on parallel orientation of fibers and maintained MSC spacing between cells on adjacent fibers (Fig. 2.3A–D). Perpendicular orientation of fibers allowed cells to migrate and spread along multiple fibers, temporarily change morphology, and switch directions at fiber intersections (Fig. 2.3E–H).

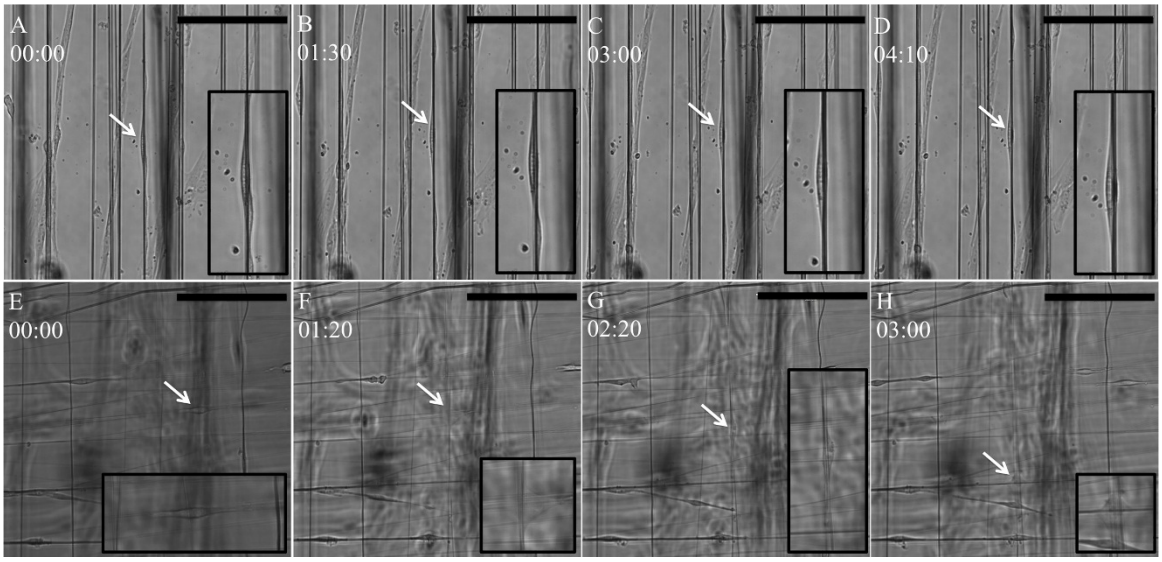

Figure 2.3: Time-lapse frames of MSCs on aligned fibers. Representative time-lapse microscopy images of equine bone marrow MSCs on aligned parallel fibrous scaffolds (A–D) and aligned perpendicular scaffolds (E–H) over 12 h. Time (hours) is indicated in the upper left corner. Arrows tack cell migration during the time-lapse. Insets show enlarged image of the cell. Scale bar 200 μm.

Fibers of perpendicular orientation promoted changes in cell migration direction and cell morphology through interaction with intersections and spreading along multiple fibers. The elongated tenocyte-like morphology was predominant before and after cells migrated through the intersections. MSC monolayers showed typical polygonal morphology on standard tissue culture treated plastic (data not shown). Viability was maintained throughout 14 days of culture on both parallel (Fig. 2.4A) and perpendicular fibers (Fig. 2.4B) showing no toxicity of cells on the polystyrene nanofibers.

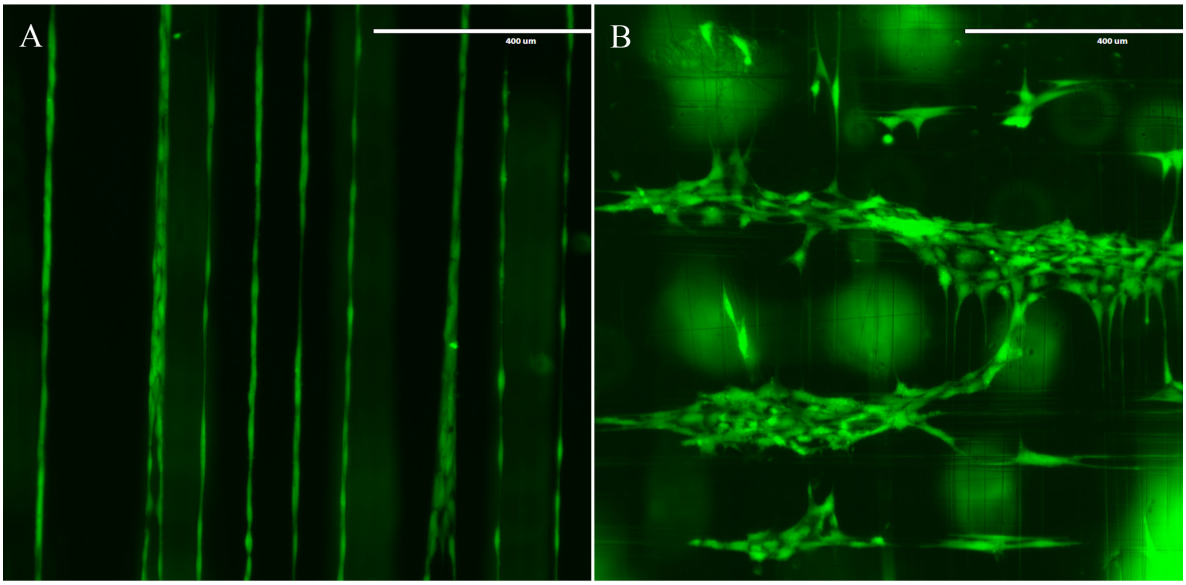

Figure 2.4: Viability of MSCs on aligned scaffolds. MSCs stained with calcein AM on parallel scaffolds (A) and perpendicular scaffolds (B) after 14 days of culture. Scale bar 400 μm.

MSCs cultured for 12 days on fibrous scaffolds elongated along aligned parallel fibers in both parallel and perpendicular oriented fibrous scaffolds as observed by fluorescence microscopy (Fig. 2.5). Intracellular F-actin stained with rhodamine phalloidin and nuclei stained with DAPI were observed along the nanofibers and in the monolayers, showed cell attachment and interaction with fibers. Perpendicular fibrous scaffolds provided fiber intersections for cell interaction (Fig. 2.5C,D), and parallel scaffolds maintained MSC spacing between fibers (Fig. 2.5A,B) leading to parallel cell orientation and spacing between fibers. The above methods have shown that fiber alignment provides environmental cues, resulting in cell elongation/tenocyte-like morphology.

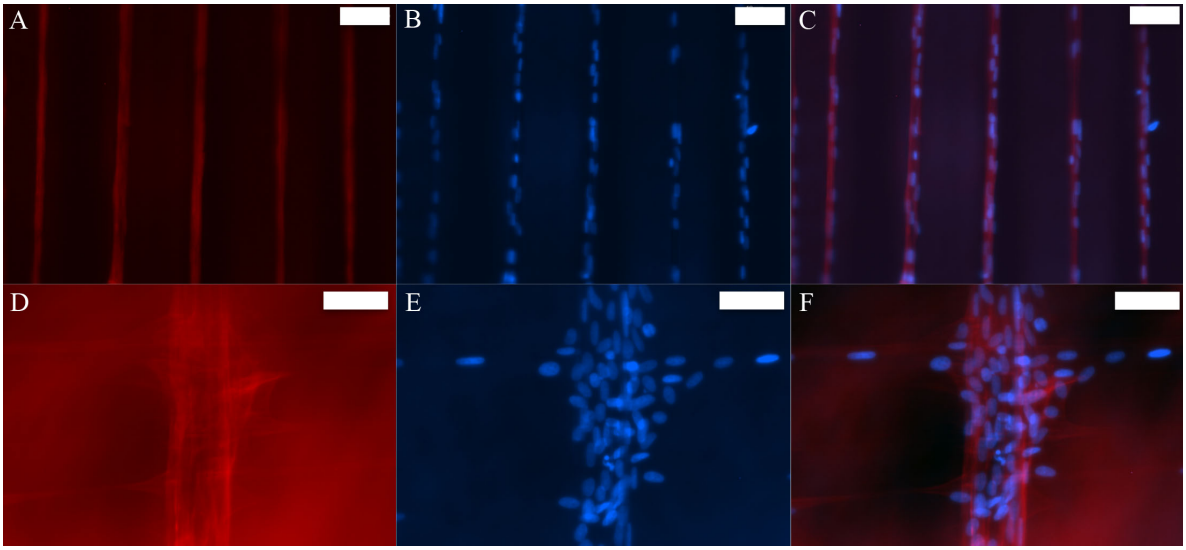

Figure 2.5: MSCs cytoskeleton and nuclei morphology on aligned scaffolds. Fluorescence microscopy images of equine bone marrow MSCs on an aligned parallel scaffolds (A–C) and an aligned perpendicular scaffolds (D–F) stained with rhodamine phalloidin (A,D); DAPI (B,E); and the merged image (C,F) on day 12 of cell culture. Scale bar 40 μm.

Tendon-Associated Gene Expression Increased Over Time

Gene expression of *scx* and *col I* custom primers and probes (Table 2.1) was analyzed on day 7 and day 14 for monolayer and scaffolds to assess tenogenesis (Fig. 2.6). There was an increasing trend in SCX expression between day 7 and 14, regardless of fiber orientation (Fig. 2.6A). Similarly, expression of COL I increased between day 7 and 14, regardless of fiber orientation (Fig 2.6B). This combined increase of both SCX and COL I expression may provide evidence of early tenogenesis.

Table 2.1: Primer and probe sequences of tendon-associated genes for qPCR analysis.

Transcript	Forward Sequence (5′-3′)	Reverse Sequence (5′-3′)	Probe Sequence (5′-3′)
GAPDH	CAAGTTCCATGGCACAGTCAAG	GGCCTTTCCGTTGATGACAA	CCGAGCACGGGAAG
Scleraxis	CGCCCAGCCCAAACAG	TTGCTCAACTTTCTCTGGTTGCT	TCTGCACCTTCTGCC
Type I Collagen	GCCAAGAAGAAGGCCAAGAA	TGAGGCCGTCCTGTATGC	ACATCCCAGCAGTCACCT

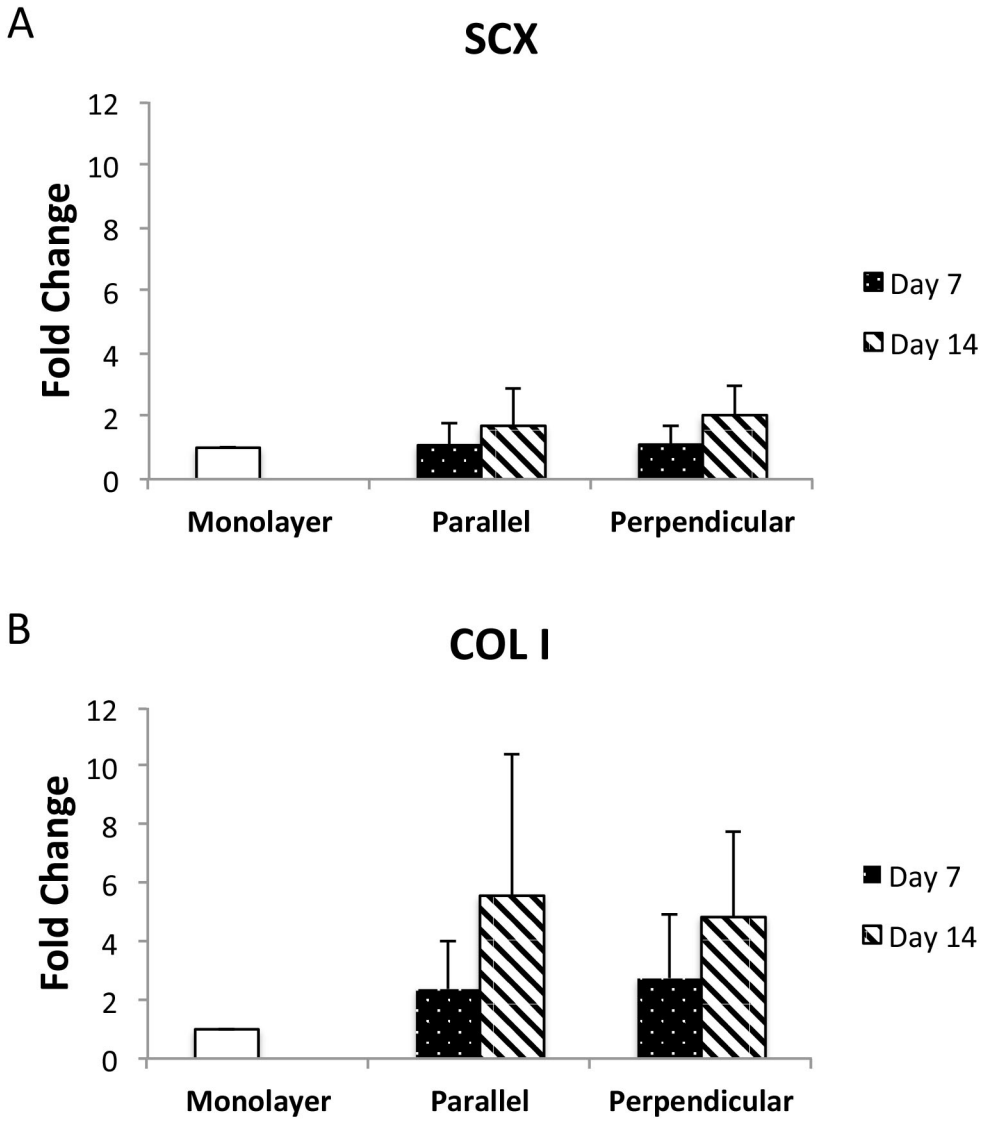

Figure 2.6: qPCR of MSCs from aligned scaffolds. Gene expression analysis of scleraxis (A) and type I collagen (B) from equine bone marrow MSCs collected from monolayers, aligned parallel scaffolds, and aligned perpendicular scaffolds on days 7 and 14. Genes were normalized to GAPDH (Glyceraldehyde 3-phosphate dehydrogenase). Gene expression of MSCs from scaffold designs is relative to monolayer controls. p value ≤ 0.05 were considered significant. Error bars represent SEM.

ECM Production Increased Over Time

Extracellular matrix production was evaluated through biochemical analysis of collagen and GAG content in the media. We found the average collagen content to increase (p = 0.0293) between days 1, 7, and 14, regardless of fiber orientation (Fig

2.7A). We also found the GAG deposition to increase over time in all three groups (monolayer, parallel, and perpendicular). There was an increase in GAG production between days ($p < 0.0001$) and an increase between all days and fiber orientation ($p = 0.0038$). In addition to the gene expression data, this increase in matrix deposition is indicative of tendon development.

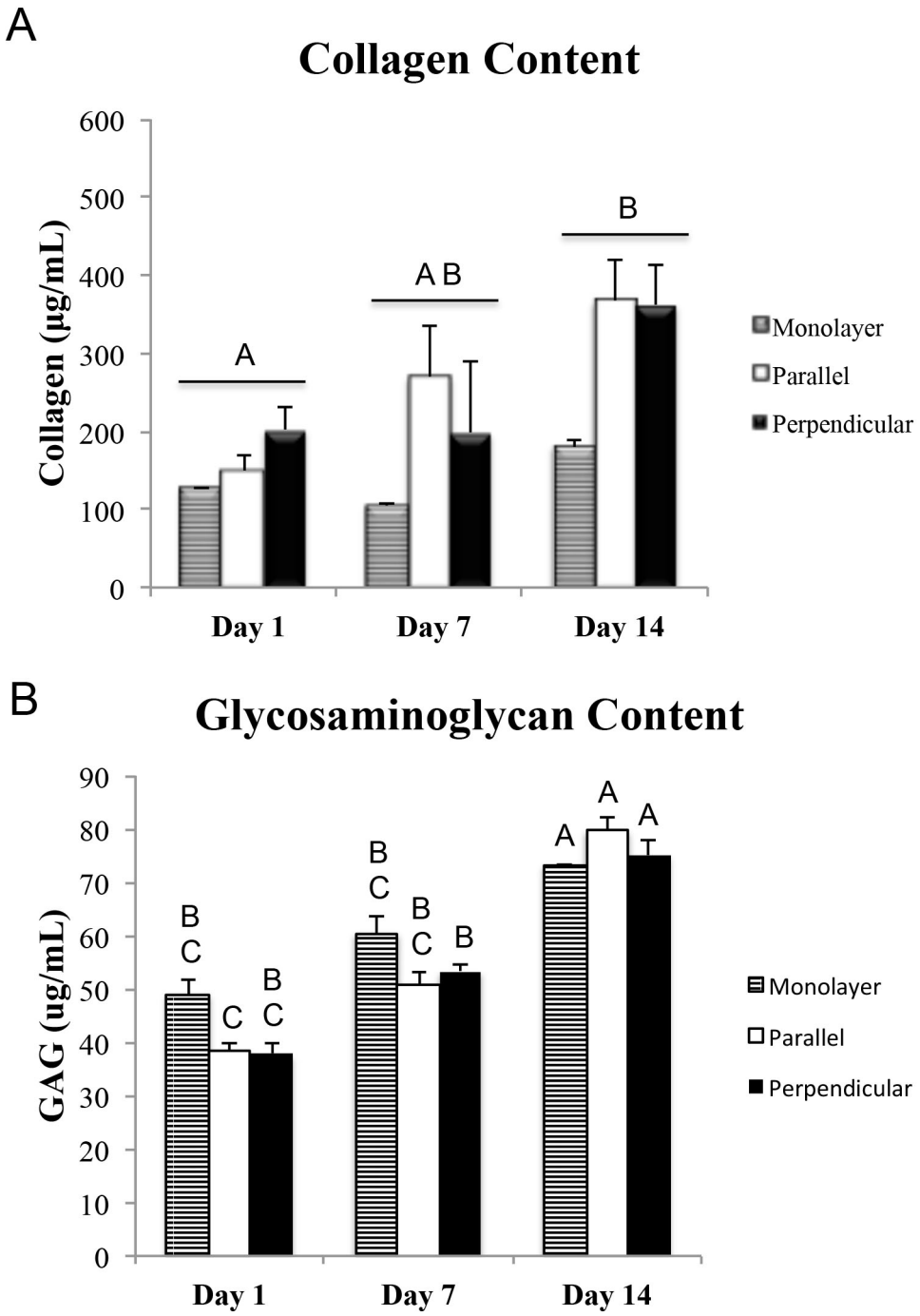

Figure 2.7: MSC production of the key matrix components. Collagen content quantification in media from cells in monolayer, aligned parallel scaffolds and aligned perpendicular scaffolds measured on days 1, 7, and 14 (A). p = 0.0038 for increased collagen production between days 1, 7, and 14, regardless of fiber orientation; GAG content quantification in media from cells in monolayer, aligned parallel scaffolds and aligned perpendicular scaffolds measured on days 1, 7, and 14 (B). p = 0.0038 for increased GAG production between all three days and fiber

orientation. p value ≤ 0.05 were considered significant. Groups not connected by the same letter are significantly different. Error bars represent SEM.

Discussion

Aligned parallel and perpendicular suspended fiber networks were used to investigate cell response to microenvironmental cues of orientation and alignment; specifically tenogenic differentiation of equine bone marrow-derived MSCs on 3D nanofibers. We found that MSCs adhered to and elongated on fibrous scaffolds of both parallel and perpendicular oriented fibers, maintained viability, and migrated along both individual and multiple fibers regardless of fiber orientation. Previous studies using aligned fibrous scaffolds have shown that MSCs elongate along aligned fibrous scaffolds to promote tenocyte-like morphologies and tendon differentiation, while random electrospun fibrous scaffolds promote polygonal cell morphology and random cell orientation [16,31,32]. Instead of randomly oriented fibers, we used aligned perpendicular fibers resulting in primarily two different morphologies. These findings show that alignment cues affected cell morphology and cell alignment, providing preliminary evidence of tenogenesis.

Further evidence of tenogenesis was demonstrated by an increasing trend of *scx* and *col I* gene expression, in response to fiber orientation from both parallel and perpendicular fibers, over time. Topographical cues from the fibers control cytoskeletal rearrangement and result in changes in cell morphology that contribute towards differentiation [33-35]. Using aligned rope-like silk scaffolds, Maharam *et al.* have previously demonstrated the association between cell morphology and tendon differentiation with increased expression of *col I* with increase in *scx* [36]. However, it was unexpected to have similar changes in gene expression of MSCs from the parallel and

perpendicular oriented fibers. This can be explained by the similarities in the cell-fiber interactions. The cells on both the parallel and perpendicular fibers interacted with the individual fibers due to fiber density. Previous studies have investigated tendon gene expression from cells cultured on fibrous scaffolds where tendon gene expression was not significantly altered, although this was a comparison between aligned and random scaffolds [37]. In another study, Gilchrist *et al.* compared aligned (parallel) and grid (perpendicular) architectural cues and observed an increase of gene expression of *scx* and *col I* from day 6 to day 12, with no significant differences in tendon gene expression between designs [22], similar to results observed in our scaffolds. Our findings suggest that alignment, rather than orientation, may be the predominant cue influencing tenogenic differentiation.

We investigated whether morphology and gene expression also correlated to the production of ECM components. We found equine MSCs produced increased amounts of collagen and GAGs over time in response to fibrous scaffolds, in accordance with previous studies. Although our study involved differences in fiber orientation compared to others, we found that the production of ECM components increased similarly. Moffat *et al.* showed an increase of collagen production from fibroblast like cells on aligned scaffolds compared to unaligned nanofiber scaffolds [38]. Therefore, increased collagen production was expected with both scaffold designs being highly aligned. We also found the GAG deposition to increase over time in all three groups from day 1, day 7 and day 14. An increase in proteogylcans may result in enhancement of fibril and fiber sliding, necessary for proper mechanical function of collagen in tendon [39]. These findings corroborate previous reports of elevated matrix production on nanofibers in response to

both parallel and perpendicular orientation of fibers. Chainani *et al.* report a similar trend of increasing collagen and GAG content over a 28-day culture period [18]. Other studies report increased scaffold production over time, with no differences between aligned and nonaligned scaffolds [15]. Thus, our findings suggest that increased matrix production over time may not be due to fiber orientation, suggesting other factors including fiber diameter may be involved.

Conclusions

The aligned nanofiber scaffolds were manufactured with fiber characteristics mimicking native tendon fibrils; alignment and nano-sized fiber diameters. In addition, these scaffold provide cell infiltration, promote tendon-like gene expression, and matrix production. Topographical cues stimulated tenogenesis and emphasized the importance of alignment in determining cell fate. In addition, our study provides insight into the importance of optimizing scaffold design through adjustable parameters that influence MSC behavior and fate. As a whole, our findings suggest that nanofiber topography alone can influence tenogenic differentiation; specifically, fiber alignment promotes cell elongation and tendon-like characteristics of tendon-related markers and matrix production for MSC differentiation. Future studies will adjust scaffold parameters to further investigate how alignment cues affect MSC response and investigate molecular mechanisms involved in tendon differentiation. Our study demonstrated that aligned scaffolds induced changes in MSC morphology, gene expression, and scaffold production that support evidence of tenogenesis. Further exploration of fibrous scaffold parameters and MSC response in varying topographical environments may help to elucidate the optimal parameters needed to stimulate tenogenesis.

Supplementary Materials

The following are available online at www.mdpi.com/link, Video S2.1: Mesenchymal stem cells on aligned parallel nanofibers, Video S2.2: Mesenchymal stem cells on aligned perpendicular nanofibers.

Acknowledgments

This study made use of Virginia Tech's Institute for Critical Technology and Applied Science and the Nanoscale Characterization and Fabrication Laboratory. The authors would like to acknowledge funding by the Stamps Family Charitable Foundation. A.S.N. would like to acknowledge partial support from NSF grant CMMI-1437101. The authors would like to thank Puja Sharma, Kevin Sheets, Daniel W. Youngstrom, Jade E. LaDow, and all other members of the STEP Laboratory and the Regenerative Medicine Research Laboratory.

Author Contributions

All authors conceived and designed the experiments; T.L. Popielarczyk performed the experiments; T.L. Popielarczyk and J.G. Barrett analyzed the data; A.S. Nain contributed reagents/materials/analysis tools; T.L. Popielarczyk wrote the paper.

Conflicts of Interest: The authors declare no conflict of interest.

References

1. Spaas JH, Guest DJ, Van de Walle GR. Tendon Regeneration in Human and Equine Athletes Ubi Sumus-Quo Vadimus (Where are We and Where are We Going to)? Sports Medicine 2012;42(10):871-890.
2. Webb WR, Dale TP, Lomas AJ, Zeng GD, Wimpenny I, El Haj AJ, Forsyth NR, Chen GQ. The application of poly(3-hydroxybutyrate-co-3-hydroxyhexanoate) scaffolds for tendon repair in the rat model. Biomaterials 2013;34(28):6683-6694.
3. Randelli P, Conforti E, Piccoli M, Ragone V, Creo P, Cirillo F, Masuzzo P, Tringali C, Cabitza P, Tettamanti G and others. Isolation and Characterization of 2 New Human Rotator Cuff and Long Head of Biceps Tendon Cells Possessing Stem Cell-Like Self-Renewal and Multipotential Differentiation Capacity. American Journal of Sports Medicine 2013;41(7):1653-1664.
4. Mazzocca AD, McCarthy MBR, Chowaniec D, Cote MP, Judson CH, Apostolakos J, Solovyova O, Beitzel K, Arciero RA. Bone Marrow-Derived Mesenchymal Stem Cells Obtained During Arthroscopic Rotator Cuff Repair Surgery Show Potential for Tendon Cell Differentiation After Treatment With Insulin. Arthroscopy-the Journal of Arthroscopic and Related Surgery 2011;27(11):1459-1471.
5. Czaplewski SK, Tsai T-L, Duenwald-Kuehl SE, Vanderby Jr R, Li W-J. Tenogenic differentiation of human induced pluripotent stem cell-derived mesenchymal stem cells dictated by properties of braided submicron fibrous scaffolds. Biomaterials 2014.
6. Leung M, Jana S, Tsao CT, Zhang MQ. Tenogenic differentiation of human bone marrow stem cells via a combinatory effect of aligned chitosan-polycaprolactone nanofibers and TGF-beta 3. Journal of Materials Chemistry B 2013;1(47):6516-6524.
7. Jones AJ, Bee JA. Age-Related and Position-Related Heterogeneity of Equine Tendon Extracellular-Matrix Composition. Research in Veterinary Science 1990;48(3):357-364.
8. Lin YL, Brama PAJ, Kiers GH, van Weeren PR, DeGroot J. Extracellular matrix compositon of the equine superficial digital flexor tendon: Relationship with age and anatomical site. Journal of Veterinary Medicine Series a-Physiology Pathology Clinical Medicine 2005;52(7):333-338.
9. Liu HH, Zhu SA, Zhang C, Lu P, Hu JJ, Yin Z, Ma Y, Chen X, OuYang HW. Crucial transcription factors in tendon development and differentiation: their potential for tendon regeneration. Cell and Tissue Research 2014;356(2):287-298.
10. Murchison ND, Price BA, Conner DA, Keene DR, Olson EN, Tabin CJ, Schweitzer R. Regulation of tendon differentiation by scleraxis distinguishes force-transmitting tendons from muscle-anchoring tendons. Development 2007;134(14):2697-2708.
11. Reed SA, Johnson SE. Expression of scleraxis and tenascin C in equine adipose and umbilical cord blood derived stem cells is dependent upon substrata and FGF supplementation. Cytotechnology 2014;66(1):27-35.

12. Birch HL, Bailey JVB, Bailey AJ, Goodship AE. Age-related changes to the molecular and cellular components of equine flexor tendons. Equine Veterinary Journal 1999;31(5):391-396.
13. Ryan CN, Sorushanova A, Lomas AJ, Mullen AM, Pandit A, Zeugolis DI. Glycosaminoglycans in Tendon Physiology, Pathophysiology, and Therapy. Bioconjugate chemistry 2015;26(7):1237-1251.
14. Kim SJ, Jang DH, Park WH, Min BM. Fabrication and characterization of 3-dimensional PLGA nanofiber/microfiber composite scaffolds. Polymer 2010;51(6):1320-1327.
15. Orr SB, Chainani A, Hippensteel KJ, Kishan A, Gilchrist C, Garrigues NW, Ruch DS, Guilak F, Little D. Aligned multilayered electrospun scaffolds for rotator cuff tendon tissue engineering. Acta Biomaterialia 2015;24:117-126.
16. Yin Z, Chen X, Chen JL, Shen WL, Nguyen TMH, Gao L, Ouyang HW. The regulation of tendon stem cell differentiation by the alignment of nanofibers. Biomaterials 2010;31(8):2163-2175.
17. Ker ED, Nain AS, Weiss LE, Wang J, Suhan J, Amon CH, Campbell PG. Bioprinting of growth factors onto aligned sub-micron fibrous scaffolds for simultaneous control of cell differentiation and alignment. Biomaterials 2011;32(32):8097-8107.
18. Chainani A, Hippensteel KJ, Kishan A, Garrigues NW, Ruch DS, Guilak F, Little D. Multilayered Electrospun Scaffolds for Tendon Tissue Engineering. Tissue Engineering Part A 2013;19(23-24):2594-2604.
19. Chen R, Huang C, Ke QF, He CL, Wang HS, Mo XM. Preparation and characterization of coaxial electrospun thermoplastic polyurethane/collagen compound nanofibers for tissue engineering applications. Colloids and Surfaces B-Biointerfaces 2010;79(2):315-325.
20. Kazanci M. Solvent and temperature effects on folding of electrospun collagen nanofibers. Materials Letters 2014;130:223-226.
21. Zhong SP, Teo WE, Zhu X, Beuerman RW, Ramakrishna S, Yung LYL. An aligned nanofibrous collagen scaffold by electrospinning and its effects on in vitro fibroblast culture. Journal of Biomedical Materials Research Part A 2006;79A(3):456-463.
22. Gilchrist CL, Ruch DS, Little D, Guilak F. Micro-scale and meso-scale architectural cues cooperate and compete to direct aligned tissue formation. Biomaterials 2014;35(38):10015-10024.
23. Kishore V, Bullock W, Sun XH, Van Dyke WS, Akkus O. Tenogenic differentiation of human MSCs induced by the topography of electrochemically aligned collagen threads. Biomaterials 2012;33(7):2137-2144.
24. Nain AS, Sitti M, Jacobson A, Kowalewski T, Amon C. Dry Spinning Based Spinneret Based Tunable Engineered Parameters (STEP) Technique for Controlled and Aligned Deposition of Polymeric Nanofibers. Macromolecular Rapid Communications 2009;30(16):1406-1412.
25. Sheets K, Wang J, Meehan S, Sharma P, Ng C, Khan M, Koons B, Behkam B, Nain AS. Cell-fiber interactions on aligned and suspended nanofiber scaffolds. Journal of Biomaterials and Tissue Engineering 2013;3(4):355-368.

26. Wang J, Nain AS. Suspended micro/nanofiber hierarchical biological scaffolds fabricated using non-electrospinning STEP technique. Langmuir 2014;30(45):13641-13649.
27. Schindelin J, Arganda-Carreras I, Frise E, Kaynig V, Longair M, Pietzsch T, Preibisch S, Rueden C, Saalfeld S, Schmid B and others. Fiji: an open-source platform for biological-image analysis. Nat Meth 2012;9(7):676-682.
28. Stewart AA, Barrett JG, Byron CR, Yates AC, Durgarn SS, Evans RB, Stewart MC. Comparison of equine tendon-, muscle-, and bone marrow-derived cells cultured on tendon matrix. American Journal of Veterinary Research 2009;70(6):750-757.
29. Farndale RW, Buttle DJ, Barrett AJ. Improved quantitation and discrimination of sulphated glycosaminoglycans by use of dimethylmethylene blue. Biochimica et Biophysica Acta (BBA)-General Subjects 1986;883(2):173-177.
30. Voleti PB, Buckley MR, Soslowsky LJ. Tendon Healing: Repair and Regeneration. Annual Review of Biomedical Engineering, Vol 14 2012;14:47-71.
31. Youngstrom DW, Barrett JG, Jose RR, Kaplan DL. Functional Characterization of Detergent-Decellularized Equine Tendon Extracellular Matrix for Tissue Engineering Applications. Plos One 2013;8(5).
32. Younesi M, Islam A, Kishore V, Anderson JM, Akkus O. Tenogenic Induction of Human MSCs by Anisotropically Aligned Collagen Biotextiles. Advanced Functional Materials 2014.
33. McBeath R, Pirone DM, Nelson CM, Bhadriraju K, Chen CS. Cell Shape, Cytoskeletal Tension, and RhoA Regulate Stem Cell Lineage Commitment. Developmental Cell;6(4):483-495.
34. Miyoshi H, Adachi T. Topography design concept of a tissue engineering scaffold for controlling cell function and fate through actin cytoskeletal modulation. Tissue Engineering 2014(ja).
35. Yin Z, Chen X, Song H-x, Hu J-j, Tang Q-m, Zhu T, Shen W-l, Chen J-l, Liu H, Heng BC and others. Electrospun scaffolds for multiple tissues regeneration in vivo through topography dependent induction of lineage specific differentiation. Biomaterials 2015;44:173-185.
36. Maharam E, Yaport M, Villanueva NL, Akinyibi T, Laudier D, He Z, Leong DJ, Sun HB. Rho/Rock signal transduction pathway is required for MSC tenogenic differentiation. Bone research 2015;3:15015.
37. Subramony SD, Dargis BR, Castillo M, Azeloglu EU, Tracey MS, Su A, Lu HH. The guidance of stem cell differentiation by substrate alignment and mechanical stimulation. Biomaterials 2013;34(8):1942-1953.
38. Moffat KL, Kwei AS-P, Spalazzi JP, Doty SB, Levine WN, Lu HH. Novel nanofiber-based scaffold for rotator cuff repair and augmentation. Tissue Engineering Part A 2008;15(1):115-126.
39. Franchi M, Torricelli P, Giavaresi G, Fini M. Role of moderate exercising on Achilles tendon collagen crimping patterns and proteoglycans. Connective tissue research 2013;54(4-5):267-274.

Chapter 3: Homing of Mesenchymal Stem Cells

I. Introduction

Mesenchymal stem cells (MSCs) exhibit great potential for treatment in various injuries, musculoskeletal diseases, [1] and inflammatory diseases including osteoarthritis, [2] rheumatoid arthritis, [3] and wound healing, [4,5]. MSCs demonstrate both trophic immunomodulatory and regenerative affects; [6,7] MSC treatment of arthritic diseases has shown replacement of damaged tissue, immunomodulation, and anti-inflammatory effects [8]. Studies of intra-articular injection of MSCs for osteoarthritis joints have shown increased function, improved pain, and reduced defect size [3,9]. The overarching barrier to optimization of these treatments is the ability of MSCs to migrate to the site of inflammation and engraft in adequate numbers to induce their therapeutic effects. Intravenous administration of MSCs commonly results in a large proportion of cells being trapped in filter organs, particularly the lungs, while the remaining cells that reach the target organ are soon removed.

Inflammation stimulates endogenous homing and the release of stem cells from the bone marrow or surrounding tissues [10]. Systemic and local administration mobilizes MSCs through the peripheral blood or is delivered locally to the injured tissue. Several factors and limitations of MSC homing control the effectiveness of these routes. MSC homing is generally defined as cell arrest within the vessel, known as localization and transendothelial migration, known as homing [10]. This review will focus on the mechanisms of endogenous and exogenous MSC homing, the stages of homing from rolling through transmigration, and *in vitro* and *in vivo* models used to study homing. Cell

culture factors determining the efficiency of homing include cell density during culture, cell age, tissue of origin, and growth conditions. Challenges in MSC delivery include the timing of delivery, administrative route, cell number, and number of doses [10]. Additionally, each tissue type has a different composition and structure that must be considered for stem cell therapy. Tendon, ligament, and cartilage are dense connective tissues that have low cellularity and vascularity that create additional challenges [1].

Gaps in our current knowledge and understanding, in addition to culture and delivery of stem cells, include cell tracking, mechanisms of trafficking, and post-homing characterization. The processes of endogenous MSC mobilization to or within the target tissue and administered MSC mobilization and tissue engraftment are not fully defined and characterized [11]. Additionally, enhancing MSC recruitment to control the leukocyte cascade can potentially regulate the immune response and prevent uncontrolled inflammation and tissue disease. Studies have investigated intravasation (cell migration from tissue into a blood vessel), extravasation (cell migration from a blood vessel into tissue), and invasion mechanisms of MSCs, immune cells, and cancer cells in *in vitro* and *in vivo* studies. These processes are tightly controlled through a series of specific cell-cell and cell-matrix interactions.

Homing Stimulators: Inflammation, Chemokines, and the Endothelium

The innate immune system seeks out invaders and initiates a localized inflammatory response when encountered. Inflammation is a normal and necessary process in healing after infection or injury. The process involves the release of cytokines, activation and dilation of blood vessels, the recruitment of leukocytes and resolution. An insufficient response leads to immunodeficiency resulting in infection or cancer, while

excessive response leads to degenerative diseases such as synovitis, [12] osteoarthritis (OA), [2] and rheumatoid arthritis (RA) [13]. Inflammation spreading into the blood stream leads to severe results such as septic shock syndrome and meningitis [14].

The endothelium consists of a layer of endothelial cells lining the luminal side of blood vessels and arteries, creating a barrier between the blood flow and the tissue stroma. The protective barrier controls the passage of molecules, ions, proteins, and cells. Endothelial cells are critical regulators of inflammation and leukocyte transmigration. These capabilities allow the endothelium to maintain homeostasis in the body; dysfunction can be a symptom of disease or lead to the development of disease. Basal conditions maintain an anticoagulant response. Injury or activation leads to production of fibrin; tissue plasminogen activator (tPA), urokinase plasminogen activator (uPA), nitric oxide (NO), plasminogen activator inhibitor-1 (PAI-1), and von Willibrand factor (vWF). Injury leads to endothelial responses of vasoconstriction, decreased barrier integrity, increased leukocyte adhesion, and inflammation. Vasoconstriction produces endothelin-1 (ET-1), PDGF-B, thromboxane, and vascular endothelial growth factor (VEGF).

Recruitment of cells to sites of inflammation and injury results in changes of morphology, cytoskeletal organization, gene expression, and cell signaling. Endothelial cell responses to inflammation include activation, adhesion, and transmigration of leukocytes in a highly controlled sequence of cell interactions including cytoskeletal organization within and between endothelial cells and immune cells. Activation can change the microenvironment from nonadhesive to adhesive recruiter and procoagulant, contributing to the inflammatory process [15].

The cytokine tumor necrosis factor - alpha (TNF-α) is produced by activated macrophages in response to stimuli and serves as a mediator of local and systemic inflammation. Local release results in the cardinal signs of inflammation of heat, pain, swelling, and redness. Systemic release depresses cardiac output, and results in microvascular thrombosis, and capillary leakage syndrome. TNF-α amplifies the response by activating the release of cytokines and mediators that promote inflammation [14].

Chemokines have been studied for their influence on leukocyte function as well as serving additional physiological and pathological functions. There are 40-50 different chemokines within four different families characterized by structural and genetic factors; CXC, C, CC, and CX_3C. Chemokines have 3 β-pleated, C-terminal alpha sheets and conserved cysteines. Rollins *et al.* described chemokines according to their family including CXC (interleukin-8, IL-8; stromal derived factor-1, SDF-1) and CC (monocyte chemoattractant protein, MCP; macrophage inflammatory proteins, MIP) chemokines [16]. More recently, chemokine mechanisms are being investigated as chemoattractants to tissue damage and disease progression for repair and intervention. For example, chemokines and their receptors have been studied for their role in MSC homing towards inflammation to myocardial infarction and to understand how culture conditions influence the therapeutic potential of MSCs [17].

The most commonly studied chemokine and receptor in migration is the SDF-1/CXCR4 axis. Granero-Molto *et al.* used a stabilized fracture model to demonstrate MSC migration towards SDF-1. Tibia fractures in mice were treated with MSCs expressing *Firefly Luciferase* for bioluminescence imaging. MSCs migrated in a CXCR4 and time-dependent manner. $CXCR4^+$ MSCs showed that the majority of lost MSCs were

maintained in the lung while the remaining MSCs were visualized at the fracture site at day 3 and were maintained for 14 days. However, CXCR4$^-$ MSCs were lost in the lung and were eliminated by day 3. MSCs without selection were dispersed throughout the lungs and both the injured and healthy tibia [6]. In another study, Gao *et al.* investigated the effects of SDF-1 in MSC migration towards tumor cell conditioned medium and identified involvement of cell signaling pathways associated with SDF-1-stimulated MSCs [18]. Inflammatory and homing molecules stimulate trafficking of otherwise dormant endogenous stem cells.

Endogenous Stem Cell Homing

Endogenous stem cell response to injury is an alternative to administration of exogenous stem cells that are limited due to isolation and cell culture procedures. Understanding the stimuli and molecular mechanisms induced is critical for recruitment of this population and maintaining viability in harsh injury conditions. Targeting stem cells (Fig. 3.1) has been studied using growth factors as chemoattractants, [19,20] biologics, and small molecules to promote regeneration. In addition to growth factors, several chemokines have been identified in endogenous MSC homing; SDF-1 (stromal derived factor 1), MCP1 (monocyte chemoattractant protein-1), MIP-1α (macrophage inflammatory protein- 1α), IL-8, RANTES (regulation on activated T cell expressed and secreted), MDC (macrophage-derived chemokine), fractalkine, SLC (secondary lymphoid tissue chemokine), and TARC (thymus and activation regulated chemokine) [21]. Studies investigating cell signaling in diseased states have identified mechanisms in endogenous stem cell recruitment [22].

Wound healing has been commonly studied as an injury model for endogenous homing [23]. Kosaraju *et al.* used a hydrogel seeded with adipose stem cells (ASCs) to induce endogenous migration, proliferation, and tubulization of bone marrow mesenchymal progenitor cells for wound healing [24]. Amplification of chemokine signaling at the wound site or modification of MSC chemokine receptors are used to enhance endogenous and exogenous stem cell homing efficiency; specifically CXCR4/SDF-1, CCL27/CCR10, and CCL21/CCR7 [25].

Stem cell niches in musculoskeletal tissues have also been extensively studied, specifically cartilage, [26] bone, [27] and tendon [28]. Chen *et al.* developed a collagen scaffold with horizontal and vertical channels with SDF-1 for cell migration into cartilage defects. An *in vivo* rabbit injury model showed cartilage regeneration after implantation of these radial oriented scaffolds with SDF-1 when compared to random oriented scaffolds without SDF-1 [29]. In another study, Zhang *et al.* developed a live hyaline cartilage graft with SDF-1 for endogenous stem cell recruitment. The graft promoted SDF-1 release and cell trafficking into the peripheral blood and the implant with enhanced chondrogenesis [30]. In addition to chemokine stimulation, transcriptional profiling has been used to identify niche mRNAs [23] and interference of signaling pathways [31]. SDF-1 delivered in an injectable hydrogel promoted recruitment of MSCs in response to chemokine from a damaged disk. This study suggests tissue-specific chemokines induce endogenous MSCs. The authors identified chemokines from damaged disk cells by proteomic analysis of their conditioned medium as CCL5/RANTES and CXCL6 [32]. Delivery of CXCR4 antagonist and SDF-1 into a titanium implant to study the CXCR4/SDF-1 chemotaxis axis improved bone anchorage and attracted the native stem cell population [33]. Lee *et al.*

identified an endogenous tendon $CD146^+$ stem/progenitor cells for tendon healing. $CD146^+$ tendon cells were treated with connective tissue growth factor (CTGF) and showed an increase in proliferation and tendon differentiation via FAK/ERK1/2 signaling [34].

Several other tissue-specific niches have been identified including those of the brain, [35] heart, [36] liver, [37] and gastrointestinal tract [38]. These niches have also been mimicked for investigation of stem cell recruitment in injury and disease states. Arvidsson *et al.* showed that after stroke, endogenous cells coordinated migration of new neurons and neuroblasts to damaged striatum and had gene expression of developing and mature biomarkers [39]. In another study, PGE_2 (prostaglandin E2) induced cardiomyocyte recruitment after myocardial infarction with optimal treatment 7-10 days after injury. Stem cell recruitment was controlled through EP2 receptor signaling and microenvironmental changes [40]. In other studies, MSC administration activated other endogenous cell populations to promote healing and re-establishment of homeostasis. Granulocyte colony-stimulating factor (G-CSF) primed bone marrow stem cells; however, local cell populations showed greater contribution to repair after chemically-induced liver injury [41]. Sémont *et al.* administered MSCs for radiation-induced gastrointestinal alterations (GIT) and showed endogenous epithelial cell homeostasis through cell proliferation and anti-apoptotic effects [42]. Endogenous stem cells are recruited in low numbers that decrease their therapeutic potential. However, large numbers of stem cells are injected via various routes including intravenous and local injection to improve efficacy.

Exogenous Stem Cell Homing

Challenges associated with exogenous stem cell homing studies are changes in expression of cell surface adhesion proteins and the associated molecular and phenotypic changes that occur after collecting and culture procedures. Additionally, the lack of local and systemic environmental cues and the absence of other cell populations normally found in the niche alter cell-matrix and cell-cell communication that regulate cell functions (Fig. 3.1). A common approach to overcome alterations due to cell culture is to engineer cell surface molecules on MSCs to restore and enhance migration capabilities. In one study, rapid engineering of MSCs with recombinant CXCR4 enhanced migration towards an SDF-1 gradient in peripheral blood post-MI. This 10 minute engineering method can be applied to a variety of stem cell therapies where chemotactic gradients last less than 48 hours [43].

Several challenges of administration affect MSC efficiency and efficacy; cell type, route of administration, number of cells, number of doses, timing after injury, and culture conditions including pre-treatments. Wei *et al.* used intranasal administration of hypoxia-treated bone marrow-derived MSCs after ischemic stroke. MSCs were delivered at $1x10^6$ cells/animal 24 hours after stroke, MSCs migrated to the vasculature of the ischemic cortex at 1.5 hours, and reparative effects were observed after 4 days [44]. The number of doses required for complete tissue repair is unknown. Guo *et al.* administered repeated doses of cardiac MSCs that showed improvement over a single dose of MSCs for myocardial infarction (MI) and ventricular function improved after each dose [45].

Chemokines are extensively used for exogenous stem cells due to their ability to enhance migration and for investigation of the associated signaling pathways that activate

corresponding cell surface receptors. Lourenco *et al.* investigated the role of macrophage migratory inhibitor factor (MIF) in MSC chemotaxis towards a tumor microenvironment. Results showed that MIF interacted dominantly with CXCR4 and activated MAPK signaling in homing to tumor sites [46]. Tissue-engineered bioactive materials have been used to enhance homing via pre-loaded scaffolds or recruitment towards a biochemical implant [47]. Naderi-Meshkin *et al.* used an injectable SDF-1 hydrogel with hypoxia-treated MSCs to induce cell retention *in vivo* [48]. In another study, a subcutaneously implanted hydrogel delivered SDF-1 and pre-conditioned human ASC homing in a rat model [48]. Song *et al.* used a SDF-1 and angiogenic peptide (Ac-SDKP) loaded hydrogel for cardiac repair after chronic myocardial infarction. Findings showed increased ventricle function, angiogenesis, and enhanced mature vessel formation [49]. In another study, chitosan biphasic biomaterial with affinity peptide binding for MSCs promoted homing and cartilage regeneration [50]. Combining factors for MSC homing may enhance efficiency and regenerative effects. The combination of VEGF and BMP-2-loaded silk scaffolds in a rabbit injury model promoted bone regeneration via mobilization, endothelial differentiation, and bone differentiation [51].

Several studies use animal models alone or in combination with an *in vitro* model. Plasminogen treatment activated CXCR4 expression of MSCs towards myocardial infarction through matrix metalloproteinase-9 (MMP-9) [52]. Bensidhoum *et al.* administered Stro-1^+ and Stro-1^- MSC subsets into NOD/SCID mice. Results differed depending on the target organ; Stro-1^+ cells were found in muscle, spleen, bone marrow, and kidneys and Stro-1^- cells localized to the lungs. Findings suggest that Stro-1^+ may be useful for tissue engraftment and Stro-1^- for hematopoietic engraftment towards

therapeutic application [53]. Colvin *et al.* studied allogeneic homing in myeloablated mice. Homing was complete in less than one hour and showed a decrease in secondary engraftment capabilities [54]. In another study, CCR7-guided MSC infusion and engraftment near T lymphocytes in secondary lymphoid organs for immunomodulation [55]. Contributions of *in vitro* and *in vitro* studies have provided insight into the processes and mechanisms that develop our foundation of MSC homing.

Several approaches are used in cell tracking as reviewed by Nguyen *et al.* and play an important role in studying and developing these treatments. Detection methods include ultrasonography, CT, MRI, PET, fluorescence, bioluminescence, and SPECT [56]. Wu *et al.* used ultrasound-targeted microbubble destruction to deliver SDF-1 to the diseased kidney, followed by administration of MSCs. Results showed an increase in MSC homing efficiency in SDF-1 primed nephropathy kidneys compared to the non-primed kidneys in normal and diseased rats [57]. Tritto *et al.* showed hematopoietic stem cell homing towards post-ischemic tissue. Direct monitoring using intravital imaging showed an increase in rolling and adhesion as ischemia duration increased [58]. In another study, Huang *et al.* used iron-based magnetic nanoparticles (MNPs) for MSC tracking and enhanced MSC surface expression of CXCR4. Therefore, the labeled MSCs could be used for *in vivo* tracking and improvement of MSC homing efficiency [59]. MSC penetration of endothelium was observed in perfusion of an isolated mouse heart model after 60-90 minutes through tissue fixation and three-dimensional (3D) reconstruction of confocal images [60]. While stem cells are promising therapies, progress has been hampered by our general lack of understanding of stem cell mechanisms of action. Investigating stem cell migration through blood vessels and interactions with the

endothelium will provide insight into these mechanisms for enhancing treatment outcomes.

II. Stages of Homing

Leukocytes have defined stages and mechanisms for transendothelial migration (TEM); rolling, tethering, adhesion, paracellular/transcellular migration, and invasion [61]. Mechanisms of MSC homing have yet to be fully defined and definitions remain general. Steingen *et al.* identified 5 stages of transmigration; initial contact, adhesion, spreading, integration, and transmigration [60]. This review will cover leukocyte, MSC, and cancer cell transmigration with a focus on MSC homing. The leukocyte cascade is often used as a foundation to study MSC behavior and cell signaling in homing. The stages of TEM are under tight spatial-temporal control and complex coordinated signaling. The schematic compares the similarities and differences in interactions between leukocytes and MSCs on the endothelium including adhesion, migration, protrusions, and transmigration (Fig. 3.1).

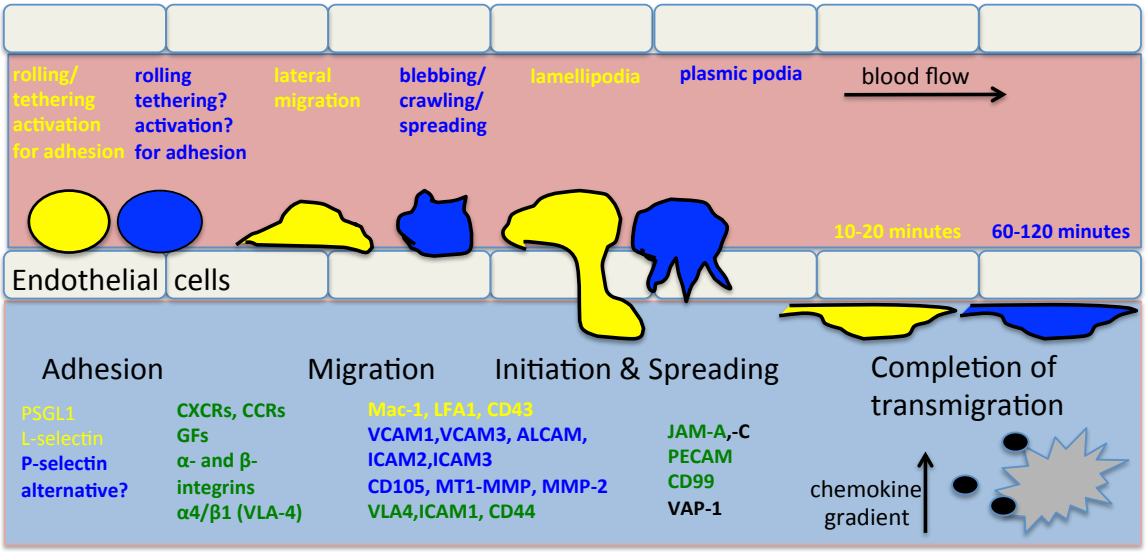

Figure 3.1: Comparison of leukocyte and MSC transendothelial migration within a capillary venule through the stages of rolling on the endothelium, migration, and transmigration in response to inflammatory conditions. Leukocytes, yellow; mesenchymal stem cells, blue; shared characteristics, green.

Rolling on the Endothelium

Leukocytes are normally found circulating in the blood; however, they can be recruited to the endothelium and initiate an inflammatory response. Chemokines typically promote activation and recruitment of leukocytes to injured tissues and trigger the immune response [62]. Chemokines produced by endothelial cells or interstitial immune cells pass through to the luminal surface and bind to glycosaminoglycans, specifically heparin sulfate glycosaminoglycans (GAGs). As postcapillary venules of the tissue are exposed to inflammatory stimuli, blood vessels narrow and blood flow decreases to allow leukocytes to come in closer contact with the endothelium. Leukocytes use L-selectin and P-selectin glycoprotein-1 (PSGL-1) for tethering and rolling on the endothelium. MSCs lack the adhesion molecules found in leukocytes and tethering and rolling require further investigation since limited studies on MSC rolling exist. However, one study investigated rolling and adhesion on human umbilical vein endothelial cells (HUVECs) with shear stress up to 2 dynes/cm^2, after TNF-α treatment. Intravital imaging showed that MSC rolling and adhesion in postcapillary venules are dependent on P-selectin in a mouse model under specific non-flow/flow conditions [63]. Adhesion molecules and integrins, activated by inflammation, aid in this contact by interacting with E-selectins and chemokine exposure on the luminal surface of the activated endothelial cells. Endothelial cells express E-selectin and bind to leukocyte ligand, PSGL1. MSCs exhibit similarities to cancer cells in morphology during the early stages of transmigration. The morphology of cancer cells can be mesenchymal or amoeboid migration, depending on the

environmental conditions. While there is still some debate as to whether MSCs become entrapped in the blood vessel or use active mechanisms to transmigrate, cancer cells use the former to become restricted in the vessel and form firm attachments. All cell types must survive intravasation and circulation, including immune cell interactions, to adhere to the endothelium.

Similar to MSC homing, metastasis is also an inefficient process as only a small subset of cancer cells will migrate from the primary tumor towards metastasis [64]. Migration occurs as a single cell or collectively through mesenchymal and amoeboid migration modes depending on microenvironmental factors. Selectin ligands for rolling include tetrasaccharide sialyl Lewis X (SeL^x) antigen, a sialofucosylated glycoform of CD44, known as hematopoietic cell E-selectin/L-selectin ligand (HCELL), PSGL1, CD24, mucin 1 (MUC1), and galectin-3-binding protein (LGALS3BP). Endothelial cells express E-selectin that may contribute to endothelial cell and cancer cell interaction after macrophage recruitment. N-cadherin is expressed by endothelial cells for cancer cell rolling and adhesion as well as expressed by cancer cells *in vitro*. Rolling has not been observed in cancer cells *in vivo*. However, ligands for E-selectin have been studied *in vitro*. Different adhesion molecules have been identified, including N-cadherin, αvβ3 integrin, β1, β4, α6β4, and α2β1 integrins. Bauer at al. profiled 45 human tumor cell transmigration and identified αvβ3 integrin as one of the key players [65]. MSCs may use mechanisms more similar to cancer cells than leukocytes at these stages.

Adhesion to the Endothelium

Chemokines bind specific chemokine receptors on the leukocyte, activating downstream signaling for integrin expression, resulting in firm adhesion and arrest.

Chemokines and cytokines also stimulate MSC recruitment. Bone marrow-derived MSCs use α1, α2, α3, α4, α5, αv, β1, β3, β4, and β5 integrins and adipose-derived MSCs (ASCs) use α1-11, αv, αx, α2b, β1- 5, and β8 integrins [66]. Krstić *et al.* studied the effects of the proinflammatory cytokine interleukin-17 (IL-17) on peripheral blood-derived MSC to enhance transmigration [67]. Leukocyte adhesion requires β1 integrins, very late antigen-4 (VLA-4), CD49d/CD21, and α4/β1 and β2 (CD18) integrins that bind to intercellular adhesion molecule-1 (ICAM1) and intercellular adhesion molecule-2 (ICAM2) on endothelial cells. Activation and binding leads to leukocyte arrest and crawling. MSCs use α integrins and β integrins alone or in combination, specifically α4/β1 binding to fibronectin [68] and various chemokine receptors depending on tissue type and extracellular matrix (ECM) proteins. Engineering MSCs is a common approach to overcome the lack of adhesion molecules after culture. Chuo *et al.* used fucosyltransferase VI transfection for fucosylation of CD44 to HCELL (hematopoietic cell E-/L-selectin ligand). HCELL positive MSCs increased homing to hypoxic endothelial cells in injured kidney when compared to HCELL negative MSCs [69]. Cancer cell adhesion mechanisms also function through CD44, MUC1, and α and β subunit integrins. MUC1 binds to ICAM, E-selectin, and galectin 3 on endothelial cells. Cancer cell receptors differ depending on cancer type and vasculature bed; tumor cells will target specific organs and their associated chemokines [70].

Transendothelial Migration

Leukocytes migrate via lamellipodia migration on the endothelium using Mac-1 (Cd11b/CD18) whereas there is no lateral migration of MSCs when determining the site of TEM. Following leukocyte migration on endothelial cells, leukocytes transmigrate

through the endothelium, the pericyte-containing basement membrane, and finally into the interstitial tissue [61,71]. TEM at endothelial cell borders is similar to cell adhesion because it is mediated by integrins and adhesion molecule combinations, specifically Mac-1 with ICAM-1 [61]. TEM occurs through a paracellular route, between the borders of endothelial cells, and a transcellular route, through the endothelial cell body. TEM initiates the inflammatory response and begins the irreversible stage of the inflammatory cascade. Leukocytes initiate TEM with a single leading edge using CD99, CD11a/CD18, CD11b/CD18, VLA-4, CD49d/CD29, and LFA-1. Several changes occur at this stage including a switch from heterophilic interactions to homophilic interactions of platelet endothelial cell adhesion molecule-1 (PECAM-1) and CD99 between leukocytes and endothelial cells. Other interactions include vascular cell adhesion protein -1 (VCAM-1), junctional adhesion molecule-A (JAM-A), and vascular endothelial cadherin (VE-cadherin) that will be discussed in the section on endothelial cell processes.

Schmidt et al. provided early evidence of MSC transmigration using both *in vitro* and *in vivo* models. Co-culture experiments showed MSC flattening and integration into the endothelial monolayer after 2 hours. Electron microscopy of perfused hearts showed direct cell to cell contacts of MSCs. Confocal microscopy visualized complete MSC transmigration through the endothelium with transmigration peaking at 50.0 +/- 8.0% at 1 hour [72]. Growth factors in the ECM can regulate MSC recruitment by activation or inactivation of signaling pathways to promote or inhibit TEM; bFGF activates or deactivates Akt signaling depending on the concentration [73]. In another study, Steingen *et al.* investigated the mechanisms in transmigration and invasion of MSCs in a co-culture system. Results showed that activation of endothelium was not required for MSC

adhesion and integration. Additionally, transmigration differences were due to endothelial cell type with myocardium venous endothelial cells resulting in the greatest transmigration of MSCs. Lastly, MSCs used plasmic podia protrusions, VACM-1, VLA-4, clustering of β1 integrin, and secretion of MMP-2 in transmigration [60]. Additionally, Law *et al.* reported that MSCs were capable of migration through blebbing and the use of multiple leading protrusions and molecules including VCAM-1, ICAM-1, ICAM-3, activated leukocyte cell adhesion molecule (ALCAM), and endoglin/CD105 [74].

Several types of endothelial cells have been used in co-culture transwell systems to study MSC homing (Table 3.1). Chamberlain *et al.* showed MSC adhesion, crawling, spreading, and transmigration across aortic endothelial cells [68]. Smith *et al.* investigated MSC intra- and extravasation through bone marrow endothelium and observed that MSCs transmigrated in both apical-to-basal and basal-to-apical directions. However, different chemokines were more effective than others, depending on the direction of TEM; CXCL22 was more efficient in the apical chamber and CCL16 was more efficient in the basal chamber [75]. Smith *et al.* studied the stages of homing by pre-treating human adipose-derived MSCs with glioma conditioned media and ECM proteins. Results showed enhanced homing towards brain cancer conditions and tumor samples *in vitro* and *in vivo* [76]. In another study, Feng *et al.* studied human MSC transmigration through human microvascular endothelial cells to mimic the microenvironment of the blood brain barrier. Results showed that MSC production of CXCL11 bound to the endothelial receptor CXCR3, disassembled tight junctions, activated endothelial ERK1/2 signaling, and promoted MSC transmigration [77]. De Becker *et al.* studied MSC migration through bone marrow endothelium; results showed that transmigration was partially regulated by

matrix metalloproteinase-2 (MMP-2) and tissue inhibitor of metalloproteinase-3 (TIMP-3) [78]. Other studies have shown supporting evidence of MMP-2 involvement in MSC TEM [60]. The Toll-like receptors (TLRs), TLR3, TLR4, TLR2/3, and TLR9 have been shown to promote MSC migration and TEM signaling [79,80]. Specifically, TLR-3 pre-treatment of umbilical MSCs induced MSC homing to an induced colitis mouse model via activation of Jagged-1 Notch-1 signaling [81].

In contrast, cancer stem cells are capable of proliferating on the endothelium before transmigration and collectively migrating, known as micrometastases that further develop into macrometastases. Proliferation can also occur after invasion of the basement membrane, result in dormancy or cell death. Transmigration occurs through interactions with selectins, integrins, CD44, cadherins, and Ig superfamily receptors. In TEM, it is unclear which routes are used *in vivo*. TEM is slower in cancer cells than in leukocytes and the endothelium exhibits a slow re-seal or no seal after prolonged opening. Cancer cell αVβ3 integrin and endothelial cell PECAM-1 interactions are observed at this stage and vascular endothelial growth factor (VEGF) and transforming growth factor beta 1 (TGF-β1) are secreted by cancer cells to disrupt VE-cadherin endothelial cell binding [70]. The most commonly studied chemokine, CXCL12/SDF-1, is secreted by target organ stromal cells. SDF-1 promotes cell adhesion and TEM of cancer cells through CXCR4 and CXCR7 ligands. Parmo-Cabañas *et al.* investigated cell signaling of bone marrow myeloma cells and myeloma-derived cells in TEM. Integrin expression of α4β1 was upregulated in response to SDF-1 exposure and modulated by cAMP activation of protein kinase A and RhoA activation of cytoskeletal rearrangement [82]. Gene expression profiling of brain cancer metastasis has identified cyclooxygenase-2 (COX2), epidermal growth

factor receptor ligand (EGFRL), heparin binding EGF-like growth factor (HBEGF), and the α-2,6-sialyltransferase ST6GALNAC5 as additional mediators of TEM [83]. Osteopontin (OPN) has been identified as a regulator required for MMP activation in cancer cell invasion [84,85]. Results showed level dependent effects on signaling contributing to cell migration, tumor growth, and metastasis. Nanomolar concentrations promoted PI3K and Akt phosphorylation and micromolar concentrations promoted PI3K production of uPA, MMP activation, and tumor growth. The authors concluded that cell type, source, and concentration levels influence signaling towards cancer progression [86]. In another study, Wu *et al.* studied cell signaling in inflammation-mediated metastasis. This includes the progression of inflammation to cancer and regulation of the tumor microenvironment through TNF-α. Additionally, this study investigated NFκB and Snail regulation of cancer progression. The authors conclude that TNF-α controls Snail and β-catenin through NFκB and Akt signaling for epithelial-mesenchymal transition (EMT) and tissue invasion [87].

As with leukocytes, CD44 and MUC1-ICAM1 are key players in cancer cell transmigration. Multiple adhesion receptors are present depending on the types of cancer and vascular cells. Multiple therapeutic targets may need to be explored for prevention of adhesion and metastasis. Both routes of transendothelial migration have been observed. Pathways of importance include the Rho-ROCK/Rac, PI-3K, p38 and ERK/MAPK, and JAK/STAT pathways for secretion, to control cancer cell protrusions, endothelial contraction, and disassembly of endothelial cell junctions in TEM [70]. Investigating these genes and signaling pathways in cancer cell TEM may contribute to our understanding of MSC TEM mechanisms.

Schnoor *et al.* reviews the differences and similarities between molecules used in TEM by different types of leukocytes; neutrophils, monocytes, macrophages, and eosinophils. All cells were found to use JAM-A, JAM-L, JAM-C, PECAM-1, DNAX accessory protein-1 (DNAM-1), CD155, and CD99. They differ in other TEM regulatory proteins; neutrophils use Mac1, norepinephrine (NE), vascular adhesion protein 1(VAP-1), and JAM-A, monocytes use VAP-1 and JAM-A, T cells use Mac1 and NE, and endothelial cell occludin and JAM-C [88]. Additional molecules have been identified in NK cells [89], neutrophils [90], and monocytes [91]. Similarly, different sources and types of stem cells may also show specific TEM mechanisms.

Other factors potentially influence TEM of leukocytes, MSCs, and cancer cells. Tumor cells can interact with the endothelium by secretion of permeability factors. For example, ascites fluid has been shown to accumulate within the luminal side of the vessels, increasing permeability of the endothelium [92]. As discussed in Chapter 1, MSCs synthesize numerous proteins that can interact with endothelial cells in a similar manner. Evidence also suggests that MSCs can undergo TEM with aid from other cell types. Intravascular MSCs interact with platelets and neutrophils to promote adhesion and TEM. In one study, 42.8 +/- 24.8% of MSCs associated with platelets and neutrophils during trafficking [93].

The contact and communication between pericytes and endothelial cells contribute to the integrity and passage through the endothelium. Changes in pericyte concentration and spreading occur throughout the microvasculature. Pericytes are more numerous and thinner on the arteriolar end and more dispersed on the venular end. Pericytes have gained more attention recently for their role in inflammation through

MyD88 signaling, [94] NOD-like receptors (NLRs), Toll-like pattern recognition receptors (TLRs), and secretion of IL-1β [95]. Leaf *et al.* showed that pericytes activated proinflammatory signaling through TLR-2/4- MyD88, and secretion of IL-1β regulated tissue injury inflammation. In another study, Nyúl-Tóth *et al.* investigated pericyte control of brain inflammation, specifically activation of non-canonical inflammasome pathway [95]. These studies provide evidence of the complex signaling that occurs within and between cell types in inflammation that could potential affect MSC TEM.

Migration likely persists through the path of least resistance through the endothelium and basement membrane [61]. The mechanical properties of the vascular bed *in vivo* and endothelial cell layer and substrate *in vitro* affect cell response. Palmieri *et al.* used a model of healthy (stiffer) cells and added a cancer (softer) cell to study cancer cell migration speed. Mechanotransduction of a soft cell mass on normal cells was enough to increase cancer cell motility with several increases in speed over the monolayer of normal healthy cells [96]. Mechanoreceptors are controlled by the stiffness of the endothelium and the underlying substrate creating a feedback loops between cells and the matrix. The site of TEM is determined by endothelial stiffness; endothelial cell cup formation increases local cell stiffness that induces more ICAM clustering. All cell types share common mechanisms that regulate different processes, specifically the RhoA-ROCK-myosin pathway control of endothelial barrier function, endothelium stiffness, and leukocyte capture, adhesion, and probing [97].

Endothelial Cell Processes

The endothelium plays critical roles in cell transmigration. After endothelial cell activation of adhesion molecules, TEM may be assisted through cup formation, loosening

of tight junctions, and sealing of the endothelium to maintain barrier integrity. Several molecules, E-selectin, ICAM-1, VCAM-1, JAM-A, JAM-C, PECAM-1, CD99, CD99L2, and VE-cadherin, contribute to the activation of various signaling pathways in transmigration [98]. Loosening of the tight junctions occurs through ICAM/VCAM crosslinking and dephosphorylation of VE-cadherin. Clustering of ICAM and VCAM at the apical side of the cell form fingerlike protrusions for cup formation around the transmigrating cell due to Rho and Src signaling. This is observed under specific conditions, normally when leukocytes adhere and cannot transmigrate. VCAM and ICAM clustering induces free calcium ions, activating myosin light chain kinase (MLCK) and contraction of actin-myosin. Crosslinking VCAM activates Rac1, increases ROS and ICAM, and activates RhoA and ROCK and actin-myosin contraction. VE-cadherin is phosphorylated through ICAM-1 signaling and vascular endothelial protein tyrosine phosphatase (VE-PTP) that associates and maintains VE-cadherin in the resting state [61].

Molecules are organized together and made available at the endothelial cell membrane by a complex known as the Lateral Border Recycling Compartment (LBRC). The LBRC holds 30% of total endothelial cell PECAM-1, CD99, and JAM-A and is targeted to the border where leukocyte TEM occurs The membrane is internalized and recycled beneath the plasma membrane of the cell borders in response to leukocyte adhesion and migration [61]. Endothelial cells also use actin binding proteins (ABPs) in TEM. Tight junctions and adherens junctions connect to the actin cytoskeleton by ABPs of endothelial cells. The organization of actin cytoskeleton requires nucleator Arp2/3 complex that nucleates actin and promotes branching and is bound to F-actin via cortactin. Other junction-cytoskeletal ABPs include alpha-catenin, vinculin, and ZO-1.

Nucleation promoting factor formins polymerize actin and function in elongation, actin recycling and depolymerization through five groups of proteins. Profilin binds G-actin bound to GTP adds actin to the barbed end of the actin filament. Additional stabilizing ABPs include ezrin/radixin/moesin (ERM) involved in stress fiber formation, mDia1, N-WASP, and VASP for nucleation and elongation of actin filaments. Filamins and IQGAP function in actin crosslinking. Cofilin binds to G-actin and F-actin to sever actin filaments. Actin capping proteins prevent additional actin from binding and inhibit filament growth. García-Ponce at el. reviewed ABPs and their contributions to stabilizing and destabilizing the endothelial barrier in detail [99].

Endothelial cells of different vascular beds will exhibit different characteristics, specific to that organ [15]. The blood brain barrier exhibits a different barrier challenge for study and therapeutics due to cellular tight junctions [100]. Different vascular beds may recruit different immune cell populations in the inflammatory response. The adhesion molecules characteristic of synovium endothelial cells include a higher expression of E-selectin and I-CAM in basal and inflammatory conditions compared to human foreskin and umbilical endothelial cells [101] and showed recruitment of mainly macrophages and T cell lymphocytes of diseased synovium in osteoarthritis [102]. MSC homing is specific to the tissue and organ endothelium and can require different therapeutic molecules for enhancement, for example MSC homing towards injury in the kidney was promoted by CD44 [103]. Selection of endothelial cell type is critical for *in vitro* studies to determine physiologically relevant mechanisms and important to account for in *in vivo* studies to elucidate mechanisms of MSCs.

III. *In Vitro* and *In Vivo* Model Systems

In vitro model systems are often simpler that *in vivo* models used to study individual factors than influence homing mechanisms. Several cell culture conditions impact the efficiency of MSC homing to sites of injury or inflammation. Classic media formulations do not compare to the native *in vivo* microenvironment. HEMOXCell is a media supplement that serves as an oxygen carrier for cells migrating to injured hypoxic sites or 3D environments. Le Pape *et al.* showed an increase in cell growth and maintenance of phenotype and differentiation properties at an optimal concentration of HEMOXCell in platelet lysate supplemented media [104]. Another approach to enhance the physiologic relevance of growth medium is to increase macromolecular crowding (MMC). The concept is that large molecules occupy space and provide the cells with greater contact. Albumin is one possible candidate for enhancing culture medium. Albumin constitutes 50% of protein in the plasma of a healthy adult and functions in regulating the distribution of fluids between intravascular and extravascular compartments. It regulates colloid oncotic pressure by drawing water into the vessel or the tissue, depending on its location and has a role in capillary membrane permeability in that it may bind in subendothelium and interstitial matrix and alter permeability to macromolecules. It has circulatory protective properties such as anticoagulant and anti-thrombotic functions and acts as a buffer by binding excessive proteins, binds and stabilizes hormones and growth peptides [105].

Another method to enhance homing is pre-treatment of MSCs. Pre-treatment of adipose-derived MSCs with valproic acid promoted overexpression of CXCR4 and CXCR6 that enhanced homing [106]. In addition to pre-treatment of MSCs, other cell

culture conditions influence *in vitro* models of transmigration. Perhaps one of the most influential factors is cell confluency. High MSC confluency has been shown to increase production of tissue inhibitor of metalloproteinase-3 (TIMP-3) that results in decreased MSC transmigration [78]. Similar detriments have been observed in highly confluent endothelial cells and cell signaling [107]. Optimal culture conditions are critical for all cell types for efficient transmigration.

The following models have been used alone or in combination to study stem cells, leukocyte, and cancer cell migration, homing, and invasion. Currently, no single method alone captures all of the contributing factors involved; each has characteristic advantages and disadvantages for the study of homing and transmigration. Specifically, 3D models are more physiologically relevant than 2D models. Hakkinen *et al.* measured cell adhesion and migration on 2D ECM coated matrices and gels of collagen, fibrin, and basement membrane extract (BME). Fibroblasts spread more on 2D matrices when compared to the spindle shape in 3D matrices and there was no spreading on BME; however, total cell area was similar. Migration was more rapid on 3D matrices, except migration was minimal on BME [108]. Besides 2D culture and hydrogels, other methods include scaffolds, bioprinting, microfluidic devices, and Boyden or transwell chambers. Cellular and molecular techniques used in studying homing processes include DNA quantification and proliferation assays, [18] qPCR, [109] western blotting, [18] overexpression of a particular gene, [110] RNA interference, [18,110] and small molecule inhibitors [18,110].

Classical 2D approaches include glass slides, cover slips, tissue-treated plastic, and the scratch assay [111]. Krstić *et al.* used a scratch assay with 0, 25, and 50 ng/ml IL-17 to study migration of treated PB-MSCs compared to untreated controls. Wound closure

was concentration dependent, with 50 ng/mL resulting in the highest number of migrated cells [67]. Tissue treated plastic has been used for adhesion and transmigration assays, cell migration on cover slips showed that MSCs on murine microvascular aortic endothelial cells flatten and integrate into the monolayer of endothelial cells. MSCs exhibited long plasmic podia, adhered to the endothelial cells by 15 minutes, integrated into the monolayer by 180 minutes, and showed endothelial growth over the MSCs by 240 minutes [60]. In another study, Chamberlain *et al.* used microslides seeded with murine aortic microvascular endothelial cells, loaded with murine MSCs, and exposed to fluid flow and chemokine CXCL9. Fluid flow increased MSC crawling and spreading and chemokine exposure contributed to increased adhesion, crawling, and spreading that contributed to transmigration [112]. More complex cell culture systems have been developed to mimic native microenvironments.

Model systems have been developed to study cell response in physiological and pathological conditions. One common technique involves the use of Boyden chambers or transwells. These systems consist of an insert that fits into a well plate and provides a plastic porous membrane support. Options for these systems include pore sizes from 0.4 – 12 um, pore densities of 1 x 10^5 – 6 x10^6, membranes of polyester (PE), polyethylene terephthalate (PET), polytetrafluoroethylene (PTFE) and polycarbonate (PC), coatings of Matrigel^{TM}, collagen, and fibronectin that fit into 6-, 12-, and 24-well plates.

Several methods of validation exist for chamber migration assays. Transendothelial electric resistance (TEER) measures electrical resistance between the area above and below the endothelium [110,113]. Horseradish peroxidase (HRP) flux measures the retention of HRP above the endothelium [77,110]. The Lucifer Yellow

Rejection assay measures the passive diffusion of lucifer yellow between the endothelial cells [113]. Solubility assays measure the distribution of tight junction protein between detergent soluble and insoluble cell fractions [77,110]. Lastly, immunofluorescence has been used to visualize endothelial cell junction proteins. Lin *et al.* tested monolayer permeability of human brain microvascular endothelial cells co-cultured with human MSCs and observed a decrease in TEER measurements, an increase in HRP flux, a shift of insoluble to soluble occludin protein, and discontinued distribution of tight junction protein-1 (ZO-1) by immunofluorescence over 12 hours [110]. These results showed that monolayer integrity decreased over time in this study. Advantages of this system are the separate chambers that allow for cell collection, removal, and fixation of the permeable membranes. Limitations of this system include maximizing the endothelial barrier, control of the chemotactic gradient, and fluid flow. One challenge of mimicking physiological vasculature is the integrity of the endothelial barrier. Since brain microvascular endothelium have tight junctions, they form stronger and more selective barriers than formed by other microvascular endothelial cells. However, even brain endothelium *in vitro* does not compare to the selective blood brain barrier *in vivo.* Gradients are more difficult to establish and maintain and fluid flow has not yet been incorporated in these systems.

Co-culture systems create an additional challenge of determining the contributions of each cell type in transmigration using current techniques. Other cell populations and blood components in physiological conditions are lacking in most *in vitro* systems; however, studies have supplemented the media in these systems with serum albumin [109]. Serum albumin was discussed previously as a major component of

blood with several physiological functions. Briefly, serum albumin increases the viscosity of the fluid in the system to more closely mimic physiological conditions. Other systems are able to overcome some of these challenges.

Gel constructs have become more common for studying cell migration in a 3D system. HUVECs were seeded on a collagen gel for studying MSC transmigration and invasion. A spherical morphology was observed at 2 hours, integration and plasmic podia were visualized at 4 hours, and MSC migration under the endothelium and invasion of the collagen gel was observed after 6 and 24 hours [60]. Other forms of gels have been used for similar purposes. Mobilization from within a spherical collagen gel was used to show MSC migration in response to IL-17 treatment [67]. The sandwich assay is a 3D model used to control chemical composition in the upper and lower matrices with cells seeded at the interface. Schor *et al.* studied dermal fibroblasts in response to platelet-derived growth factor-AB (PDGF-AB) and TGF-βs in the sandwich model and observed symmetrical migration with isotrophic distribution and then directional migration in anisotropic distribution [114]. Endothelial spheroids where used to attract MSCs and showed MSC adhesion to the spheroids at 2 hours and invasion at 4 and 6 hours. This was an alternative method of demonstrating the interaction between endothelial cells and MSCs [60].

Microfluidic devices have been used as models to investigate chemotaxis and to mimic a vascular environment. Schwartz *et al.* developed a microfluidic device to study dendritic cell chemotaxis and haptotaxis towards gradients of immobilized CCL21 and mobilized CCL19 that resulted in different migration patterns [115]. Manneschi *et al.* developed and validated a microfluidic chip to study extravasation. Micropillars were

incorporated in the design between two parallel microchannels to function as the permeable membrane to study vascular transport and cell migration [116].

Combining these methods is one approach to navigate the limitations of *in vitro* systems. Smith *et al.* combined multiple models of transwell chambers, microfluidic devices, nano-patterned migration assays, and SCID mice to study transmigration of pre-treated MSCs through the endothelium of the blood brain barrier towards brain tumors [76]. Combining these models offered strong evidence for pre-treatment of MSCs for enhancing stem cell therapies. Different models are more suitable for investigating MSC mechanisms depending on the stages of homing being studied. Few studies specific to the mechanisms of MSC transmigration have been published.

IV. Stem Cell Migration and Homing Mechanisms

Several studies investigate the cellular mechanisms of MSC migration; however, little information exists on the processes and cellular and molecular mechanisms of MSC transmigration through an endothelial barrier. Pre-treatment, chemoattractant, cell type, cell culture system, and environmental conditions influence activation of signaling pathways. Studies investigated the effects of pre-treatment with cytokines and growth factors on mechanisms of MSC migration. Gao *et al.* investigated the effects of SDF-1 in MSC migration towards tumor cell conditioned medium and identified roles for signal transducer and activator of transcription 3 (Stat3) and focal adhesion kinase (FAK) [18]. Chemokines have been linked to specific integrin expression and cell signaling. Feng *et al.* observed that MSCs produced CXCL11 that bound to the endothelial receptor CXCR3

and activated endothelial ERK1/2 signaling and MSC transmigration in a blood brain barrier model [77]. The CXCL12/CXCR4 axis and the CXCL5/CXCR2 axis have been observed in ASC transmigration [66]. IL-17 enhanced MSC adhesion and transmigration, with the localization of urokinase in cell protrusions, and activated ERK1/2 MAPK signaling [67]. TGF-β1 signaling in the bone marrow environment downregulated the expression of *sdf-1* at mRNA and protein levels and showed decreased SDF-1 dependent α1β4 integrin adhesion, chemotaxis, and TEM in bone marrow cell trafficking [117].

Studies examining changes in MSC morphology and cell signaling pathways provide insight for transmigration studies. ASCs use lysophosphatidic acid-1 (LPA-1), MAPK/ERK1/2, PI3K-Akt, Rho/ROCK, and PDGF-BB signaling pathways for migration that have the potential for identification of therapeutic targets [66]. Maijenburg at al. studied genes in MSC migration towards SDF-1 and showed that the highest expression of *nur77* and *nurr1* in migratory MSCs towards SDF-1 and PDGF [109]. Cytoskeleton regulators include actin and microtubule molecules and ROCK signaling. Lin *et al.* observed the involvement of both ROCK and PI3K signaling in human MSC transmigration across human brain microvascular endothelium. Findings showed decrease MSC transmigration with overexpression of a PI3K dominant negative mutant, a decrease in transmigration after RNA interference of ROCK, and similar results of MSC transmigration after PI3K, ROCK, and PKC inhibitor treatment [110]. In another study, Maijenburg *et al.* studied the role of orphan genes in MSC transmigration; results showed involvement of NFκB through *nur77* and *nurr1* [109]. These pathways require further investigation to determine mechanisms of MSC transmigration and identification of target molecules to enhance MSC homing.

Endothelial Cell Source	Stem Cell Source	Migration Stimulus	Findings
Human bone marrow-derived	Human bone marrow-derived MSCs	10% FCS	TEM through bone marrow ECs is partially regulated by MMP-2. High confluency induces TIMP-3 that decreases TEM [78].
Human brain microvascular	Human adipose-derived MSCs	CM from F60 or U87 MG	Pre-treatment with GCM, fibronectin, or laminin increased homing efficiency towards glioblastoma [76].
Human umbilical vein	Human bone marrow-derived MSCs	10% FBS 10% Nu-serum	PI3K and ROCK pathways regulate TEM through brain microvascular ECs [110].
Human brain microvascular	peripheral blood-MSCs	10% FBS	IL-17 induced uPa and promoted increased MSC migration, adhesion, and TEM via ERK1/2 MAPK signaling [67].
Human brain microvascular	Human bone marrow-derived MSCs	MSC-derived CXCL11	The CXCR3/CXCL11 axis interrupts EC junctions via ERK1/2 signaling and enhances MSC TEM [77].
Human bone marrow	Human MSCs	CXCL12, CXCL13, CXCL16, CCL11, CCL22	CXCl16 was the most efficient chemokine in TEM in the apical-to-basal direction and CCL22 was the most efficient chemokine in TEM in the basal-to-apical direction. MSCs flattened and extended filopodia protrusions into the ECs. MSCs showed directional preferences for different chemokines [75].
Human umbilical vein	Human bone marrow-derived MSCs	chemerin, chemerin-9, or CM	CM medium increased MSC migration. Chemerin stimulated MSC phosphorylation of p42/44, p38, and JNK II kinases. Chemerin induced MIF expression and secretion that promoted MSC migration at high concentrations of chemerin [118].
Murine aortic	Murine MSCs	CXCL9, CXCL16, CXCL20, CXCL25	CXCL9 enhanced adhesion, crawling, and spreading towards MSC TEM. Shear stress enhanced crawling and spreading after MSC adhesion. MSC formed filopodia, followed by pseudopodia protrusions extending in multiple directions [112].
Human microendothelial	Human bone marrow-derived MSCs	CM from cancer cell lines and breast cancer samples	MSCs selected for α2, α3, and α5 integrins showed increased homing towards tumor sites. Homing was dependent on inhibition of metellopeptidases. MSCs were capable of transporting oncolytic adenovirus to tumors [119].

Table 3.1: Summary of co-culture transwell systems used for studying mesenchymal stem cell homing through an endothelial cell layer. EC, endothelial cell, GCM, glioma conditioned medium, uPA, urokinase type plasminogen activator.

Future Directions

Defining the mechanisms of MSC homing in comparison to the leukocyte cascade will be critical in controlling endogenous and exogenous stem cell trafficking to sites of inflammation or injury or regulate immune cell functions. New experimental findings that 1) elucidate the cellular and molecular mechanisms of MSC homing, 2) understand signaling between MSCs and endothelial cells, and 3) determine how MSCs may control immune cell function could greatly impact the efficiency and efficacy of stem cell therapies. The next chapter presents a study that identifies three signaling pathways

involved in MSC transmigration and a potential target for enhanced homing. Harnessing the full potential of MSCs will lead to new therapies for injury, inflammation, and diseases.

References

1. Fong ELS, Chan CK, Goodman SB. Stem cell homing in musculoskeletal injury. Biomaterials 2011;32(2):395-409.
2. Nöth U, Steinert AF, Tuan RS. Technology insight: adult mesenchymal stem cells for osteoarthritis therapy. Nature clinical practice Rheumatology 2008;4(7):371-380.
3. Ansboro S, Roelofs AJ, De Bari C. Mesenchymal stem cells for the management of rheumatoid arthritis: immune modulation, repair or both? Current opinion in rheumatology 2017;29(2):201-207.
4. Ennis WJ, Sui A, Bartholomew A. Stem cells and healing: impact on inflammation. Advances in wound care 2013;2(7):369-378.
5. Khosrotehrani K. Mesenchymal stem cell therapy in skin: why and what for? Experimental dermatology 2013;22(5):307-310.
6. Granero‐Moltó F, Weis JA, Miga MI, Landis B, Myers TJ, O'Rear L, Longobardi L, Jansen ED, Mortlock DP, Spagnoli A. Regenerative effects of transplanted mesenchymal stem cells in fracture healing. Stem cells 2009;27(8):1887-1898.
7. Shen WL, Chen JL, Zhu T, Chen LK, Zhang W, Fang Z, Heng BC, Yin Z, Chen X, Ji JF and others. Intra-Articular Injection of Human Meniscus Stem/Progenitor Cells Promotes Meniscus Regeneration and Ameliorates Osteoarthritis Through Stromal Cell-Derived Factor-1/CXCR4-Mediated Homing. Stem Cells Translational Medicine 2014;3(3):387-394.
8. Chen FH, Tuan RS. Mesenchymal stem cells in arthritic diseases. Arthritis research & therapy 2008;10(5):223.
9. Jo CH, Lee YG, Shin WH, Kim H, Chai JW, Jeong EC, Kim JE, Shim H, Shin JS, Shin IS. Intra‐articular injection of mesenchymal stem cells for the treatment of osteoarthritis of the knee: a proof‐of‐concept clinical trial. Stem cells 2014;32(5):1254-1266.
10. Karp JM, Teo GSL. Mesenchymal stem cell homing: the devil is in the details. Cell stem cell 2009;4(3):206-216.
11. Karp JM, Teol GSL. Mesenchymal Stem Cell Homing: The Devil Is in the Details. Cell Stem Cell 2009;4(3):206-216.
12. El-Gabalawy H. The challenge of early synovitis: multiple pathways to a common clinical syndrome. Arthritis Research & Therapy 1999;1(1):31.
13. Szekanecz Z, Kim J, Koch AE. Chemokines and chemokine receptors in rheumatoid arthritis. 2003. Elsevier. p 15-21.
14. Tracey KJ. The inflammatory reflex. Nature 2002;420(6917):853-859.
15. Sutton NR, Baek A, Pinsky DJ. Endothelial Cells and Inflammation. Encyclopedia of Medical Immunology: Springer; 2014. p 367-381.
16. Rollins. Chemokines. Blood 1997.
17. Wang S, Wu Y. The role of chemokines in mesenchymal stromal cell homing to sites of inflammation, including infarcted myocardium. The Biology and Therapeutic Application of Mesenchymal Cells 2017:314-322.

18. Gao H, Priebe W, Glod J, Banerjee D. Activation of signal transducers and activators of transcription 3 and focal adhesion kinase by stromal cell‐derived factor 1 is required for migration of human mesenchymal stem cells in response to tumor cell‐conditioned medium. Stem Cells 2009;27(4):857-865.
19. Nakatomi H, Kuriu T, Okabe S, Yamamoto S-i, Hatano O, Kawahara N, Tamura A, Kirino T, Nakafuku M. Regeneration of hippocampal pyramidal neurons after ischemic brain injury by recruitment of endogenous neural progenitors. Cell 2002;110(4):429-441.
20. Benraiss A, Chmielnicki E, Lerner K, Roh D, Goldman SA. Adenoviral brain-derived neurotrophic factor induces both neostriatal and olfactory neuronal recruitment from endogenous progenitor cells in the adult forebrain. Journal of Neuroscience 2001;21(17):6718-6731.
21. Vanden Berg-Foels WS. In situ tissue regeneration: chemoattractants for endogenous stem cell recruitment. Tissue Engineering Part B: Reviews 2013;20(1):28-39.
22. Dimmeler S, Ding S, Rando TA, Trounson A. Harnessing the potential of endogenous stem cells. Nature 2014;201:4.
23. Tumbar T, Guasch G, Greco V, Blanpain C, Lowry WE, Rendl M, Fuchs E. Defining the epithelial stem cell niche in skin. Science 2004;303(5656):359-363.
24. Kosaraju R, Rennert RC, Maan ZN, Duscher D, Barrera J, Whittam AJ, Januszyk M, Rajadas J, Rodrigues M, Gurtner GC. Adipose-derived stem cell-seeded hydrogels increase endogenous progenitor cell recruitment and neovascularization in wounds. Tissue Engineering Part A 2016;22(3-4):295-305.
25. Hocking AM. The role of chemokines in mesenchymal stem cell homing to wounds. Advances in wound care 2015;4(11):623-630.
26. Biology and Engineering of Stem Cell Niches: Mica Haley; 2017.
27. Yin T, Li L. The stem cell niches in bone. The Journal of clinical investigation 2006;116(5):1195-1201.
28. Costa-Alameida R, Gonçalves A, Gershovich P, Rodrigues M, Reis R, Gomes M. Tendon stem cell niche. Tissue-Specific Stem Cell Niche: Springer; 2015. p 221-244.
29. Chen P, Tao J, Zhu S, Cai Y, Mao Q, Yu D, Dai J, Ouyang H. Radially oriented collagen scaffold with SDF-1 promotes osteochondral repair by facilitating cell homing. Biomaterials 2015;39:114-123.
30. Zhang F, Leong W, Su K, Fang Y, Wang D-A. A transduced living hyaline cartilage graft releasing transgenic stromal cell-derived factor-1 inducing endogenous stem cell homing in vivo. Tissue Engineering Part A 2013;19(9-10):1091-1099.
31. Fleming HE, Janzen V, Celso CL, Guo J, Leahy KM, Kronenberg HM, Scadden DT. Wnt signaling in the niche enforces hematopoietic stem cell quiescence and is necessary to preserve self-renewal in vivo. Cell stem cell 2008;2(3):274-283.
32. Grad S, Peroglio M, Li Z, Alini M. Endogenous Cell Homing for Intervertebral Disk Regeneration. Journal of the American Academy of Orthopaedic Surgeons 2015;23(4):264-266.
33. Karlsson J, Harmankaya N, Palmquist A, Atefyekta S, Omar O, Tengvall P, Andersson M. Stem cell homing using local delivery of plerixafor and stromal

derived growth factor-1alpha for improved bone regeneration around Ti-implants. Journal of Biomedical Materials Research Part A 2016;104(10):2466-2475.
34. Lee CH, Lee FY, Tarafder S, Kao K, Jun Y, Yang G, Mao JJ. Harnessing endogenous stem/progenitor cells for tendon regeneration. The Journal of clinical investigation 2015;125(7):2690-2701.
35. Riquelme PA, Drapeau E, Doetsch F. Brain micro-ecologies: neural stem cell niches in the adult mammalian brain. Philosophical Transactions of the Royal Society of London B: Biological Sciences 2008;363(1489):123-137.
36. Urbanek K, Cesselli D, Rota M, Nascimbene A, De Angelis A, Hosoda T, Bearzi C, Boni A, Bolli R, Kajstura J. Stem cell niches in the adult mouse heart. Proceedings of the National Academy of Sciences 2006;103(24):9226-9231.
37. Itoh T. Liver Stem Cell Niche. Tissue-Specific Stem Cell Niche: Springer; 2015. p 83-97.
38. Yen T-H, Wright NA. The gastrointestinal tract stem cell niche. Stem Cell Reviews and Reports 2006;2(3):203-212.
39. Arvidsson A, Collin T, Kirik D, Kokaia Z, Lindvall O. Neuronal replacement from endogenous precursors in the adult brain after stroke. Nature medicine 2002;8(9):963-970.
40. Hsueh YC, Wu JM, Yu CK, Wu KK, Hsieh PC. Prostaglandin E2 promotes post-infarction cardiomyocyte replenishment by endogenous stem cells. EMBO molecular medicine 2014;6(4):496-503.
41. Yannaki E, Athanasiou E, Xagorari A, Constantinou V, Batsis I, Kaloyannidis P, Proya E, Anagnostopoulos A, Fassas A. G-CSF–primed hematopoietic stem cells or G-CSF per se accelerate recovery and improve survival after liver injury, predominantly by promoting endogenous repair programs. Experimental hematology 2005;33(1):108-119.
42. Semont A, Mouiseddine M, Francois A, Demarquay C, Mathieu N, Chapel A, Saché A, Thierry D, Laloi P, Gourmelon P. Mesenchymal stem cells improve small intestinal integrity through regulation of endogenous epithelial cell homeostasis. Cell Death & Differentiation 2010;17(6):952-961.
43. Won Y-W, Patel AN, Bull DA. Cell surface engineering to enhance mesenchymal stem cell migration toward an SDF-1 gradient. Biomaterials 2014;35(21):5627-5635.
44. Wei N, Yu SP, Gu X, Taylor TM, Song D, Liu X-f, Wei L. Delayed intranasal delivery of hypoxic-preconditioned bone marrow mesenchymal stem cells enhanced cell homing and therapeutic benefits after ischemic stroke in mice. Cell transplantation 2013;22(6):977-991.
45. Guo Y, Wysoczynski M, Nong Y, Tomlin A, Zhu X, Gumpert AM, Nasr M, Muthusamy S, Li H, Book M. Repeated doses of cardiac mesenchymal cells are therapeutically superior to a single dose in mice with old myocardial infarction. Basic research in cardiology 2017;112(2):18.
46. Lourenco S, Teixeira VH, Kalber T, Jose RJ, Floto RA, Janes SM. Macrophage migration inhibitory factor–CXCR4 is the dominant chemotactic axis in human mesenchymal stem cell recruitment to tumors. The Journal of Immunology 2015;194(7):3463-3474.

47. Yu Y, Sun B, Yi C, Mo X. Stem cell homing-based tissue engineering using bioactive materials. Frontiers of Materials Science 2017:1-13.
48. Naderi-Meshkin H, Matin MM, Heirani-Tabasi A, Mirahmadi M, Irfan-Maqsood M, Edalatmanesh MA, Shahriyari M, Ahmadiankia N, Moussavi NS, Bidkhori HR. Injectable hydrogel delivery plus preconditioning of mesenchymal stem cells: exploitation of SDF-1/CXCR4 axis toward enhancing the efficacy of stem cells' homing. Cell biology international 2016;40(7):730-741.
49. Song M, Jang H, Lee J, Kim JH, Kim SH, Sun K, Park Y. Regeneration of chronic myocardial infarction by injectable hydrogels containing stem cell homing factor SDF-1 and angiogenic peptide Ac-SDKP. Biomaterials 2014;35(8):2436-2445.
50. Huang H, Zhang X, Hu X, Shao Z, Zhu J, Dai L, Man Z, Yuan L, Chen H, Zhou C. A functional biphasic biomaterial homing mesenchymal stem cells for in vivo cartilage regeneration. Biomaterials 2014;35(36):9608-9619.
51. Zhang W, Zhu C, Wu Y, Ye D, Wang S, Zou D, Zhang X, Kaplan DL, Jiang X. VEGF and BMP-2 promote bone regeneration by facilitating bone marrow stem cell homing and differentiation. Eur Cell Mater 2014;27(1):1-11.
52. Gong Y, Zhao Y, Li Y, Fan Y, Hoover-Plow J. Plasminogen regulates cardiac repair after myocardial infarction through its noncanonical function in stem cell homing to the infarcted heart. Journal of the American College of Cardiology 2014;63(25 Part A):2862-2872.
53. Bensidhoum M, Chapel A, Francois S, Demarquay C, Mazurier C, Fouillard L, Bouchet S, Bertho JM, Gourmelon P, Aigueperse J and others. Homing of in vitro expanded Stro-1(-) or Stro-1(+) human mesenchymal stem cells into the NOD/SCID mouse and their role in supporting human CD34 cell engraftment. Blood 2004;103(9):3313-3319.
54. Colvin GA, Lambert JF, Dooner MS, Cerny J, Quesenberry PJ. Murine allogeneic in vivo stem cell homing. Journal of Cellular Physiology 2007;211(2):386-391.
55. Li H, Jiang Y, Jiang X, Guo X, Ning H, Li Y, Liao L, Yao H, Wang X, Liu Y. CCR7 guides migration of mesenchymal stem cell to secondary lymphoid organs: a novel approach to separate GvHD from GvL effect. Stem Cells 2014;32(7):1890-1903.
56. Nguyen PK, Riegler J, Wu JC. Stem cell imaging: from bench to bedside. Cell stem cell 2014;14(4):431-444.
57. Wu S, Li L, Wang G, Shen W, Xu Y, Liu Z, Zhuo Z, Xia H, Gao Y, Tan K. Ultrasound-targeted stromal cell-derived factor-1-loaded microbubble destruction promotes mesenchymal stem cell homing to kidneys in diabetic nephropathy rats. International journal of nanomedicine 2014;9:5639.
58. Tritto I, Falzetti F, Bettini M, Porchetta I, Zuchi C, Biscottini E, Coiro S, Tabilio A, Ambrosio G. In vivo direct monitoring of stem cell homing in postischemic tissues. Journal of Molecular and Cellular Cardiology 2007;42:S96-S96.
59. Huang X, Zhang F, Wang Y, Sun X, Choi KY, Liu D, Choi J-s, Shin T-H, Cheon J, Niu G. Design considerations of iron-based nanoclusters for noninvasive tracking of mesenchymal stem cell homing. ACS nano 2014;8(5):4403-4414.
60. Steingen C, Brenig F, Baumgartner L, Schmidt J, Schmidt A, Bloch W. Characterization of key mechanisms in transmigration and invasion of

mesenchymal stem cells. Journal of Molecular and Cellular Cardiology 2008;44(6):1072-1084.
61. Muller W. Getting leukocytes to the site of inflammation. Veterinary Pathology Online 2013;50(1):7-22.
62. Baggiolini M. Chemokines and leukocyte traffic. Nature 1998;392(6676):565.
63. Rüster B, Göttig S, Ludwig RJ, Bistrian R, Müller S, Seifried E, Gille J, Henschler R. Mesenchymal stem cells display coordinated rolling and adhesion behavior on endothelial cells. Blood 2006;108(12):3938-3944.
64. Fidler IJ. The organ microenvironment and cancer metastasis. Differentiation 2002;70(9-10):498-505.
65. Bauer K, Mierke C, Behrens J. Expression profiling reveals genes associated with transendothelial migration of tumor cells: a functional role for αvβ3 integrin. International journal of cancer 2007;121(9):1910-1918.
66. Zhao Y, Zhang H. Update on the mechanisms of homing of adipose tissue–derived stem cells. Cytotherapy 2016;18(7):816-827.
67. Krstić J, Obradović H, Jauković A, Okić-Đorđević I, Trivanović D, Kukolj T, Mojsilović S, Ilić V, Santibañez JF, Bugarski D. Urokinase type plasminogen activator mediates Interleukin-17-induced peripheral blood mesenchymal stem cell motility and transendothelial migration. Biochimica et Biophysica Acta (BBA)-Molecular Cell Research 2015;1853(2):431-444.
68. Chamberlain J. Concise Review: Mesenchymal Stem Cells: Their Phenotype,Differentiation Capacity, Immunological Features, andPotential for Homing. 2007.
69. Chou K-J, Lee P-T, Chen C-L, Hsu C-Y, Huang W-C, Huang C-W, Fang H-C. CD44 fucosylation on mesenchymal stem cell enhances homing and macrophage polarization in ischemic kidney injury. Experimental Cell Research 2017;350(1):91-102.
70. Reymond N, d'Agua BB, Ridley AJ. Crossing the endothelial barrier during metastasis. Nature Reviews Cancer 2013;13(12):858-870.
71. Teo GS, Ankrum JA, Martinelli R, Boetto SE, Simms K, Sciuto TE, Dvorak AM, Karp JM, Carman CV. Mesenchymal Stem Cells Transmigrate Between and Directly Through Tumor Necrosis Factor‐α‐Activated Endothelial Cells Via Both Leukocyte‐Like and Novel Mechanisms. Stem Cells 2012;30(11):2472-2486.
72. Schmidt A, Ladage D, Steingen C, Brixius K, Schinköthe T, Klinz F-J, Schwinger RH, Mehlhorn U, Bloch W. Mesenchymal stem cells transmigrate over the endothelial barrier. European journal of cell biology 2006;85(11):1179-1188.
73. Schmidt A, Ladage D, Schinköthe T, Klausmann U, Ulrichs C, Klinz FJ, Brixius K, Arnhold S, Desai B, Mehlhorn U. Basic fibroblast growth factor controls migration in human mesenchymal stem cells. Stem cells 2006;24(7):1750-1758.
74. Law S, Chaudhuri S. Mesenchymal stem cell and regenerative medicine: regeneration versus immunomodulatory challenges. Am J Stem Cells 2013;2(1):22-38.
75. Smith H, Whittall C, Weksler B, Middleton J. Chemokines stimulate bidirectional migration of human mesenchymal stem cells across bone marrow endothelial cells. Stem cells and development 2011;21(3):476-486.

76. Smith CL, Chaichana KL, Lee YM, Lin B, Stanko KM, O'Donnell T, Gupta S, Shah SR, Wang J, Wijesekera O. Pre-Exposure of Human Adipose Mesenchymal Stem Cells to Soluble Factors Enhances Their Homing to Brain Cancer. Stem cells translational medicine 2015;4(3):239-251.
77. Feng Y, Yu H-M, Shang D-S, Fang W-G, He Z-Y, Chen Y-H. The involvement of CXCL11 in bone marrow-derived mesenchymal stem cell migration through human brain microvascular endothelial cells. Neurochemical research 2014;39(4):700-706.
78. De Becker A, Van Hummelen P, Bakkus M, Broek IV, De Wever J, De Waele M, Van Riet I. Migration of culture-expanded human mesenchymal stem cells through bone marrow endothelium is regulated by matrix metalloproteinase-2 and tissue inhibitor of metalloproteinase-3. Haematologica 2007;92(4):440-449.
79. Tomchuck SL, Zwezdaryk KJ, Coffelt SB, Waterman RS, Danka ES, Scandurro AB. Toll-Like Receptors on Human Mesenchymal Stem Cells Drive Their Migration and Immunomodulating Responses. Stem cells 2008;26(1):99-107.
80. Shirjang S, Mansoori B, Solali S, Hagh MF, Shamsasenjan K. Toll-like receptors as a key regulator of mesenchymal stem cell function: an up-to-date review. Cellular Immunology 2016.
81. Qiu Y, Guo J, Mao R, Chao K, Chen B, He Y, Zeng Z, Zhang S, Chen M. TLR3 preconditioning enhances the therapeutic efficacy of umbilical cord mesenchymal stem cells in TNBS-induced colitis via the TLR3-Jagged-1-Notch-1 pathway. Mucosal immunology 2017;10(3):727-742.
82. Parmo-Cabañas M, Bartolomé RA, Wright N, Hidalgo A, Drager AM, Teixidó J. Integrin α4β1 involvement in stromal cell-derived factor-1α-promoted myeloma cell transendothelial migration and adhesion: role of cAMP and the actin cytoskeleton in adhesion. Experimental cell research 2004;294(2):571-580.
83. Bos PD, Zhang XH-F, Nadal C, Shu W, Gomis RR, Nguyen DX, Minn AJ, van de Vijver MJ, Gerald WL, Foekens JA. Genes that mediate breast cancer metastasis to the brain. Nature 2009;459(7249):1005-1009.
84. Rangaswami H, Bulbule A, Kundu GC. JNK1 differentially regulates osteopontin-induced nuclear factorinducing kinase/MEKK1-dependent activating protein-1-mediated promatrix metalloproteinase-9 activation. Journal of Biological Chemistry 2005;280(19):19381-19392.
85. Xie Z, Singh M, Siwik DA, Joyner WL, Singh K. Osteopontin Inhibits Interleukin-1β-stimulated Increases in Matrix Metalloproteinase Activity in Adult Rat Cardiac Fibroblasts ROLE OF PROTEIN KINASE C-ζ. Journal of Biological Chemistry 2003;278(49):48546-48552.
86. Rangaswami H, Bulbule A, Kundu GC. Osteopontin: role in cell signaling and cancer progression. Trends in cell biology 2006;16(2):79-87.
87. Wu Y-d, Zhou B. TNF-α/NF-κB/Snail pathway in cancer cell migration and invasion. British journal of cancer 2010;102(4):639-644.
88. Schnoor M, Alcaide P, Voisin M-B, van Buul JD. Crossing the vascular wall: common and unique mechanisms exploited by different leukocyte subsets during extravasation. Mediators of inflammation 2015;2015.

89. Mukherjee S, Kim J, Mooren OL, Shahan ST, Cohan M, Cooper JA. Role of cortactin homolog HS1 in transendothelial migration of natural killer cells. PloS one 2015;10(2):e0118153.
90. Leow-Dyke S, Allen C, Denes A, Nilsson O, Maysami S, Bowie AG, Rothwell NJ, Pinteaux E. Neuronal Toll-like receptor 4 signaling induces brain endothelial activation and neutrophil transmigration in vitro. Journal of neuroinflammation 2012;9(1):230.
91. Tsubota Y, Frey JM, Tai PW, Welikson RE, Raines EW. Monocyte ADAM17 promotes diapedesis during transendothelial migration: identification of steps and substrates targeted by metalloproteinases. The Journal of Immunology 2013;190(8):4236-4244.
92. Senger DR, Galli SJ, Dvorak AM, Perruzzi CA, Harvey VS, Dvorak HF. Tumor cells secrete a vascular permeability factor that promotes accumulation of ascites fluid. Science 1983;219(4587):983-985.
93. Teo GSL, Yang Z, Carman CV, Karp JM, Lin CP. Intravital imaging of mesenchymal stem cell trafficking and association with platelets and neutrophils. Stem Cells 2015;33(1):265-277.
94. Abbott JD, Huang Y, Liu D, Hickey R, Krause DS, Giordano FJ. Stromal cell-derived factor-1 alpha plays a critical role in stem cell recruitment to the heart after myocardial infarction but is not sufficient to induce homing in the absence of injury. Circulation 2004;110(21):3300-3305.
95. Nyúl-Tóth Á, Kozma M, Nagyőszi P, Nagy K, Fazakas C, Haskó J, Molnár K, Farkas AE, Végh AG, Váró G. Expression of pattern recognition receptors and activation of the non-canonical inflammasome pathway in brain pericytes. Brain, Behavior, and Immunity 2017.
96. Palmieri B, Bresler Y, Wirtz D, Grant M. Multiple scale model for cell migration in monolayers: Elastic mismatch between cells enhances motility. Scientific reports 2015;5:11745.
97. Schaefer A, Hordijk PL. Cell-stiffness-induced mechanosignaling–a key driver of leukocyte transendothelial migration. J Cell Sci 2015;128(13):2221-2230.
98. Muller WA. Mechanisms of leukocyte transendothelial migration. Annual Review of Pathology: Mechanisms of Disease 2011;6:323-344.
99. García-Ponce A, Citalán-Madrid AF, Velázquez-Avila M, Vargas-Robles H, Schnoor M. The role of actin-binding proteins in the control of endothelial barrier integrity. Thrombosis and haemostasis 2015;113(1):20-36.
100. Pardridge WM. Molecular biology of the blood-brain barrier. The Blood-Brain Barrier: Biology and Research Protocols 2003:385-399.
101. To SS, Newman PM, Hyland VJ, Robinson BG, Schrieber L. Regulation of adhesion molecule expression by human synovial microvascular endothelial cells in vitro. Arthritis & Rheumatism 1996;39(3):467-477.
102. Mathiessen A, Conaghan PG. Synovitis in osteoarthritis: current understanding with therapeutic implications. Arthritis research & therapy 2017;19(1):18.
103. Herrera M, Bussolati B, Bruno S, Morando L, Mauriello-Romanazzi G, Sanavio F, Stamenkovic I, Biancone L, Camussi G. Exogenous mesenchymal stem cells localize to the kidney by means of CD44 following acute tubular injury. Kidney international 2007;72(4):430-441.

104. Le Pape F, Cosnuau‐Kemmat L, Richard G, Dubrana F, Férec C, Zal F, Leize E, Delépine P. HEMOXCell, a New Oxygen Carrier Usable as an Additive for Mesenchymal Stem Cell Culture in Platelet Lysate‐Supplemented Media. Artificial Organs 2017;41(4):359-371.
105. Fanali G, di Masi A, Trezza V, Marino M, Fasano M, Ascenzi P. Human serum albumin: from bench to bedside. Molecular aspects of medicine 2012;33(3):209-290.
106. Hashemzadeh MR, Seyedi Z, Rafiei S, Hassanzadeh-Moghaddam M, Edalatmanesh MA. Chemokine receptor's expression in human adipose derived mesenchymal stem cells primed with valproic acid. Comparative Clinical Pathology 2017;26(1):115-120.
107. Dejana E. Endothelial cell–cell junctions: happy together. Nature reviews Molecular cell biology 2004;5(4):261-270.
108. Hakkinen KM, Harunaga JS, Doyle AD, Yamada KM. Direct comparisons of the morphology, migration, cell adhesions, and actin cytoskeleton of fibroblasts in four different three-dimensional extracellular matrices. Tissue Engineering Part A 2010;17(5-6):713-724.
109. Maijenburg MW, Gilissen C, Melief SM, Kleijer M, Weijer K, ten Brinke A, Roelofs H, Van Tiel CM, Veltman JA, de Vries CJ. Nuclear receptors Nur77 and Nurr1 modulate mesenchymal stromal cell migration. Stem cells and development 2011;21(2):228-238.
110. Lin M-N, Shang D-S, Sun W, Li B, Xu X, Fang W-G, Zhao W-D, Cao L, Chen Y-H. Involvement of PI3K and ROCK signaling pathways in migration of bone marrow-derived mesenchymal stem cells through human brain microvascular endothelial cell monolayers. Brain research 2013;1513:1-8.
111. Liang C-C, Park AY, Guan J-L. In vitro scratch assay: a convenient and inexpensive method for analysis of cell migration in vitro. Nature protocols 2007;2(2):329-333.
112. Chamberlain G, Smith H, Rainger GE, Middleton J. Mesenchymal stem cells exhibit firm adhesion, crawling, spreading and transmigration across aortic endothelial cells: effects of chemokines and shear. PloS one 2011;6(9):e25663.
113. Rastogi H, Pinjari J, Honrao P, Praband S, Somani R. The impact of permeability enhancers on assessment for monolayer of colon adenocarcinoma cell line (CACO-2) used in in vitro permeability assay. Journal of Drug Delivery and Therapeutics 2013;3(3):20-29.
114. Schor S, Ellis I, Harada K, Motegi K, Anderson A, Chaplain M, Keatch R, Schor A. A novel "sandwich" assay for quantifying chemo‐regulated cell migration within 3‐dimensional matrices: Wound healing cytokines exhibit distinct motogenic activities compared to the transmembrane assay. Cell motility and the cytoskeleton 2006;63(5):287-300.
115. Schwarz J, Bierbaum V, Merrin J, Frank T, Hauschild R, Bollenbach T, Tay S, Sixt M, Mehling M. A microfluidic device for measuring cell migration towards substrate-bound and soluble chemokine gradients. Scientific Reports 2016;6.

116. Manneschi C, Pereira R, Marinaro G, Bosca A, Francardi M, Decuzzi P. A microfluidic platform with permeable walls for the analysis of vascular and extravascular mass transport. Microfluidics and Nanofluidics 2016;20(8):1-12.
117. Wright N, de Lera TL, García-Moruja C, Lillo R, García-Sánchez F, Caruz A, Teixidó J. Transforming growth factor-β1 down-regulates expression of chemokine stromal cell–derived factor-1: functional consequences in cell migration and adhesion. Blood 2003;102(6):1978-1984.
118. Kumar JD, Holmberg C, Kandola S, Steele I, Hegyi P, Tiszlavicz L, Jenkins R, Beynon RJ, Peeney D, Giger OT. Increased expression of chemerin in squamous esophageal cancer myofibroblasts and role in recruitment of mesenchymal stromal cells. PloS one 2014;9(8):e104877.
119. Bolontrade MF, Sganga L, Piaggio E, Viale DL, Sorrentino MA, Robinson A, Sevlever G, García MG, Mazzolini G, Podhajcer OL. A specific subpopulation of mesenchymal stromal cell carriers overrides melanoma resistance to an oncolytic adenovirus. Stem cells and development 2012;21(14):2689-2702.

Chapter 4: Mesenchymal Stem Cell Homing to Sites of Inflammation

Abstract

Mesenchymal sfJtem cells (MSCs) have great potential to improve clinical outcomes for many inflammatory and degenerative diseases whether through intravenously delivered MSCs or through mobilization and migration of endogenous MSCs to injury sites, termed "stem cell homing". Stem cell homing involves the processes of attachment to and transmigration through endothelial cells lining the vasculature and migration through the tissue stroma to a site of injury or inflammation. While the process of leukocyte transendothelial migration is well understood, far less is known about stem cell homing. In this study, transwells that mimic the vasculature were used to monitor transbarrier movement of human mesenchymal stem cells in response to chemokine exposure. Specifically, transwell membranes lined with human synovial microvascular endothelial cells (HSynMECs) were partitioned from the tissue injury-mimetic site containing chemokine stromal cell-derived factor- 1 (SDF-1). MSCs were loaded in the apical chambers containing endothelial cell-lined membrane, mimicking the vessel, and observed for morphology and transmigration of cells, with SDF-1 in the basal chamber. Two population subsets of MSCs were studied: migrated cells that initiated transmigration on the membrane top and nonmigrated cells in the apical chamber that failed to transmigrate. We hypothesized that cells would adhere to and migrate through the endothelial lining with SDF-1 exposure and that gene and protein expression changes would be observed between migratory and nonmigratory cells. We validated a vasculature model for MSC transmigration, demonstrated kinetics of MSC

transmigration over time, performed gene and protein expression of PI3K, MAPK, and Jak/Stat pathways, and quantified cell transmigration after inhibition of specific cell signaling pathways. Our model supported MSC transmigration and identified key signaling pathways regulating MSC transmigration. These findings allowed us to identify key regulatory molecules involved in MSC homing, specifically mechanisms of transmigration, towards development of targeted therapies.

Introduction

Mesenchymal stem cells (MSCs) have been extensively studied for their trophic and regenerative effects in treatment of various injuries, diseases, and inflammatory conditions [1-4]. The efficacy of MSCs to treat inflammation and tissue injury by intravenous or intra-arterial injection has likely been limited due to lack of knowledge of the underlying molecular mechanisms of stem cell homing [5]. Stem cell homing is activated by inflammation and involves the processes of localization and extravasation, where cells arrest in the vasculature and adhere to and migrate through the vascular lining [6]. Stem cells alter their phenotype during cell culture for expansion of cell numbers; alterations include differential expression of cell surface proteins important for cell-cell signaling and adhesion [7]. This process inhibits the efficacy of cell therapies and requires a better understanding of the basic cellular processes to enable proper targeting of cells to areas of injury. Furthermore, the process of stem cell homing introduces the possibility of using molecular cues for stem cell homing as drugs to enhance endogenous stem cell release and migration to areas of inflammation or injury, potentially obviating the need for stem cell culture prior to treatment. The mechanisms involved in transmigration of MSCs are not fully understood, in contrast to the well-characterized leukocyte

transendothelial migration (TEM). While many similarities between leukocyte and stem cell transmigration exist, there are mechanistic differences in their responses [8]. Both the timing of migration and the morphologic changes during transmigration differ between the cell types. Interestingly, MSCs exhibit morphology more akin to metastatic tumor and embryonic germ cell transmigration than to leukocyte migration [9]. A better understanding of these processes opens the potential that differential homing of stem cells rather than leukocytes to areas of inflammation could be achieved, allowing a reduced inflammatory response, and enhanced regenerative response for these injuries. Luu *et al.* showed that MSC secretion of interleukin-6 (IL-6) suppressed cytokine production after endothelial cell activation and inhibited leukocyte TEM [10]. Understanding the crosstalk between cell types will aid in elucidating these processes.

Most studies investigating homing have used animal models of disease, or simplified migration assays using filter-based co-culture systems. Boyden chambers or transwell assays are commonly used to study adhesion, migration and invasion on various endothelial cell types [11-17]. Smith *et al.* used human brain microvascular endothelial cells to mimic the blood brain barrier and human adipose-derived MSCs with conditioned medium as the chemoattractant in a transmigration invasion assay. This system provided a method to study enhancement of MSC transmigration for engraftment to brain tumors [18]. Other studies investigated various signaling pathways involved in cytoskeletal organization and regulation of cell migration towards a chemoattractant. For example, migration studies showed that SDF-1 stimulates the activity of the PI3K and Jak/Stat signaling pathways [19]. Gao *et al.* provided evidence for SDF-1 activation of Jak2/Stat3, Erk1/2 and NFκB signaling pathways resulting in activation of focal adhesion kinase

(FAK) and cytoskeletal changes inducing MSC migration [20].

Homing studies have used growth factors, chemokines, or a combination of the two to mimic inflammation and injury to promote chemotaxis to activate adhesion and transmigration [21]. Chemokine (C-X-C motif) ligand 12 (CXCL12), also known as SDF-1, has been extensively studied for its influence on mechanisms of stem cell homing and healing [4,22,23]. Another study showed that chemokines were most effective at chemotaxis of MSCs between concentrations of 10 – 100 ng/ml [24]. Zhao *et al.* used a combination of SDF-1 and cytokines to show an increase in bone marrow-derived progenitor cell homing to ischemic transplanted heart and provided evidence for the regeneration of myocardiocytes and blood vessels [25]. Additionally, growth factors including platelet derived growth factor-AB (PDGF-AB), insulin growth factor-1 (IGF-1), hepatic growth factor (HGF), and epidermal growth factor (EGF) have shown to be potent for MSC chemotaxis [26]. MSC trafficking to sites of injury and inflammation has been studied in musculoskeletal tissue for promoting healing and enhancing regeneration [3]. Osteoarthritis (OA) and rheumatoid arthritis (RA) are examples of chronic inflammation affecting the synovium of joints that leads to degradation of cartilage and bone. Synovitis induces pathogenic changes in the endothelium, leading to the transendothelial migration of inflammatory cells [27]. Several chemokines are found in the RA synovium and joint fluid, including SDF-1 [28] and synergistic effects of cytokines and growth factors [29].

In this study, we used a modified transwell system to mimic the vasculature for elucidating the underlying mechanisms involved in transmigration of MSCs towards inflammation. Synovial endothelial cells were used to line the membrane and MSCs were loaded into the upper chambers while chemokine was loaded into the lower chamber.

Bovine serum albumin (BSA) was used in culture media to implement macromolecular crowding (MMC) [30] to promote cell growth and increase physiological relevance of the model. Our hypotheses were 1) human bone marrow-derived MSCs will transmigrate through the monolayer of human synovial microvascular endothelial cells after SDF-1 exposure, 2) gene and protein expression will differ between migrated and nonmigrated MSCs, and 3) PI3K-Akt, MAPK, and Jak/Stat pathways will be activated in MSC transmigration in response to an inflammatory environment. This vascular model could be used to study MSC transmigration for use in strategies to inhibit inflammation while promoting regeneration, as well as for small molecule screening to identify molecules that attract endogenous stem cells and inhibit leukocyte recruitment to areas of injury or inflammation.

Materials and Methods

Experimental Design

Transwell systems were used for studying MSC homing to identify potential target molecules to enhance MSC transmigration for therapeutic applications. Transwell fibronectin-coated inserts were lined with a monolayer of human synovial microvascular endothelial cells. Monolayer integrity was tested using a lucifer yellow (LY) rejection assay, confocal microscopy, and ELISA. Human bone marrow-derived MSCs were loaded into the upper chamber and 100 ng/ml SDF-1 was loaded into the lower chamber of the transwell. Control transwells contained serum-free medium without chemoattractant in the lower chamber. One MSC line and one endothelial cell line were used in this study in triplicate. Migrated cells were collected for cell quantification from each compartment of the transwell; apical chamber, top and bottom of the membrane, and

the basal chamber. Nonmigrated cells were collected from the apical chamber and migratory cells from the top of the membrane for gene expression and protein analyses. Twelve transwell samples were pooled per population subset, migrated and nonmigrated MSCs for qPCR; three transwell samples were pooled per population subset for western blotting. Three transwell samples were used for each transmigration assay with inhibitors for PI3K-Akt, MAPK, and Jak/Stat signaling pathways to quantify their effect on MSC transmigration.

Cell Lines and Cell Culture

Human bone marrow mesenchymal stem cells were obtained from American Type Culture Collection and cultured in mesenchymal stem cell basal medium with growth kit (Manassas, VA). All MSCs in this study were used at passage 4. Human synovial microvascular endothelial cells were obtained from Angio-Proteomie and cultured in ENDO-Growth Medium (EGM) (Boston, MA). All endothelial cells in this study were used at passages 7-8. Cells were expanded in culture at 37°C, 5% CO^2 and 90% humidity and fed every other day until 80% confluent.

Preparation of Transwell Permeable Supports

Polyester terephthalate (PET) transwell membranes of 8 um pore size in 24 well plates were used to study cell transmigration (Corning, NY, #3464). Membranes were coated for 1 hour with 20 μg/mL human fibronectin (Corning, NY). Endothelial cells were seeded < 70% confluency onto the inserts at a density of 2 x 10^5 cells/membrane in 100 ul of complete endothelial cell medium supplemented with 42.0 g/L BSA (Sigma, Missouri). Apical chambers were placed in 600 ul of complete endothelial cell growth medium (EGM) supplemented with 42.0 g/mL BSA for 48 hours.

Lucifer Yellow Rejection Assay

Integrity of the endothelial cell monolayer was validated using the LY Rejection Assay [31]. Endothelial cells were incubated in 60 uM LY CH, potassium salt (Sigma, Missouri) for one hour to measure apical and basal chamber fluorescence at 480 nm with a HIDEX Chameleon V microplate reader (HIDEX, Finland). Percent LY rejection was calculated with the following equation.

% LY Rejection = 100 * (1-RFU $_{basal}$ / RFU $_{apical}$) [32]

Mesenchymal Stem Cell Transmigration Assay

MSCs were loaded in the apical chamber of the transwell at a density of $1x10^5$ cells in serum free (SF) MSC medium supplemented with 42.0 g/mL BSA. For SDF-1 exposure, basal chambers were loaded with the same medium with and without human recombinant stromal cell-derived factor-1 alpha (SDF-1α) (Thermo Fisher, Waltham, MA) at a concentration of 100 ng/mL. For inhibitor treatment, 2.1 nM Crenolanib, PDGFR inhibitor (Thermo Fisher); 11 nM A-674563, Akt inhibitor (Selleckchem); 20 μM Tyrphostin 490, Jak inhibitor (Sigma); and 50 μM ALX-166; Grb2 inhibitor (ENZO) were added to SF medium supplemented with BSA. MSCs were pre-treated with inhibitors for 1 hour before loading into the apical chamber of the transwell. Cells were collected from each compartment of the transwell; apical chamber, top of the membrane, bottom of the membrane, and the basal chamber and identified as nonmigrated and migrated cells. Cell number was quantified using a Quant-iT dsDNA Assay kit, broad range (Thermo Fisher, Waltham, MA), referencing human MSCs as the standard.

Fluorescence Microscopy and Confocal Microscopy

MSCs were incubated in 10 μM Vybrant CFDA SE Cell Tracer for 30 minutes, washed, and loaded into the upper chamber. Transwell membranes were stained with 20 μM CellTracker Red for 30 minutes, washed, and fixed in 4% PFA for fluorescence confocal imaging to visualize the endothelial cell monolayer and MSC morphology. Fluorescence microscopy was performed with an AMG EVOS fl digital inverted fluorescence microscope or a Nikon TE2000 Widefield and C2si laser scanning confocal microscope (Light Microscopy and Imaging Facility, James Madison University, VA).

Endothelial Cell and Mesenchymal Stem Cell Separation

Cultures were placed on ice and cells were collected from the apical chamber and the top of the membrane with 0.05% trypsin-EDTA (Thermo Fisher, Waltham, MA) after 4 hours of SDF-1 exposure. Mixed cell populations were incubated with human anti-CD31 microbeads (Milteni Biotec), loaded into the MS columns, collected on ice, and washed with chilled degased buffer according to the manufacturer's instructions.

RNA Isolation, Quantification, and Quantitative PCR

After MSC isolation, MSCs were lysed in TRIzol and RNA was isolated using phenol. (Thermo Fisher Scientific, Waltham, MA). An RNeasy Mini Kit (Qiagen, USA) was used to purify the RNA; this procedure includes an on-column DNase treatment to reduce genomic template contamination. RNA quantification was performed using a NanoDrop 2000c (Thermo Fisher Scientific, Waltham, MA). RNA was converted to cDNA using RT^2 PreAmp cDNA synthesis and RT^2 PreAmp cDNA synthesis primer mix for human PI3K-Akt and Jak/Stat signaling pathway PCR arrays following the manufacturer's instructions (Qiagen, Germantown, MD) and Thermal Cycler (Eppendorf, Hauppauge, NY). A Real Time 7500 PCR System (Thermo Fisher Scientific, USA) was

used to run quantitative PCR (qPCR) of RT^2 Profiler PCR Arrays for human PI3K-Akt (PAHS-0553) and Jak/Stat (PAHS-0331Z) signaling pathways (Qiagen) at 50 ng of cDNA per 25 µl PCR reaction. Relative quantitation was calculated using the Comparative C_T method ($2^{\wedge-\Delta\Delta C_T}$) [33]. All array controls were in the acceptable range. Gene expression was normalized to MSC apical control samples using RPLP0 and compared to MSC membrane samples.

Western Blotting Analysis

Samples were collected from the apical chamber and top of the insert membranes in cold RIPA buffer (Thermo Fisher) with protease and phosphatase inhibitor cocktails (Sigma). A Bradford assay kit (Thermo Fisher) was used to quantify proteins from the apical chamber and top of the insert membranes according to the manufacturer's instructions. Twenty micrograms of total protein per lane were loaded in a Mini-PROTEAN TGX stain free pre-cast gels of 4-12% polyacrylamide with Precision Plus Dual Color standards and transferred to immune-blot low fluorescence PVDF. All western blotting supplies were from Bio-Rad (Hercules, CA) unless noted otherwise. Phospho-PDGF-RA pTyr754 antibody (1:1000), phospho-AKT pSer473 antibody (1:1000), phospho-Jak2 antibody (1ug), phospho-GRB2 antibody (1ug), and α-tubulin (1:500) primary antibodies and Pierce goat anti-rabbit IgG peroxidase conjugated secondary antibody (1:10000). All antibodies were from Thermo Fisher. Clarity Western ECL substrate was used for chemiluminescence detection with an Alpha Innotech FluorChem SP. Spot densitometry analysis was performed in AlphaView Software (ProteinSimple). Samples were normalized to α-tubulin for densitometric analysis for membrane top and apical samples.

Enzyme-Linked Immunosorbent Assay

Transwells were prepared as previously described. A Human CXCL12/SDF-1α Quantikine ELISA kit (Thermo Fisher, USA) was used to measure the SDF-1 gradient across the transwell insert membrane. Media samples were collected from the apical and basal chambers at 0, 4, 8, 12, and 16 hours. A Human PDGF-AB Quantikine ELISA kit (Thermo Fisher, USA) was used the measure endothelial cell production of PDGF in response to SDF-1 after 4 hours. Media samples were collected from the apical chambers, both with and without SDF-1 exposure. Media without SDF-1 supplementation was used as the control.

Statistical Analysis

Quantitative data was reported as mean +/- standard deviation (SEM). Comparisons were made between groups and within groups by analysis of variance (ANOVA) with Tukey's *post hoc* test. A Wilcoxon Rank Sum test was used to compare gene expression of migrated and nonmigrated MSCs. *A priori* significance was determined using p value ≤ 0.05.

Results

Synovial Microvascular Endothelial Cells Form and Maintain Barrier Function

Monolayer integrity was evaluated via LY rejection and SDF-1 concentration (Fig. 4.1). An increase in LY rejection was observed at 6 hours between the samples with no BSA supplementation and with BSA supplementation. At 6 hours, no BSA resulted in a 46.3% average LY rejection and 56.3% average LY rejection. LY rejection levels peaked at 24 hours in both treatment groups and were maintained through 96 hours (Fig.

4.1A). LY rejection and SDF-1 concentration were measured at 0, 4, 8, 12, and 16 hours. Monolayer integrity was maintained at 90.1% with and without SDF-1 exposure at 0 hours through 12 hours without and with SDF-1 exposure. At 16 hours, percent LY rejection decreased to 87.4% after SDF-1 exposure (Fig. 4.1B). No detection of SDF-1 was observed in the apical chambers. However, the concentration of SDF-1 decreased in the basal chamber by 4 hours and continued to decrease at 8 hours to 29.7 ng/ml. SDF-1 concentration levels began to increase at 12 hours and 16 hours to 35.0 ng/ml (Fig. 4.1C).

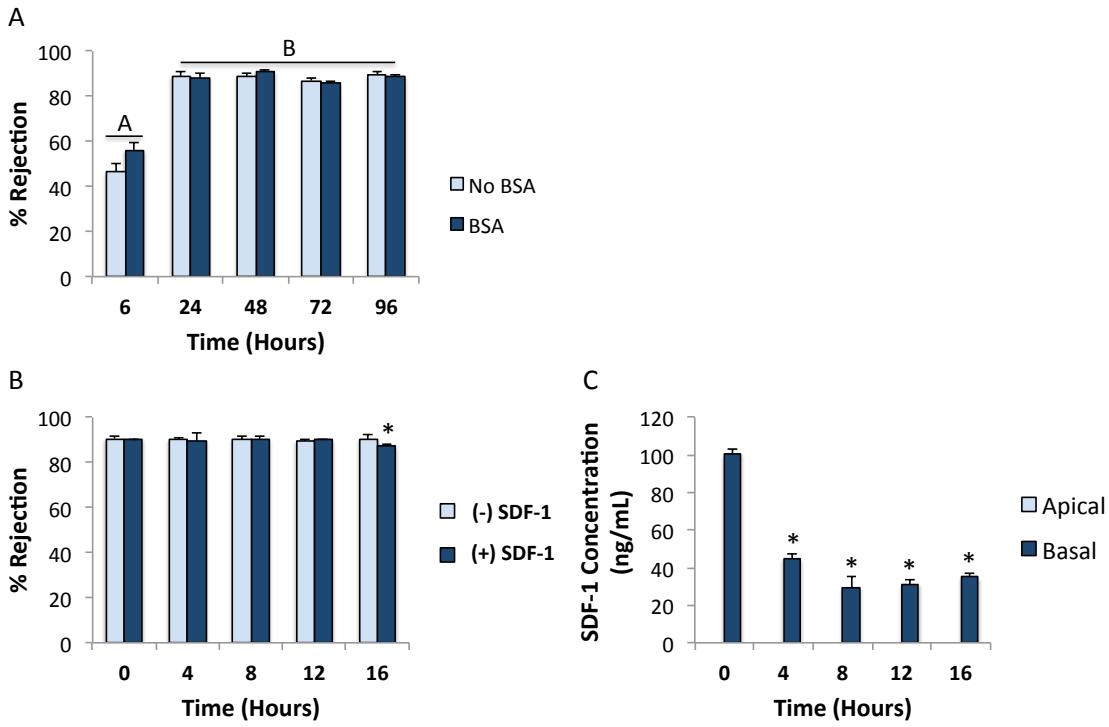

Figure 4.1: Human synovial microvascular endothelial cell monolayer barrier integrity. Transwell membranes were seeded with synovial microvascular endothelial cells with no BSA supplementation of the endothelial growth media and with BSA supplementation of endothelial growth media. Monolayers were then tested with the lucifer yellow rejection assay at 6, 24, 48, 72, and 96 hours. Data not connected by the same letter are significantly different. (A). Human synovial microvascular endothelial cell monolayer barrier integrity was tested with the lucifer yellow rejection assay at 0, 4, 8, 12, and 16 hours. Significance denoted with an asterisk (*) (B). ELISA was used to measure the SDF-1 gradient across the seeded membrane. Media samples were collected from the apical and basal chambers after 0, 4, 8, 12, and 16 hours of SDF-1 exposure. Significance

denoted with an asterisk (*) (C). Error bars represent SEM. A p value ≤ 0.05 was considered significant.

MSCs Migrate Through Synovial Endothelium After SDF-1 Exposure

Cytoplasmic staining of MSCs was visualized by fluorescence microscopy (Fig. 4.2A). MSCs migrated through the endothelial cells towards the bottom of the membrane without SDF-1 and with SDF-1; however, cell number was greater with SDF-1 exposure. Additionally, MSC number was quantified in each of the four transwell compartments and divided into upper compartments for nonmigrated cells and lower compartments for migrated cells (Fig. 4.2B). An increase in cell number was observed for migratory MSCs when SDF-1 was loaded compared to migratory MSCs without SDF-1. Without SDF-1 exposure, 65.1 $^{+}$/- 2.38% of the cells were located on the top of the membrane and 34.9 $^{+}$/- 2.1% were on the bottom of the membrane. After SDF-1 exposure, 59.8 $^{+}$/- 1.32% of the cells were nonmigratory and 40.2 $^{+}$/- 0.8% were migratory.

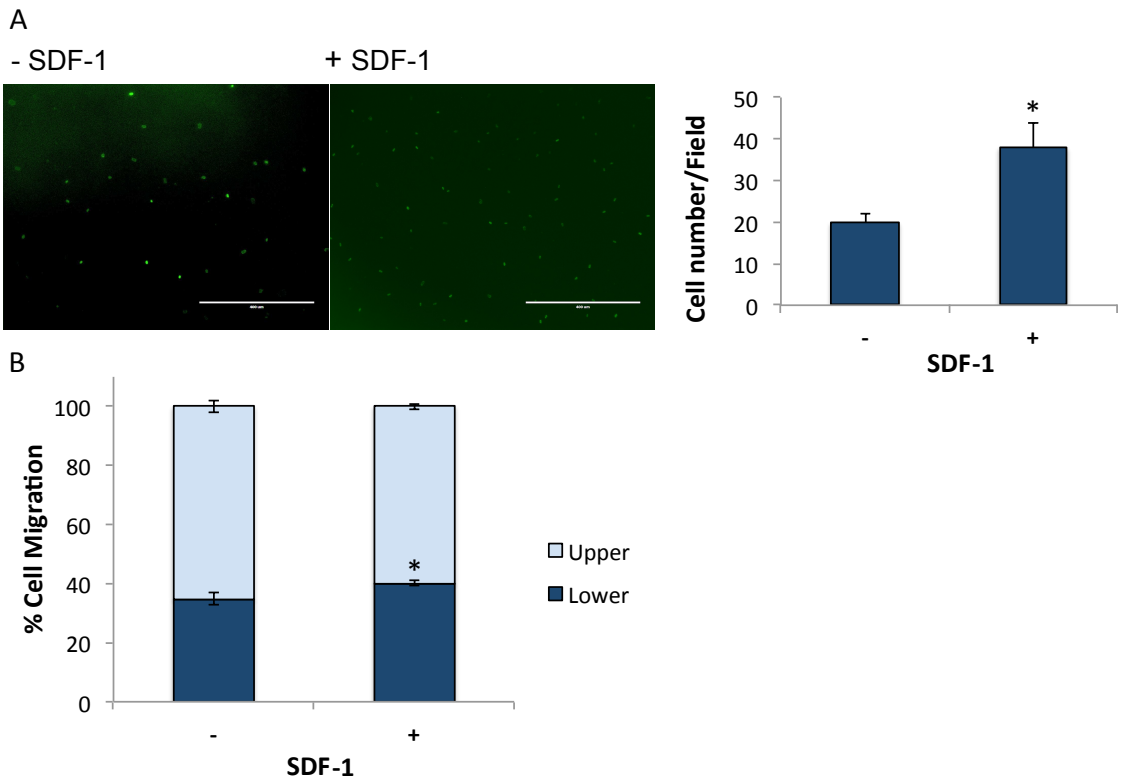

Figure 4.2: Transendothelial migration of human MSCs through human synovial microvascular endothelium in response to SDF-1. Fluorescence staining of human MSCs adhered to the bottom of the membrane with and without loaded SDF-1. Semi-quantification of MSC number/field was performed with ImageJ from fluorescence images (A). Cell number was quantified for the apical chamber, membrane, and basal chamber without and with loaded SDF-1. (B). Upper, nonmigrated MSCs from the apical and membrane top; Lower, migrated MSCs from beneath the membrane and basal chamber. Error bars represent SEM. Scale bar = 400 um. A p value ≤ 0.05 was considered significant and denoted with an asterisk (*).

MSC Transendothelial Migration Peaked at 4 hours in the Vasculature Model

Endothelial cell-seeded membranes were loaded with MSCs and exposed to SDF-1 as previously described for 0 - 16 hours for the co-culture group (Fig. 4.3). Stained endothelial cells and MSCs were visualized with fluorescence microscopy. The top of the membrane supported the endothelial cell cuboidal morphology to form a monolayer and

the adhered MSCs. MSCs were capable of migration through the endothelium and membrane. The bottom of the membrane showed MSCs in the process of transmigration as the membrane pores were filled with the MSCs and completion of transendothelial migration (Fig. 4.3A). Additionally, fluorescence confocal Z-stacked images were compiled from images from the top of the transwell membrane, through the membrane, and to the bottom of the membrane (Video S4.1). MSC migration through the endothelial membrane was similar between the four transwell compartments as previously described at 0, 4, 8, 12, and 16 hours. At 0 hours 94.3 $^{+}$/- 4.1% of the cells were located in the upper compartments and 5.7 $^{+}$/- 0.4% were in the lower compartments. By 4 hours, 58.3 $^{+}$/- 10.8% of the cells were located in the upper compartments and 41.7 $^{+}$/- 6.1% were in the lower compartments (Fig. 4.3B).

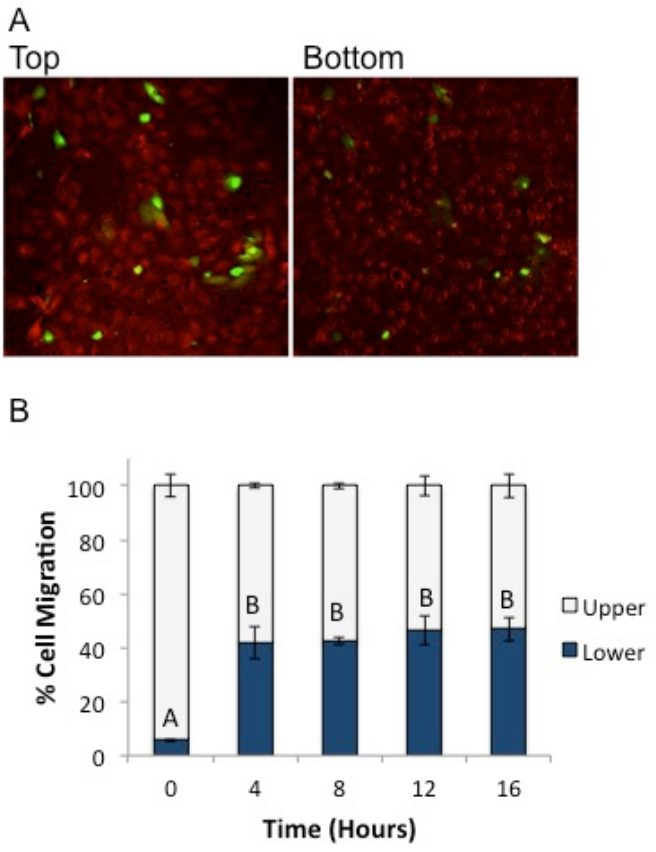

Figure 4.3: Transmigration of human MSCs through human synovial microvascular endothelium. Representative fluorescence confocal images of stained human MSCs (green) and human endothelial cells (red) from the top (left) and bottom (right) of the membrane with loaded SDF-1 at 4 hours. 20x magnification (A). Cell number was quantified for the apical chamber, membrane, and basal chamber with loaded SDF-1 for 0, 4, 8, 12, and 16 hours (B). Top, top of the membrane; Bottom, bottom of the membrane, Upper, nonmigratory MSCs from the apical and membrane top; Lower, migratory MSCs from beneath the membrane and basal chamber. Error bars represent SEM. Data not connected by the same letter are significantly different. Data not connected by the same letter are significantly different. A p value ≤ 0.05 was considered significant.

PI3K, MAPK, and Jak/Stat-associated Genes are Expressed in Migratory MSCs

All genes for the PI3K-Akt and Jak/Stat signaling pathway arrays were expressed in transmigrating MSCs, specifically upregulation of 33 genes of the PI3K-Akt signaling array and upregulation of 15 genes of the Jak/Stat signaling array were observed. Several of these PI3K-associated genes regulate cytoskeletal organization, MAPK signaling, migration, and other cell processes. Four key genes were selected for further investigation (Fig. 4.4, Fig. 4.7). Migrating MSCs showed a 19-fold increase in gene expression of *akt1*, a 4-fold increase in gene expression of *grb2*, and a 10-fold increase in gene expression of *pdgfra* relative to nonmigrated control MSCs. Several genes regulating cell growth, migration, and other cell processes in Jak/Stat signaling were upregulated relative to nonmigrated control MSCs. Migrating MSCs had a 26-fold increase in gene expression of *jak2*.

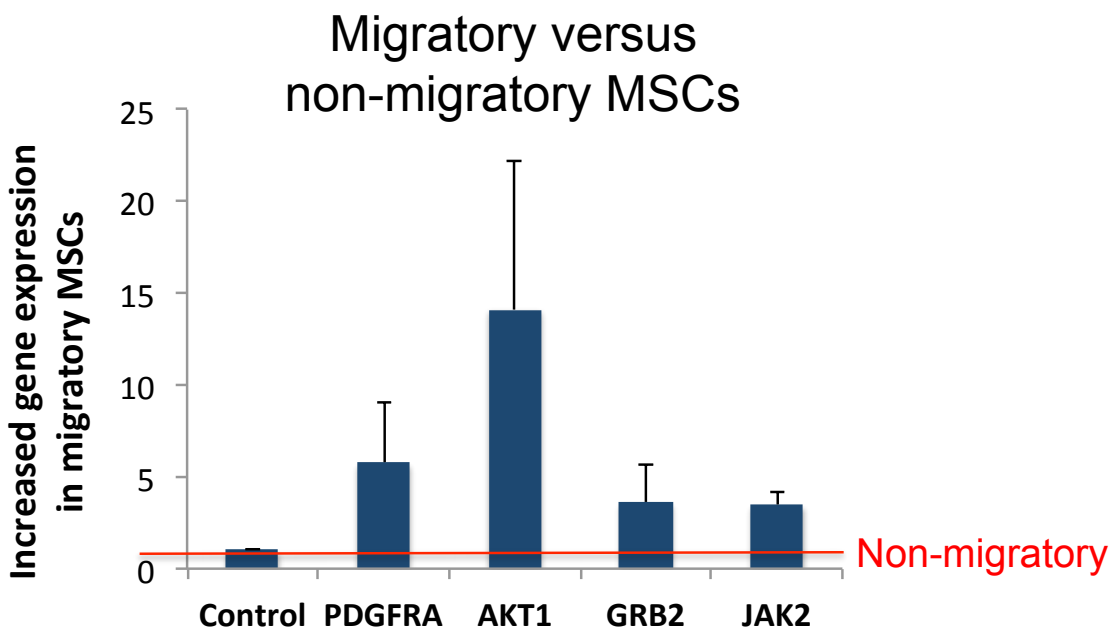

Figure 4.4: qPCR of genes involved in the PI3K-Akt, MAPK, and Jak/Stat signaling pathways were investigated in MSC transmigration. RPLPO was used as the reference gene. Fold change was calculated relative to control nonmigratory cells. Error bars represent SEM. A p value ≤ 0.05 was considered significant.

SDF-1 Stimulated Endothelial Cell PDGF Production and MSC PI3K-Akt, MAPK and Jak/Stat Signaling

Endothelial cell production of PDGF was measured in the media of the apical chambers (Fig. 4.5A, Fig. 4.7). PDGF was not detectable in media from the apical chamber of endothelial cells not exposed to SDF-1. Media samples from apical chambers with SDF-1-stimulated endothelial cells and media samples from apical chambers with SDF-1-stimulated endothelial cells and MSCs resulted in increased levels of PDGF. Spot densitometry analysis was performed for cells from the top of the membrane relative to control samples (Fig 4.5B). Two bands were observed for tubulin membrane top samples in all three groups. Increased phosphorylation was observed for PDGFRA, Akt1, and

Jak2 in the migratory MSCs. Additionally, phosphorylation of Jak2 showed the greatest increase (Fig.4 .7). Results were inconclusive for Grb2.

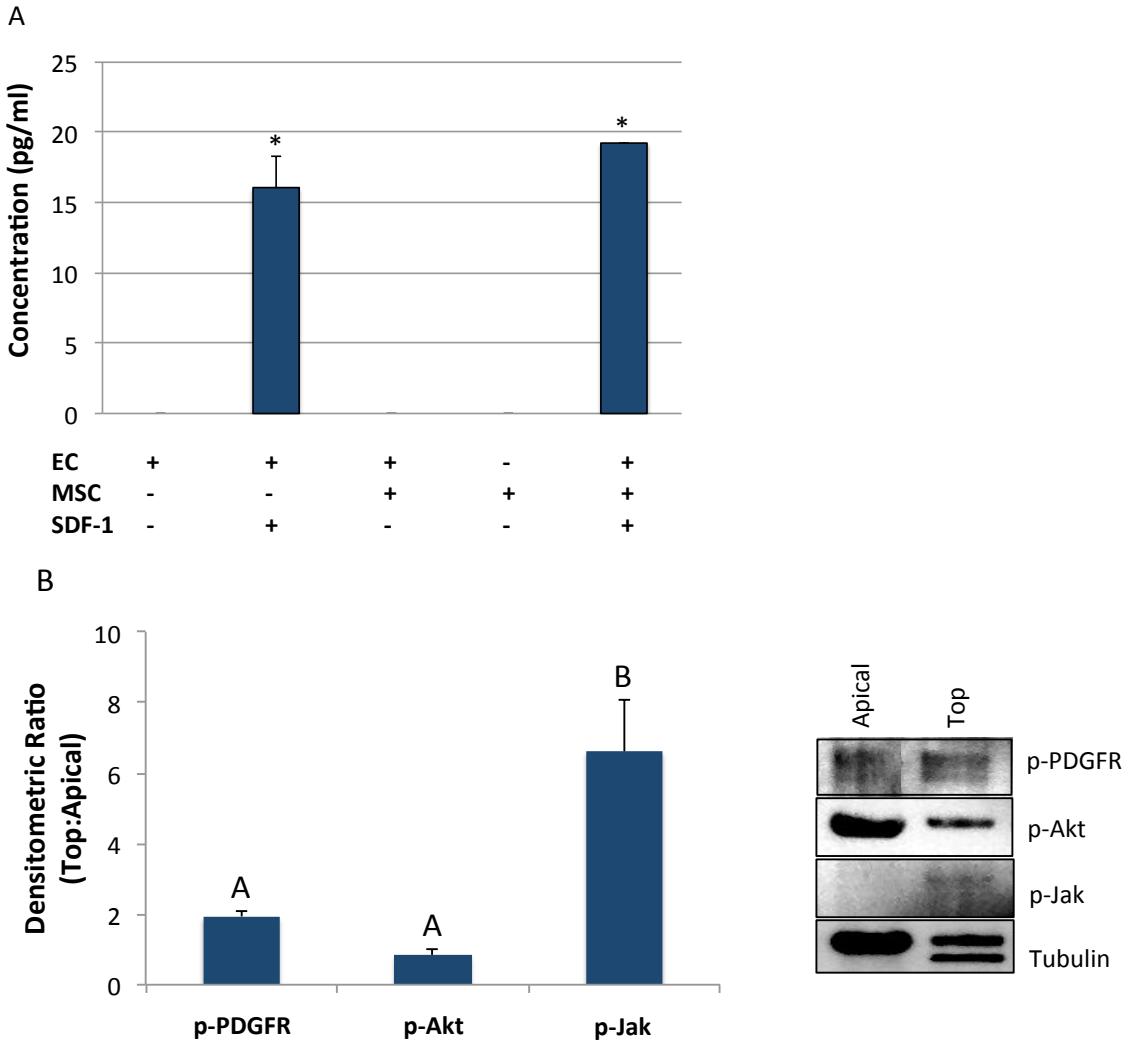

Figure 4.5: PDGF production and phosphorylation of target proteins. ELISA for SDF-1-stimulated endothelial cell production of PDGF (A). Western blot analysis of p-PDGFR, p-Akt, p-Jak, and p-Grb2 signaling in cells collected from the top of the membrane and the apical chamber after SDF-1 exposure. Densitometry analysis was calculated for apical and membrane top samples, relative to alpha-tubulin (B). Top, cells collected from the top of the membrane; Apical, cells collected from the apical chamber. Data not connected by the same letter are significantly different. A p value ≤ 0.05 was considered significant.

Mesenchymal Stem Cell Transmigration is Regulated by PDGFRA, Akt1, Jak2, and Grb2

Transmigration assays were performed for co-culture of endothelial cells with MSCs in response to inhibitors of the three signaling pathways (Fig. 4.6). Decreased MSC transmigration was observed with inhibitor treatment with Crenolanib, A-674563, Tyr 490, and ALX-166 (Fig 4.6A). ALX-166 showed the greatest decrease, followed by Tyr 490, and Crenolanib compared to the No SDF-1 treatment group. A-674563 decreased MSC transmigration compared to the DMSO treatment group. MSC transmigration through the endothelial membrane was quantified for each of the four transwell compartments and calculated for the upper and lower compartments as previously described (Fig. 4.6B). All inhibitors showed decreased cell transmigration to the membrane bottom compared to the DMSO treatment group. Cell transmigration after inhibitor treatment was similar to basal levels of transmigration. Decreased cell transmigration after inhibitor treatments was similar to basal levels of transmigration, except for Crenolanib.

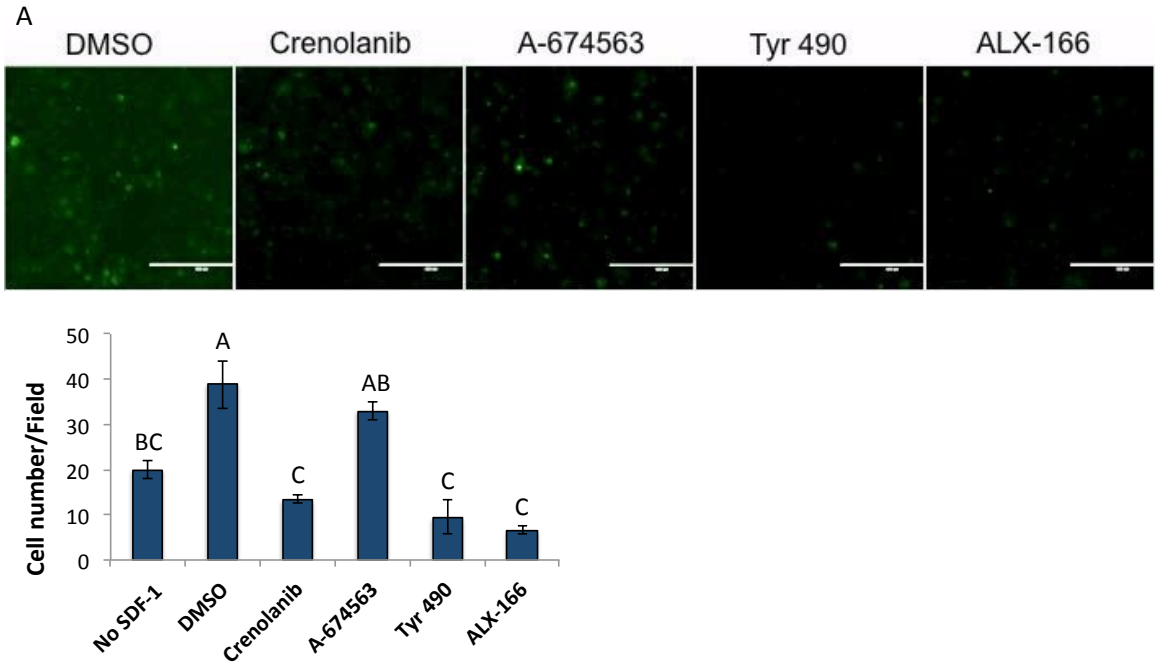

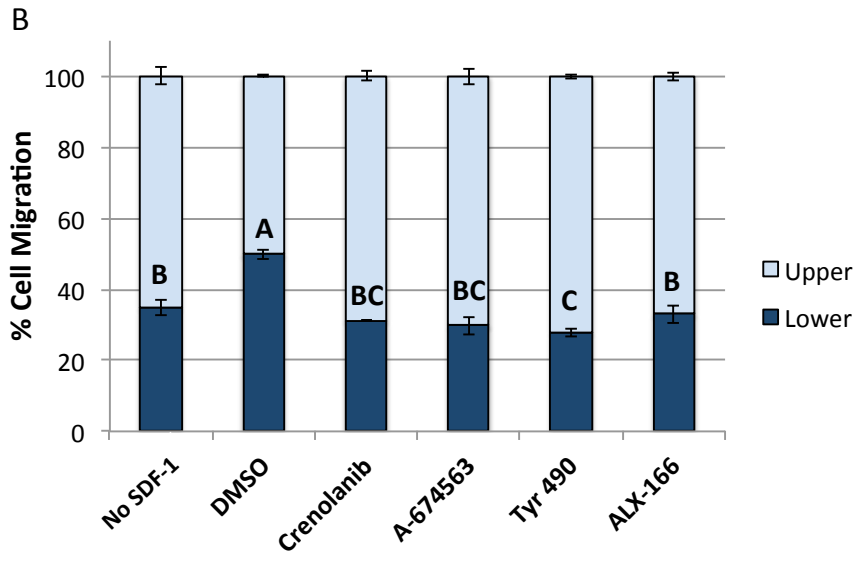

Figure 4.6: Transmigration of human MSCs through human synovial microvascular endothelium in response to inhibitors. Fluorescence images of stained human MSCs adhered to the membrane bottom after inhibitor treatment. Semi-quantification of MSCs per field. (A). Cell number was quantified for the apical chamber, membrane, and basal chamber with SDF-1 and inhibitor treatment for co-culture of endothelial cells and MSCs (B). Crenolanib, PDGFR inhibitor; A-674563, Akt inhibitor; Tyr 490, Jak inhibitor, ALX-166, Brb2 inhibitor; Upper, nonmigrated MSCs from the apical and membrane top; Lower, migrated MSCs from the membrane bottom and basal chamber. Error bars represent SEM. Scale bar = 400 um. Data not connected by the same letter are significantly different. A p value ≤ 0.05 was considered significant.

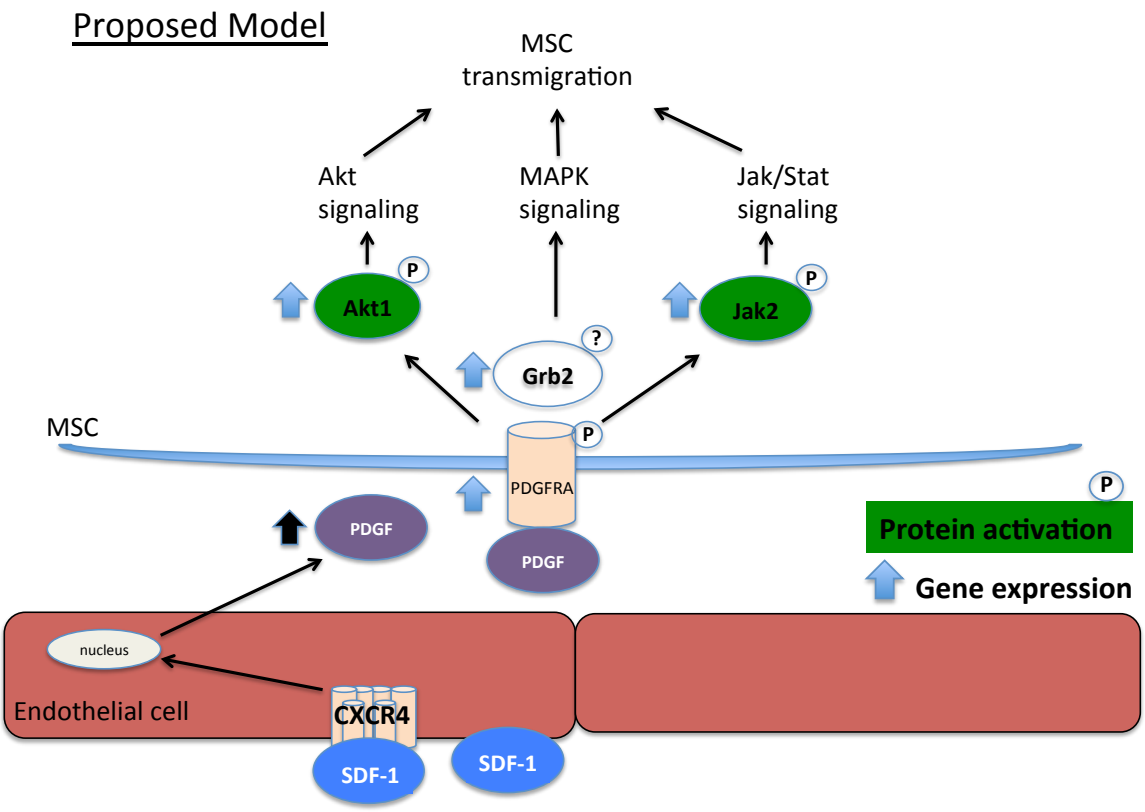

Figure 4.7: Model showing the downstream effects of SDF-1 exposure to human synovial microvascular endothelial cells on MSCs. SDF-1 binds to CXCR4 on endothelial cells and produces PDGF. PDGF binds to PDGFR on MSCs and activates the PI3K-Akt, MAPK, and Jak/Stat signaling pathways. Blue arrows indicate and increase in gene expression and green indicates protein activation via phosphorylation.

Discussion

Homing of exogenous and endogenous MSCs is a multi-step process activated by chemokines and cytokines from inflammatory sites [34]. Studies have investigated MSC homing in comparison to the leukocyte cascade; however, co-culture models involving MSC and endothelial cell interactions are limited. A complete endothelial monolayer barrier was achieved in our transwell system and allowed for transmigration of MSCs. The critical component of this system was monolayer growth and the maintenance of its barrier integrity. As expected, BSA supplementation showed an early increase in LY

rejection of the endothelium compared to monolayers cultured without BSA. Perhaps this is due to increased synthesis of ECM proteins, resulting in promotion of endothelial cell proliferation and increased cell-matrix adhesions. MMC has been used in other studies that showed increased matrix production, [30] cell proliferation, metabolism, and differentiation of MSCs *in vitro* [35]. Maijenburg *et al.* supplemented media with 0.25% BSA; [36] however, MSC migration was studied in the absence of endothelial cells and its effects were not reported. We then tested barrier integrity after SDF-1 exposure and measured SDF-1 concentration in the chambers. Results showed that barrier integrity was maintained through 16 hours of SDF-1 exposure and no SDF-1 was detected in the apical chambers, confirming barrier integrity. Smith *et al.* also used 100 ng/ml SDF-1 in a similar system without detrimental affects [37]. Decreased SDF-1 concentration in the basal chamber may be due to degradation or immobilization of SDF-1 on endothelial cells [38] and appeared to increase again over time. This may be due to endothelial cell and/or MSC production of SDF-1 as studies have shown that PDGF may stimulate SDF-1 production as well [39,40]. The increased MSC transmigration that was observed after the addition of SDF-1 was not due to chemotaxis towards SDF-1 because SDF-1 was contained in the basal chamber by the endothelial barrier. Therefore other possibilities were examined. After model validation, we examined the kinetics of MSC transmigration over time with SDF-1 exposure.

The timing of cell collection has an effect on the stage of migration, collecting MSCs too early may capture the earlier stages before transmigration changes occur and collecting MSCs too late may capture MSCs in the later stages and miss critical changes involved in transmigration. No time-course has been investigated for these purposes.

However, another study has distinguished between these steps of transmigration, quantifying MSC migration as not started, in progress, and completed transmigration [41]. It was expected that cell number would decrease in the upper compartments (nonmigrated cells) of the transwell system and increase in the lower compartments (migrated cells) of the system over time; however migrated MSCs peaked at 4 hours and remained constant through 16 hours. One possible explanation for these results is that a chemotactic SDF-1 gradient was not established; therefore there was no correlated increase of migratory MSCs in response to SDF-1. Fluorescence confocal microscopy allowed visualization of MSC transmigration through the endothelial cell barrier at 4 hours. Teo *et al.* showed similar images of MSC transmigration at 60 minutes on a two-dimensional surface [41]. It was also unexpected that endothelial cells would migrate along with MSCs; however, endothelial progenitor cells have been shown to migrate towards SDF-1 [42]. Results showed that our transwell modifications supported complete monolayer growth and barrier integrity of endothelial cells that could be maintained up to 16 hours with SDF-1 exposure and induce MSC transmigration through a synovial endothelium.

Differences in gene expression of PI3K-Akt and Jak/Stat-associated genes were observed between migrated and nonmigrated MSCs. Fluorescence staining showed adhered MSCs on the membrane top and the MSCs viewed from the bottom of the membrane filled the pores, providing evidence that transmigration was initiated. For this reason, it was determined that 4 hours was an appropriate time for cell collection as it captured MSCs in the process of transmigration and potentially decreased irrelevant changes in gene expression not correlated to initiation of transmigration. It was unexpected that transmigration would occur this quickly. Previous studies have

investigated migration at 4 hours with endothelial cells and transmigration at 12-48 hours [7,43,44]. Other studies report MSC transmigration completion at 60-120 minutes *in vitro*; [41] however, this does not account for adhesion time. Several genes were upregulated at 4 hours suggesting that other cell processes are occurring simultaneously and may not be specific to transmigration or endothelial cell interactions. Additionally, MSCs may be at different steps of the transmigration stage at time of collection. These results also suggest that multiple pathways may be activated.

In addition to gene expression, we investigated activation of signaling pathways in migrated versus nonmigrated MSCs. There was an increase in fold change for many of the growth factor receptors, i.e. PDGFR. We measured PDGF levels in the media and found that PDGF was present after 4 hours in samples with endothelial cells only and endothelial cells loaded with MSCs. The results showed low level production of PDGF by endothelial cells and/or MSCs. Ponte *et al.* showed more efficient migration of MSCs towards growth factors when compared to chemokines/cytokines, with PDGF-AB promoting the greatest chemotaxis [26]. In another study, mouse iPSCs migrated towards glioma conditioned media via tumor growth factor secretion [45]. This evidence suggests that MSCs migrated in response to PDGF, produced by SDF-1-stimulated endothelial cells. Hamdan *et al.* showed that the SDF-1/CXCR4 axis controls PDGF-BB expression, resulting in pericyte differentiation and expansion of tumor vasculature [46]. Western blot analysis showed two bands for membrane top tubulin. This could be explained by post-translation modifications, specifically acetylation observed in migratory cells [47]. The increase in PDGFR phosphorylation observed in each groups was expected and provided evidence towards activation of PDGFR signaling in MSC transmigration. However, while

the changes in Akt phosphorylation between migrated and nonmigrated cells within each group were significant, the low signals for p-Grb2 made results inconclusive. Gene expression data, in addition to western blot analysis, suggested that endothelial cell-MSC interaction may activate PDGFRA/Akt1, PDGFRA/Grb2 and/or PDGFRA/Jak/Stat signaling.

Inhibiting key targets of these pathways demonstrated decreased MSC transmigration. The inhibitors of PDGFRA, Akt1, Jak2, and Grb2 inhibitors showed decreased transmigration to varying degrees, suggesting differences in effectiveness and regulation by multiple signaling pathways. Although our study showed similarities in migration of the different cell types, this suggests involvement of similar molecular mechanisms in migration between MSCs and endothelial cells. Similarly, Lin *et al.* studied inhibition of ROCK, PI3K, and PKC to show decreased MSC transmigration in response to PI3K and ROCK inhibitors, suggesting a role for PI3K and cytoskeletal pathways in involvement [48]. These findings corroborate previous reports of multiple cell signaling pathways involved in transmigration. Another study proposed a model demonstrating the involvement of the MEK/ERK, Jak/Stat3, cytoskeletal organization, and NFκB signaling pathways and their relationship to one another in SDF-1-stimulated MSC migration [20]. Thus, our findings suggest that MSC transmigration involves the interaction of PI3K/Akt, Jak/Stat, and MAPK signaling pathways. Specifically, Jak2 has the potential for use as a therapeutic target in enhancing MSC homing to inflammation.

Conclusions

Our study validates a vascular model that demonstrates the differences between migratory and nonmigratory MSCs and the mechanisms of MSC transmigration. This

was the first study using a modified transwell system for investigation of human MSC transmigration through a synovial microvascular endothelium to show activation of multi-pathway signaling. MSC transmigration may be driven by activation of PDGFRA/PI3K/Akt, PDGFRA/MAPK/Grb2, and PDGFR/Jak2/Stat signaling, as a result of SDF-1 stimulated endothelial cell production of PDGF. Future studies are needed to fully investigate the effects of endothelial cell growth factor and cytokine production on MSC transmigration and the complex interactions between signaling pathways. The development of relevant *in vitro* models will aid in our understanding of the interactions between vessel endothelium and stem cells and the mechanisms involved in transmigration. Therapeutic applications of MSCs may be developed to control the inflammatory process through interference of the leukocyte cascade and immune regulation for tissue healing.

Acknowledgements

The authors would like to thank Dr. Kristopher Kubow for his assistance and training with confocal microscopy at James Madison University's Light Microscopy and Imaging Facility. The authors would like to acknowledge funding by Virginia Tech's Internal Research Competition and the Stamps Family Charitable Foundation.

References

1. Ansboro S, Roelofs AJ, De Bari C. Mesenchymal stem cells for the management of rheumatoid arthritis: immune modulation, repair or both? Current opinion in rheumatology 2017;29(2):201-207.
2. Chen FH, Tuan RS. Mesenchymal stem cells in arthritic diseases. Arthritis research & therapy 2008;10(5):223.
3. Fong ELS, Chan CK, Goodman SB. Stem cell homing in musculoskeletal injury. Biomaterials 2011;32(2):395-409.
4. Shen WL, Chen JL, Zhu T, Chen LK, Zhang W, Fang Z, Heng BC, Yin Z, Chen X, Ji JF and others. Intra-Articular Injection of Human Meniscus Stem/Progenitor Cells Promotes Meniscus Regeneration and Ameliorates Osteoarthritis Through Stromal Cell-Derived Factor-1/CXCR4-Mediated Homing. Stem Cells Translational Medicine 2014;3(3):387-394.
5. Barsotti MC, Di Stefano R, Spontoni P, Chimenti D, Balbarini A. Role of endothelial progenitor cell mobilization after percutaneous angioplasty procedure. Curr Pharm Des 2009;15(10):1107-22.
6. Karp JM, Teo GSL. Mesenchymal stem cell homing: the devil is in the details. Cell stem cell 2009;4(3):206-216.
7. De Becker A, Van Hummelen P, Bakkus M, Broek IV, De Wever J, De Waele M, Van Riet I. Migration of culture-expanded human mesenchymal stem cells through bone marrow endothelium is regulated by matrix metalloproteinase-2 and tissue inhibitor of metalloproteinase-3. Haematologica 2007;92(4):440-449.
8. Kang SK, Shin IS, Ko MS, Jo JY, Ra JC. Journey of Mesenchymal Stem Cells for Homing: Strategies to Enhance Efficacy and Safety of Stem Cell Therapy. Stem Cells International 2012.
9. Teo GS, Ankrum JA, Martinelli R, Boetto SE, Simms K, Sciuto TE, Dvorak AM, Karp JM, Carman CV. Mesenchymal stem cells transmigrate between and directly through tumor necrosis factor-alpha-activated endothelial cells via both leukocyte-like and novel mechanisms. Stem Cells 2012;30(11):2472-86.
10. Thin Luu N, Mcgettrick HM, Buckley CD, Newsome PN, Ed Rainger G, Frampton J, Nash GB. Crosstalk between mesenchymal stem cells and endothelial cells leads to downregulation of cytokine‐induced leukocyte recruitment. Stem cells 2013;31(12):2690-2702.
11. Ponte AL, Marais E, Gallay N, Langonne A, Delorme B, Herault O, Charbord P, Domenech J. The in vitro migration capacity of human bone marrow mesenchymal stem cells: comparison of chemokine and growth factor chemotactic activities. Stem cells 2007;25(7):1737-1745.
12. Mauney J, Olsen BR, Volloch V. Matrix remodeling as stem cell recruitment event: a novel in vitro model for homing of human bone marrow stromal cells to the site of injury shows crucial role of extracellular collagen matrix. Matrix Biology 2010;29(8):657-663.
13. Kwon YW, Heo SC, Jeong GO, Yoon JW, Mo WM, Lee MJ, Jang I-H, Kwon SM, Lee JS, Kim JH. Tumor necrosis factor-α-activated mesenchymal stem cells promote endothelial progenitor cell homing and angiogenesis. Biochimica et Biophysica Acta (BBA) - Molecular Basis of Disease 2013;1832(12):2136-2144.

14. Gong Y, Zhao Y, Li Y, Fan Y, Hoover-Plow J. Plasminogen regulates cardiac repair after myocardial infarction through its noncanonical function in stem cell homing to the infarcted heart. Journal of the American College of Cardiology 2014;63(25_PA):2862-2872.
15. Di Scipio F, Sprio A, Folino A, Carere M, Salamone P, Yang Z, Berrone M, Prat M, Losano G, Rastaldo R. Injured cardiomyocytes promote dental pulp mesenchymal stem cell homing. Biochimica et Biophysica Acta (BBA)-General Subjects 2014;1840(7):2152-2161.
16. Chen W, Li M, Cheng H, Yan Z, Cao J, Pan B, Sang W, Wu Q, Zeng L, Li Z. Overexpression of the mesenchymal stem cell Cxcr4 gene in irradiated mice increases the homing capacity of these cells. Cell biochemistry and biophysics 2013;67(3):1181-1191.
17. Belema-Bedada F, Uchida S, Martire A, Kostin S, Braun T. Efficient Homing of Multipotent Adult Mesenchymal Stem Cells Depends on FROUNT-Mediated Clustering of CCR2. Cell Stem Cell 2008;2(6):566-575.
18. Smith CL, Chaichana KL, Lee YM, Lin B, Stanko KM, O'Donnell T, Gupta S, Shah SR, Wang J, Wijesekera O. Pre-exposure of human adipose mesenchymal stem cells to soluble factors enhances their homing to brain cancer. Stem cells translational medicine 2015;4(3):239-251.
19. Mellado M, Rodríguez-Frade JM, Mañes S, Martínez-A C. Chemokine signaling and functional responses: the role of receptor dimerization and TK pathway activation. Annual review of immunology 2001;19(1):397-421.
20. Gao H, Priebe W, Glod J, Banerjee D. Activation of signal transducers and activators of transcription 3 and focal adhesion kinase by stromal cell‐derived factor 1 is required for migration of human mesenchymal stem cells in response to tumor cell‐conditioned medium. Stem Cells 2009;27(4):857-865.
21. Yagi H, Soto-Gutierrez A, Parekkadan B, Kitagawa Y, Tompkins RG, Kobayashi N, Yarmush ML. Mesenchymal stem cells: mechanisms of immunomodulation and homing. Cell transplantation 2010;19(6):667.
22. Lutz M, Rosenberg M, Kiessling F, Eckstein V, Heger T, Krebs J, Ho AD, Katus HA, Frey N. Local injection of stem cell factor (SCF) improves myocardial homing of systemically delivered c-kit plus bone marrow-derived stem cells. Cardiovascular Research 2008;77(1):143-150.
23. Jung Y, Wang J, Schneider A, Sun YX, Koh-Paige AJ, Osman NI, McCauley LK, Taichman RS. Regulation of SDF-1 (CXCL12) production by osteoblasts; a possible mechanism for stem cell homing. Bone 2006;38(4):497-508.
24. Chamberlain G, Smith H, Rainger GE, Middleton J. Mesenchymal stem cells exhibit firm adhesion, crawling, spreading and transmigration across aortic endothelial cells: effects of chemokines and shear. PloS one 2011;6(9):e25663.
25. Zhao TM, Zhang DS, Millard RW, Ashraf M, Wang YG. Stem cell homing and angiomyogenesis in transplanted hearts are enhanced by combined intramyocardial SDF-1 alpha delivery and endogenous cytokine signaling. American Journal of Physiology-Heart and Circulatory Physiology 2009;296(4):H976-H986.
26. Ponte. The in vitro migration capacity of human bone marrow mesenchymal stem cells: Comparison of chemo- kine and growth factor chemotactic activities. 2007.

27. Middleton J, Americh L, Gayon R, Julien D, Aguilar L, Amalric F, Girard J-P. Endothelial cell phenotypes in the rheumatoid synovium: activated, angiogenic, apoptotic and leaky. Arthritis Research and Therapy 2004;6(2):60-77.
28. Szekanecz Z, Kim J, Koch AE. Chemokines and chemokine receptors in rheumatoid arthritis. 2003. Elsevier. p 15-21.
29. Higgs R. Rheumatoid arthritis: synergistic effects of growth factors drive an RA phenotype in fibroblast-like synoviocytes. Nature Reviews Rheumatology 2010;6(7):383-383.
30. Chen C, Loe F, Blocki A, Peng Y, Raghunath M. Applying macromolecular crowding to enhance extracellular matrix deposition and its remodeling in vitro for tissue engineering and cell-based therapies. Advanced drug delivery reviews 2011;63(4):277-290.
31. Kimberly A. Foster a b, Michael L. Avery c, Mehran Yazdanian b,, c KLA. Characterization of the Calu-3 cell line as a tool to screen pulmonary drug delivery. International Journal of Pharmaceutics 2000.
32. Inc C. Corning HTS Transwell-96 Permeable Support Protocols for Drug Transport. Corning Inc; 2007. p Application Note.
33. Leutenegger CM, Mislin CN, Sigrist B, Ehrengruber MU, Hofmann-Lehmann R, Lutz H. Quantitative real-time PCR for the measurement of feline cytokine mRNA. Veterinary Immunology and Immunopathology 1999;71(3–4):291-305.
34. Karp JM, Teol GSL. Mesenchymal Stem Cell Homing: The Devil Is in the Details. Cell Stem Cell 2009;4(3):206-216.
35. Patrikoski M, Lee MHC, Mäkinen L, Ang XM, Mannerström B, Raghunath M, Miettinen S. Effects of Macromolecular Crowding on Human Adipose Stem Cell Culture in Fetal Bovine Serum, Human Serum, and Defined Xeno-Free/Serum-Free Conditions. Stem Cells International 2017;2017.
36. Maijenburg MW, Gilissen C, Melief SM, Kleijer M, Weijer K, ten Brinke A, Roelofs H, Van Tiel CM, Veltman JA, de Vries CJ. Nuclear receptors Nur77 and Nurr1 modulate mesenchymal stromal cell migration. Stem cells and development 2011;21(2):228-238.
37. Smith H, Whittall C, Weksler B, Middleton J. Chemokines stimulate bidirectional migration of human mesenchymal stem cells across bone marrow endothelial cells. Stem cells and development 2011;21(3):476-486.
38. Schwarz J, Bierbaum V, Merrin J, Frank T, Hauschild R, Bollenbach T, Tay S, Sixt M, Mehling M. A microfluidic device for measuring cell migration towards substrate-bound and soluble chemokine gradients. Scientific Reports 2016;6.
39. Kamprom W, Kheolamai P, Yaowalak U, Supokawej A, Wattanapanitch M, Laowtammathron C, Issaragrisil S. Effects of mesenchymal stem cell-derived cytokines on the functional properties of endothelial progenitor cells. European journal of cell biology 2016;95(3):153-163.
40. Song N, Huang Y, Shi H, Yuan S, Ding Y, Song X, Fu Y, Luo Y. Overexpression of platelet-derived growth factor-BB increases tumor pericyte content via stromal-derived factor-1α/CXCR4 axis. Cancer research 2009;69(15):6057-6064.
41. Teo GS, Ankrum JA, Martinelli R, Boetto SE, Simms K, Sciuto TE, Dvorak AM, Karp JM, Carman CV. Mesenchymal Stem Cells Transmigrate Between and

Directly Through Tumor Necrosis Factor-α-Activated Endothelial Cells Via Both Leukocyte-Like and Novel Mechanisms. Stem Cells 2012;30(11):2472-2486.

42. Moore M, Hattori K, Heissig B, SHIEH JH, Dias S, Crystal R, Rafii S. Mobilization of endothelial and hematopoietic stem and progenitor cells by adenovector-mediated elevation of serum levels of SDF-1, VEGF, and angiopoietin-1. Annals of the New York Academy of Sciences 2001;938(1):36-47.
43. Krstić J, Obradović H, Jauković A, Okić-Đorđević I, Trivanović D, Kukolj T, Mojsilović S, Ilić V, Santibañez JF, Bugarski D. Urokinase type plasminogen activator mediates Interleukin-17-induced peripheral blood mesenchymal stem cell motility and transendothelial migration. Biochimica et Biophysica Acta (BBA)-Molecular Cell Research 2015;1853(2):431-444.
44. Smith CL, Chaichana KL, Lee YM, Lin B, Stanko KM, O'Donnell T, Gupta S, Shah SR, Wang J, Wijesekera O. Pre-Exposure of Human Adipose Mesenchymal Stem Cells to Soluble Factors Enhances Their Homing to Brain Cancer. Stem cells translational medicine 2015;4(3):239-251.
45. Koizumi S, Gu C, Amano S, Yamamoto S, Ihara H, Tokuyama T, Namba H. Migration of mouse-induced pluripotent stem cells to glioma-conditioned medium is mediated by tumor-associated specific growth factors. Oncology letters 2011;2(2):283-288.
46. Hamdan R, Zhou Z, Kleinerman ES. Blocking SDF-1α/CXCR4 Downregulates PDGF-B and Inhibits Bone Marrow–Derived Pericyte Differentiation and Tumor Vascular Expansion in Ewing Tumors. Molecular cancer therapeutics 2014;13(2):483-491.
47. Perdiz D, Mackeh R, Poüs C, Baillet A. The ins and outs of tubulin acetylation: more than just a post-translational modification? Cellular signalling 2011;23(5):763-771.
48. Lin M-N, Shang D-S, Sun W, Li B, Xu X, Fang W-G, Zhao W-D, Cao L, Chen Y-H. Involvement of PI3K and ROCK signaling pathways in migration of bone marrow-derived mesenchymal stem cells through human brain microvascular endothelial cell monolayers. Brain research 2013;1513:1-8.

Chapter 5: Conclusions and Future Directions

Summary of Results

The occurrences of tendon injuries are on the rise and there is currently no cure. Regenerative medicine strives to harness the full potential of stem cells that have great potential for development of new therapeutics for tendon healing. Knowledge of the microenvironmental factors influencing cell behavior and the ability to mimic these in *in vitro* studies hold the key to elucidating cellular and molecular mechanisms of tissue injury and repair. This dissertation introduces two important processes of MSCs; cell differentiation for tissue repair and MSC homing towards inflammation and tissue injury (Fig 5.1).

In the first study, manufactured STEP scaffolds were used to study whole cell populations towards tenogenesis. Scaffolds of highly aligned organization where used to mimic the alignment of collagen and spatial distribution of tenocytes found in native tendon. It was hypothesized that scaffold of aligned orientation would promote MSC differentiation towards tenogenesis. Scaffolds promoted an elongated tenocyte-like morphology, increased gene expression of tendon-associated biomarkers, and increased production of collagen and GAG. Together, these results provided evidence of tenogenesis and emphasized the importance of appropriate scaffold parameters in mimicking native tissue and the control of cellular behaviors.

In the second study, we examined the mechanisms of MSC homing, specifically the process of transmigration towards inflammation or injury. While many studies have investigated MSC migration, very few have studied MSC transmigration with the involvement of endothelium. A co-culture system, using modified transwell chambers

was used to mimic the vasculature to determine the mechanisms of MSC transmigration. Human synovial microvascular endothelial cells were seeded on the top of the permeable membrane and human bone marrow-derived MSCs were loaded in the upper chamber as SDF-1 was loaded in the lower camber. We hypothesized that cells would adhere to and migrate through the endothelial cell lining of this vasculature model with SDF-1 exposure and that gene and protein expression changes related to PI3K, MAPK, and Jak/Stat signaling would be observed between migratory and nonmigratory cells. Results showed complete barrier integrity and maintenance in this vasculature model. Gene expression changes of several genes involved in the PI3K, MAPK, and Jak/Stat signaling pathways between migrated and nonmigrated MSCs were observed, specifically *pdgfra*, *akt1*, *jak2*, and *grb2*. Evidence showed that SDF-1 was not directly involved in MSC transmigration, rather SDF-1 stimulated endothelial cell production of PDGF and pathway activation. Furthermore, decreased cell migration in the presence of PDGFR, Akt1, Jak2, and Grb2 inhibitors suggested activation and control of transmigration through multiple signaling pathways after PDGFR activation. It was concluded that human bone marrow-derived MSC transmigration through human synovial microvascular endothelial cells is partially regulated by PDGFRA, PI3K-Akt, MAPK, and Jak/Stat signaling.

The number of potential stem cell therapies and the different approaches that can be used to develop stem cell therapies is vast. These two studies highlight the need to understand the microenvironmental cues that control cell signaling for the processes of MSC migration, engraftment, and regenerative/trophic effects. This knowledge of the interactions between microenvironmental factors and MSCs will provide the answers for development of therapeutic treatments.

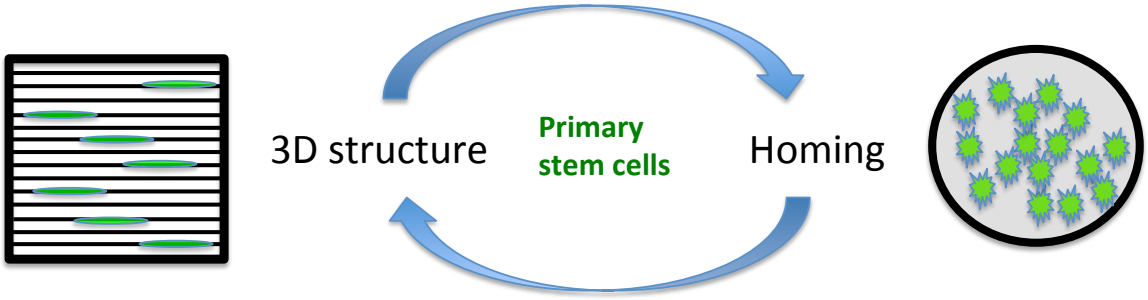

Figure 5.1: Stem cell therapies using primary stem cells.

Manufacturing 3D structures to mimic native tissue structure for support of differentiated stem cells for implantation and administration of stem cells through intravenous, intra-arterial, or local injection are two methods of cell therapies.

Future Directions

Chapter 2 describes a study using aligned, MSC-seeded STEP scaffolds that promoted an elongated tenocyte-like morphology, increased gene expression of tendon-associated biomarkers, and increased deposition of matrix proteins. Evidence suggested that alignment was the dominant factor influencing tenogenic differentiation as both scaffold designs resulted in similar cell responses. Modifications to scaffold design, including fiber diameter, density, and architecture, could be implemented to further study MSC response to topographical cues. Additionally, this study focused on the cellular responses to topography. Future studies using STEP-manufactured scaffolds include examination of the underlying molecular mechanisms of topographical cues on MSCs towards tenogenic differentiation.

Chapter 4 describes a study using a modified Transwell system to investigate the molecular mechanisms of MSCs through synovial endothelium in response to SDF-1 exposure. Further experiments using this Transwell system include investigation of SDF-1 induced PDGF and PDGF-induced SDF-1 signaling between endothelial cells and MSCs, investigation of the relationship between other endothelial cell and MSC growth

factors and chemokine signaling pathways, and 3) the cross-talk between multiple signaling pathways involved in MSC transmigration. Additionally, this model lends itself to several modifications including media composition and further investigation of the affects of bovine serum albumin (BSA) within the vasculature, composition of extracellular matrix proteins for endothelial cell adhesion and MSC invasion, and additional cell populations to include direct comparisons to leukocytes and interactions with other cells of the vasculature or immune system to be tailored to the target tissue.

Appendix A: STEP Aligned Nanofibers

Seeding Density and Scaffold Preparation

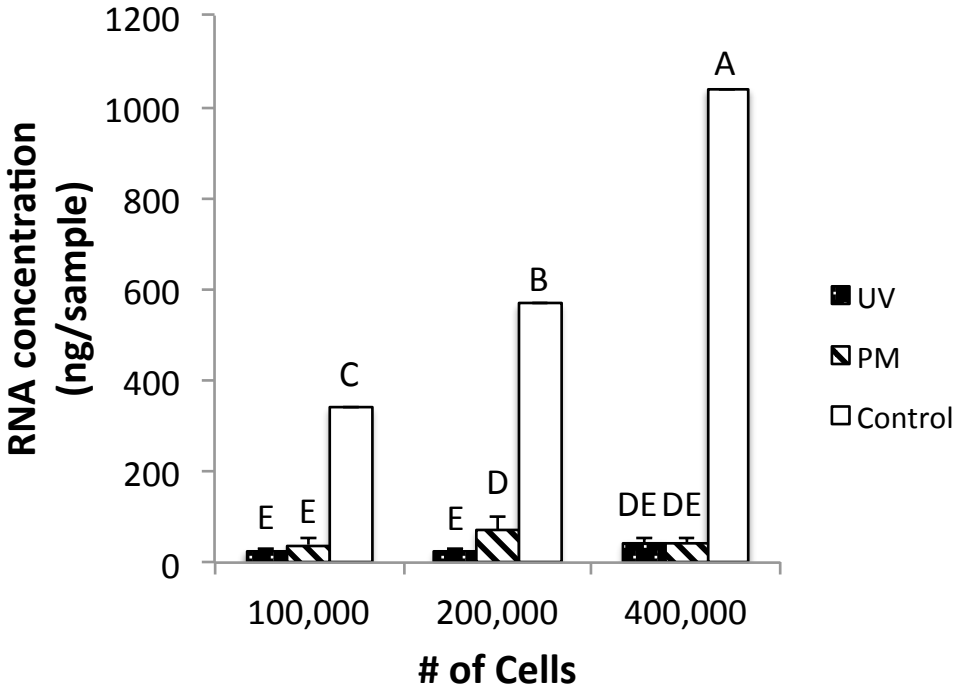

Figure A.1: Nanofiber seeding of equine bone marrow-derived mesenchymal stem cells. Nanofibers seeded with 100,00, 200,000, and 400,000 equine bone marrow-derived MSCs on UV and fibronectin-coated fibers, plasma-treated and fibronectin-coated fibers, and culture-treated plastic controls. UV, ultraviolet light; PM, plasma-treated. Error bars represent SEM. Data not connected by the same letter are significantly different. p value ≤ 0.05 was considered significant.

Appendix B: Mesenchymal Stem Cell Homing

Human Umbilical Vein Endothelial Cell Seeding Density and Barrier Integrity

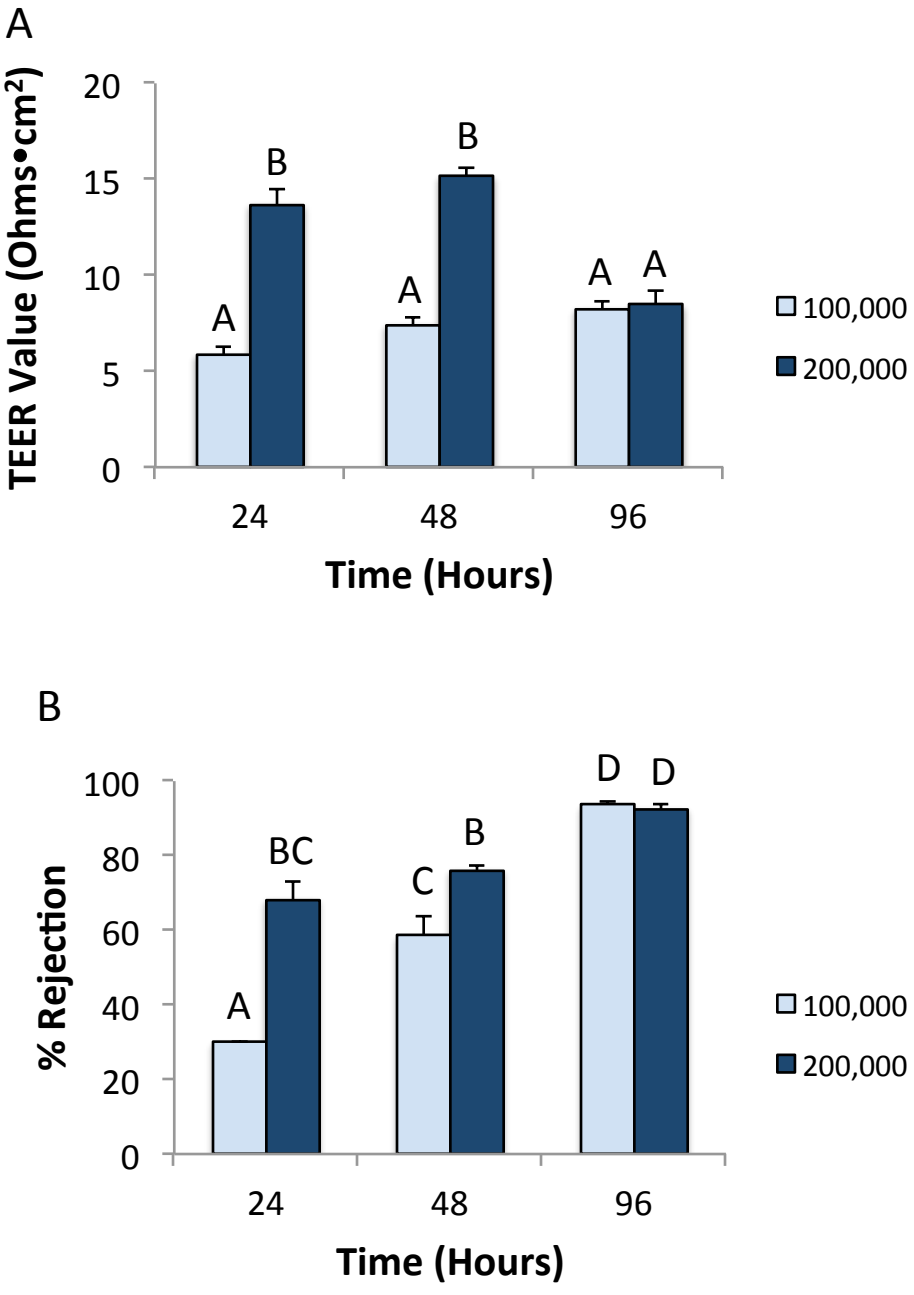

Figure B.1: Human umbilical vein endothelial cell seeding density affected barrier integrity. HUVECs were seeded onto fibronectin-coated Transwell membranes at 1x105 and 2x105 cells per membrane. TEER measurements were calculated at 24,

48, and 96 hours (A). Percent Lucifer Yellow rejection was calculated at 24, 48, and 96 hours (B). Error bars represent SEM. Data not connected by the same letter are significantly different. p value ≤ 0.05 was considered significant.

Human Umbilical Vein Endothelial Cell Barrier Integrity

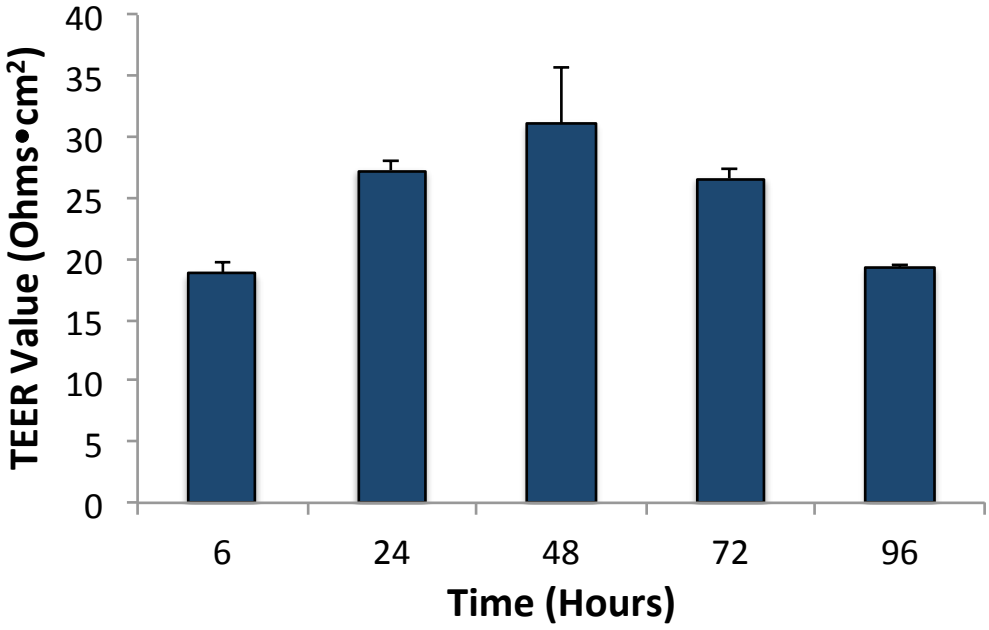

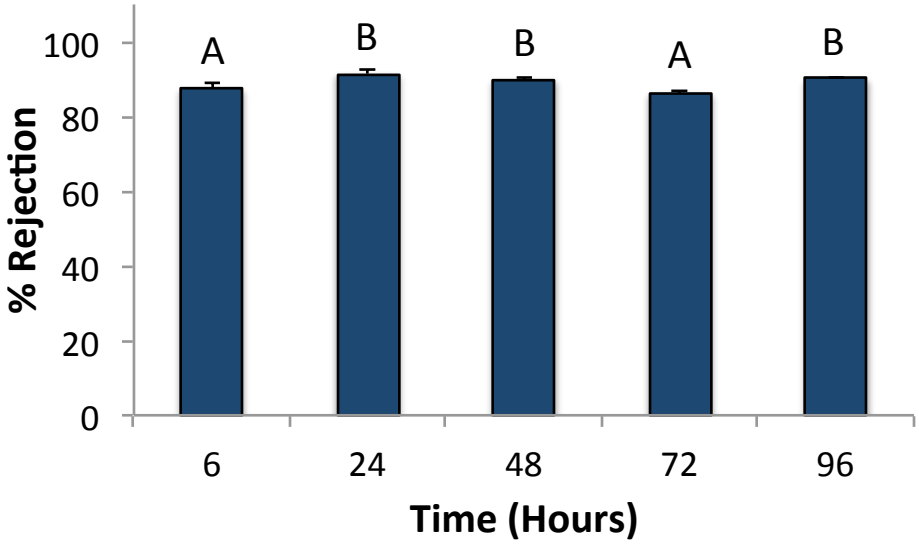

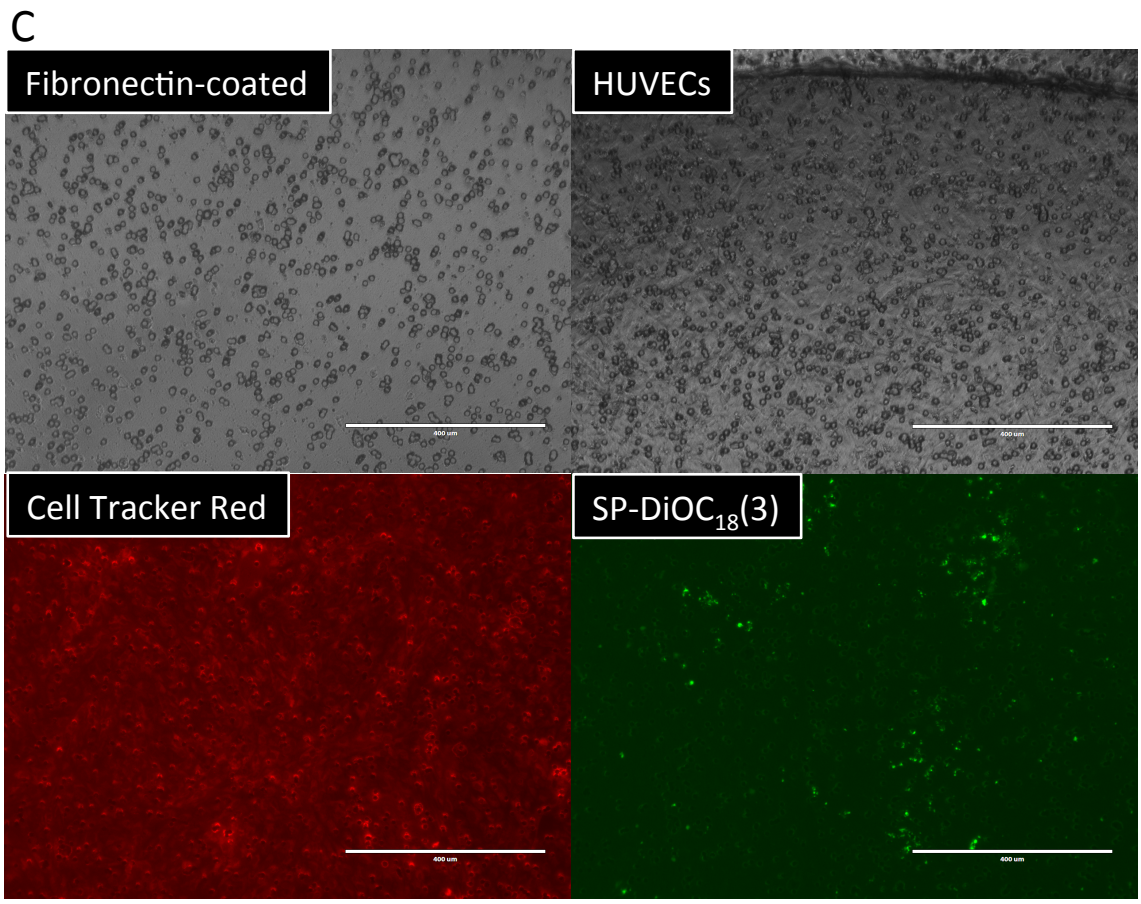

Figure B.2: Human umbilical vein endothelial cell monolayer barrier integrity changed over time. HUVECs were seeded onto fibronectin-coated Transwell membranes at 2x105 cells per membrane. TEER measurements were calculated at 6, 24, 48, 72, and 96 hours (A). Percent lucifer yellow rejection was calculated at 6, 24, 48, 72, and 96 hours (B). Human umbilical vein endothelial cell (HUVEC) monolayer barrier integrity via fluorescence microscopy on day 2. HUVECs seeded at 2x105 per Transwell membrane were stained with Cell Tracker Red and SP-$DiOC_{18}(3)$ (green) and visualized with fluorescence microscopy. Scale bar is 400 µm (C). Error bars represent SEM. Data not connected by the same letter are significantly different. p value ≤ 0.05 was considered significant.

Human Synovial Microvascular Endothelial Cell Barrier Integrity

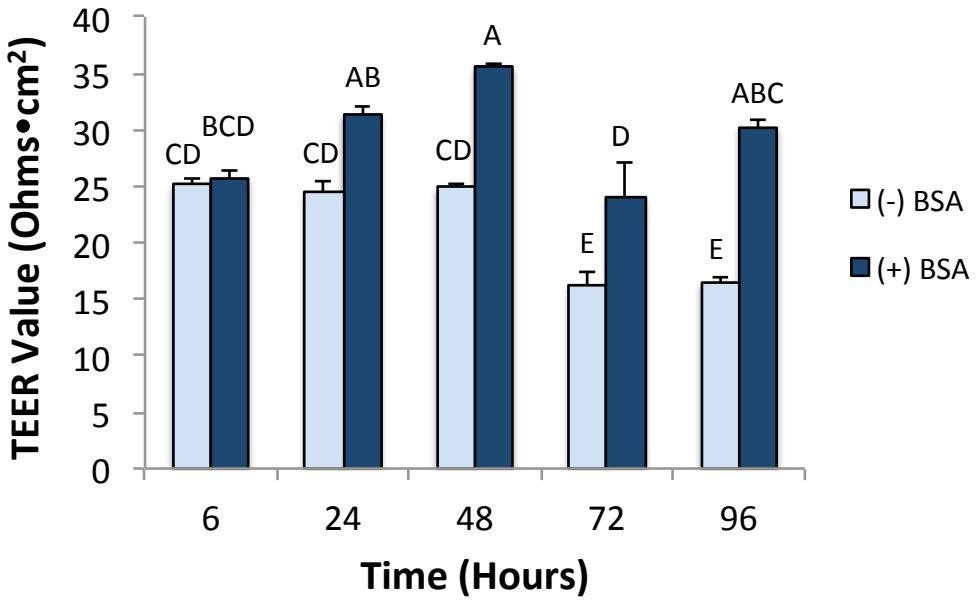

Figure B.3: Human synovial microvascular endothelial cell monolayer barrier integrity changed over time. HSynMEC monolayer integrity +/- BSA supplementation measured via TEER measurements at 6, 24, 48, 72, and 96 hours. Error bars represent SEM. Data not connected by the same letter are significantly different. p value ≤ 0.05 was considered significant.

Chemokine and Cytokine Treatment on Barrier Integrity

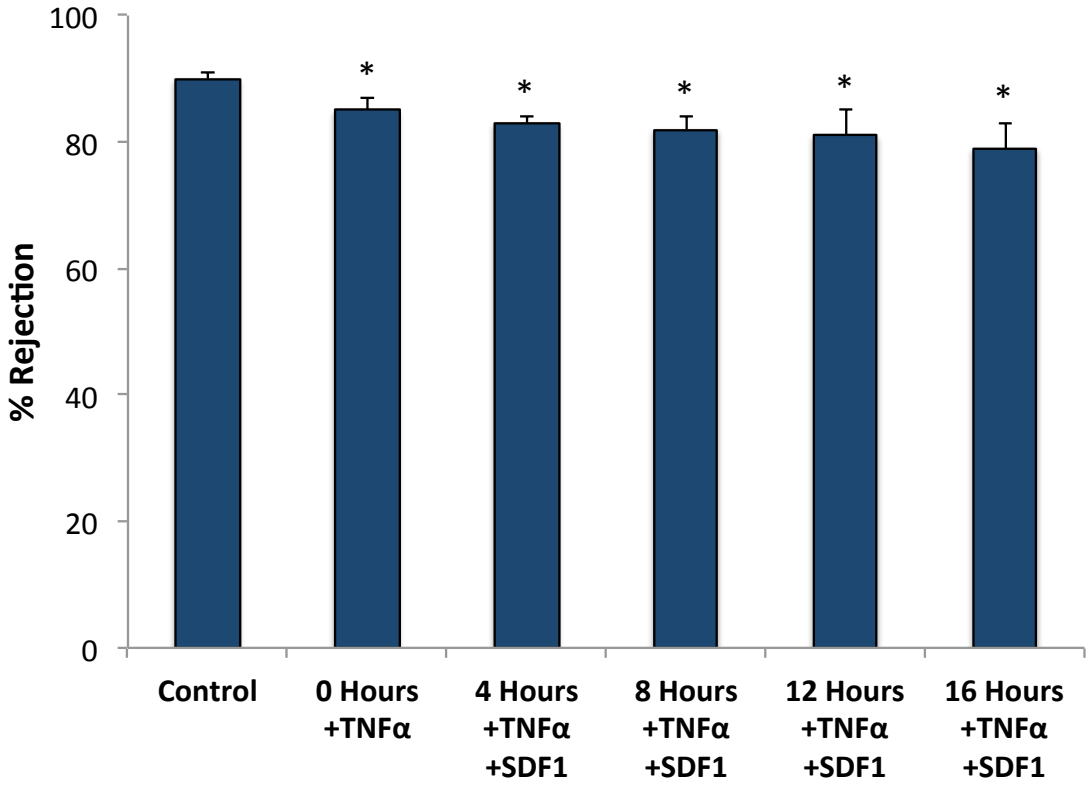

Figure B.4: Human synovial microvascular endothelial cell monolayer barrier integrity with BSA supplementation, TNF-α, and SDF-1. Monolayer integrity was measured via lucifer yellow rejection assay at 0, 4, 8, 12, and 16 hours. Control was untreated monolayer. Error bars represent SEM. p value ≤ 0.05 was considered significant.

Cell Collection Methods

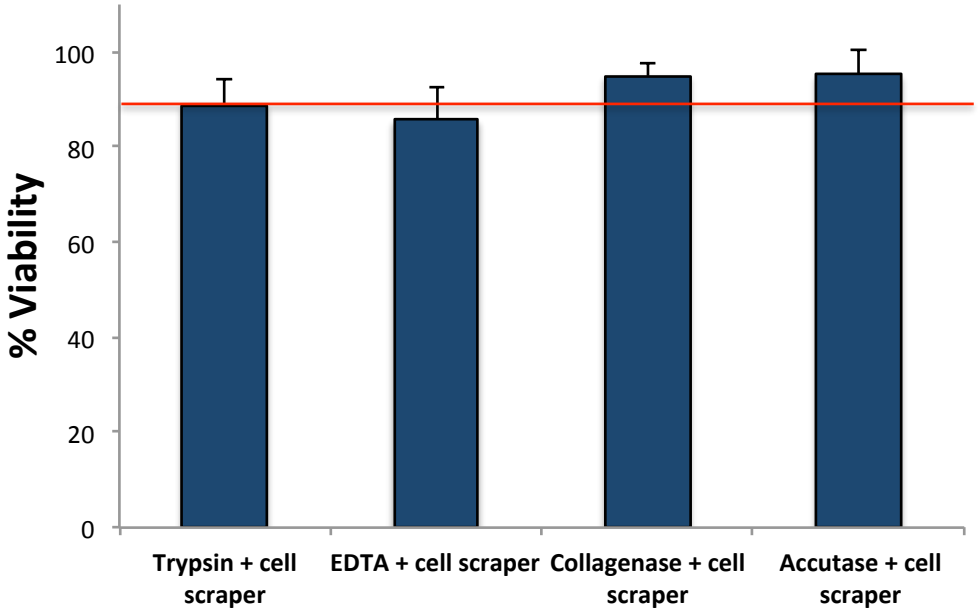

Figure B.5: Human bone marrow-derived mesenchymal stem cells were collected from transwell membranes. Methods included trypsin, EDTA, collagenase, and Accutase, followed by a cell scraper and % viability calculation. Percent viability greater that 90% (red line) was required for experimental conditions. Error bars represent SEM.

Time-course Transmigration Assay

Human Synovial Microvascular Endothelial Cells

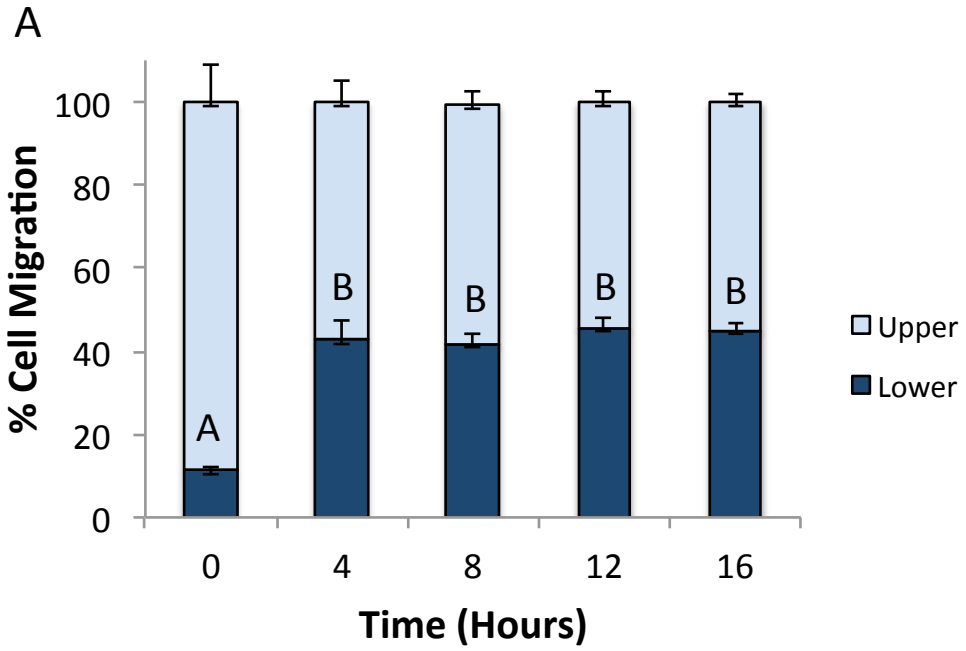

Human Mesenchymal Stem Cells

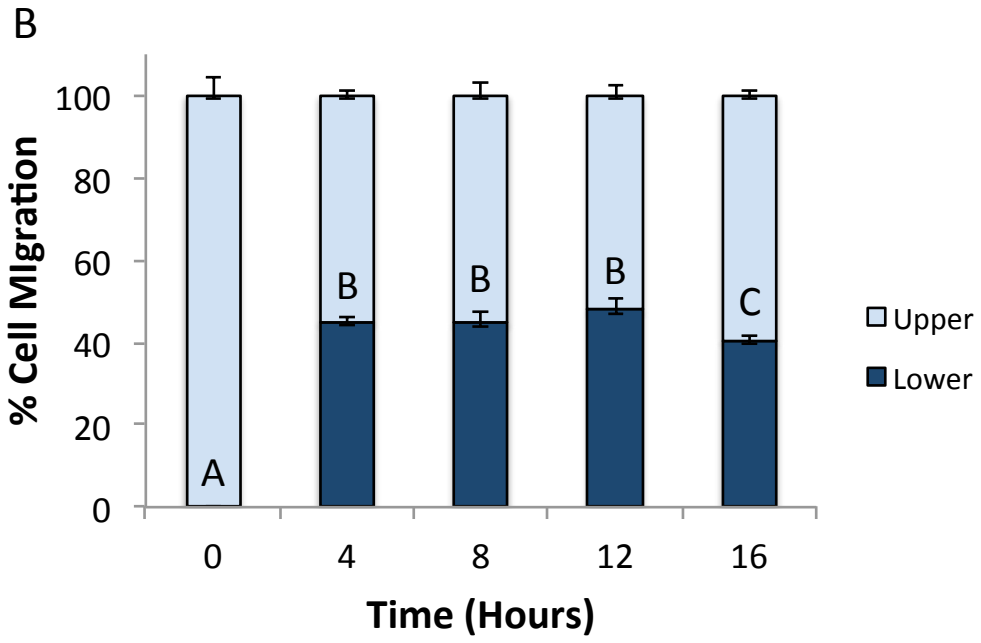

Figure B.6: Time-course transmigration assay. Human synovial microvascular endothelial cells were seeded on top of the membrane. Human bone marrow-derived mesenchymal stem cells (MSCs) were loaded into the apical chamber and SDF-1 into the basal chamber. Endothelial cells (A) and MSCs (B) were collected at 0, 4, 8,

12, and 16 hours using Quanti-iT dsDNA assay kit. Upper, apical chamber and membrane top; Lower, basal chamber and membrane bottom. Error bars represent SEM. Data not connected by the same letter are significantly different. p value ≤ 0.05 was considered significant.

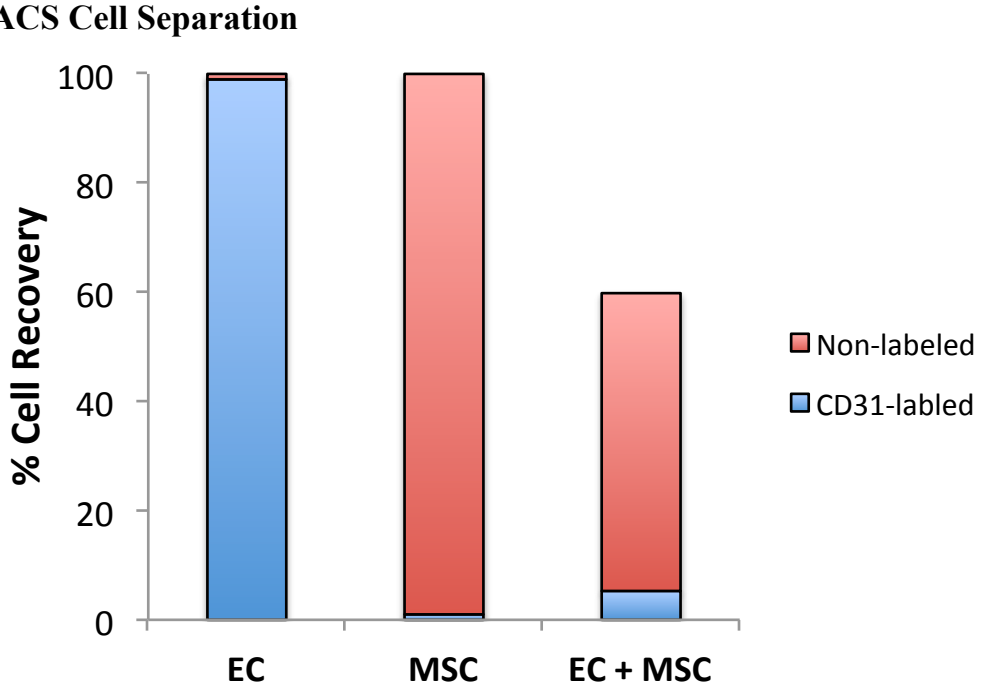

Figure B.7: MACS cell separation. Human anti-CD31 microbeads were used to separate human synovial microvascular endothelial cells from human bone marrow-derived mesenchymal stem cells (MSCs).

RT^2 Profiler qPCR Signaling Pathway Arrays

Cytoskeletal regulators

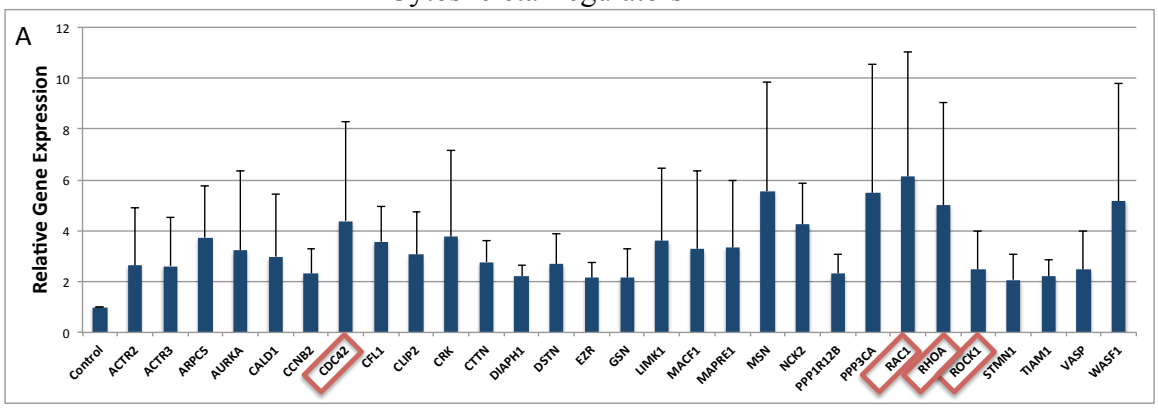

PI3K-Akt signaling pathway

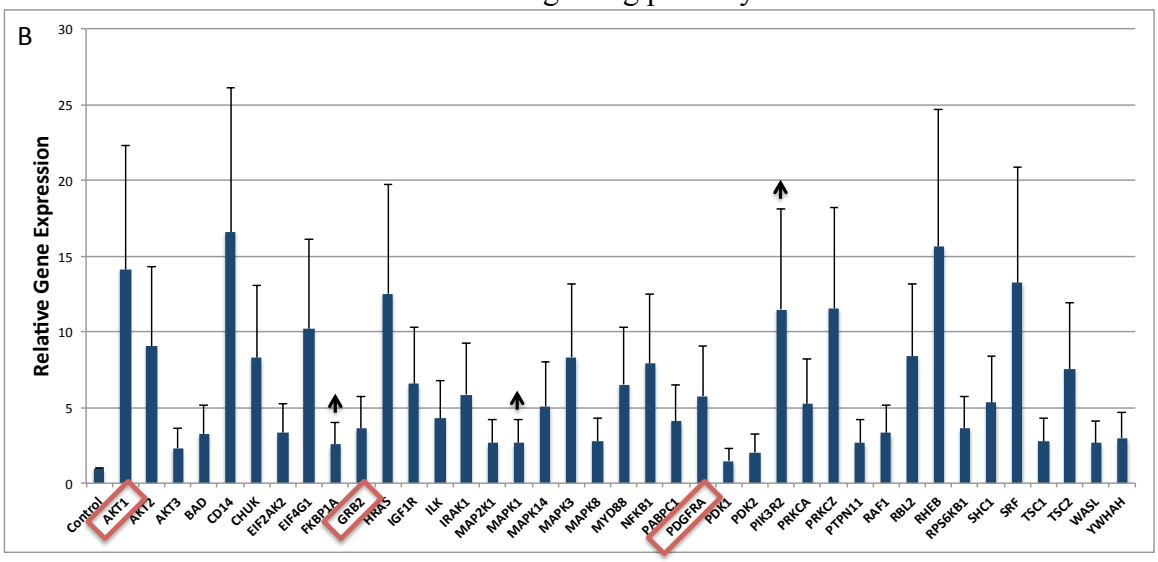

Jak/Stat signaling pathway

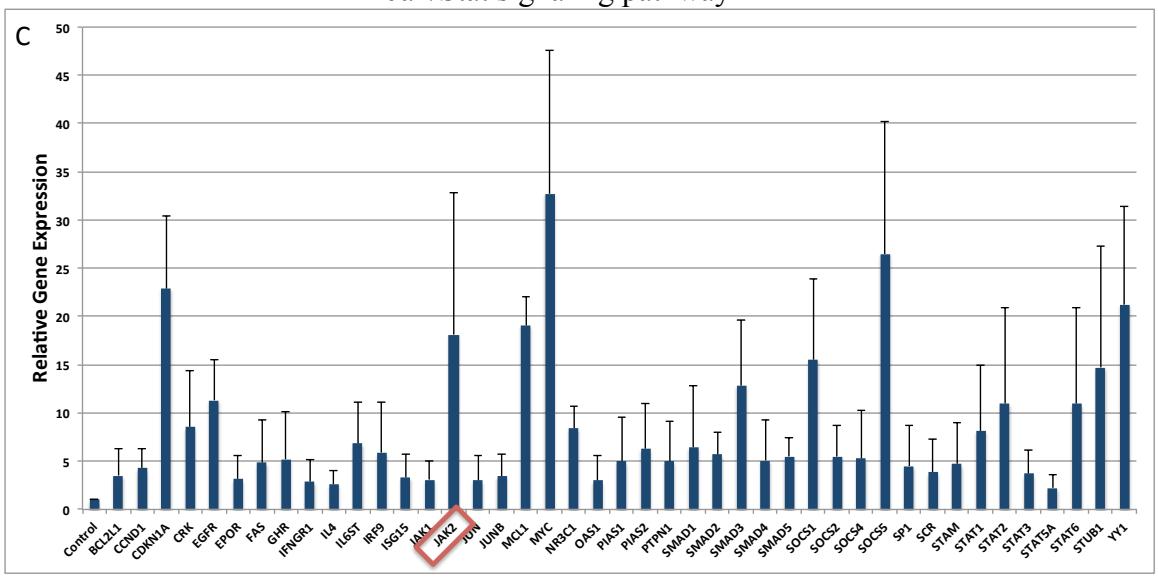

Figure B.8: MSC gene expression analysis. Migratory and non-migratory MACS-separated human bone marrow-derived mesenchymal stem cells were used for qPCR analysis of cytoskeletal regulators (A), PI3K-Akt signaling (B), and Jak/Stat signaling (C). Samples were normalized to RPLP0 and gene expression represents the increase of migratory cells relative to non-migratory cells. Key genes are highlighted in the red boxes. Error bars represent SEM. p value ≤ 0.05 was considered significant.

Western Blotting and Densitometry Analysis

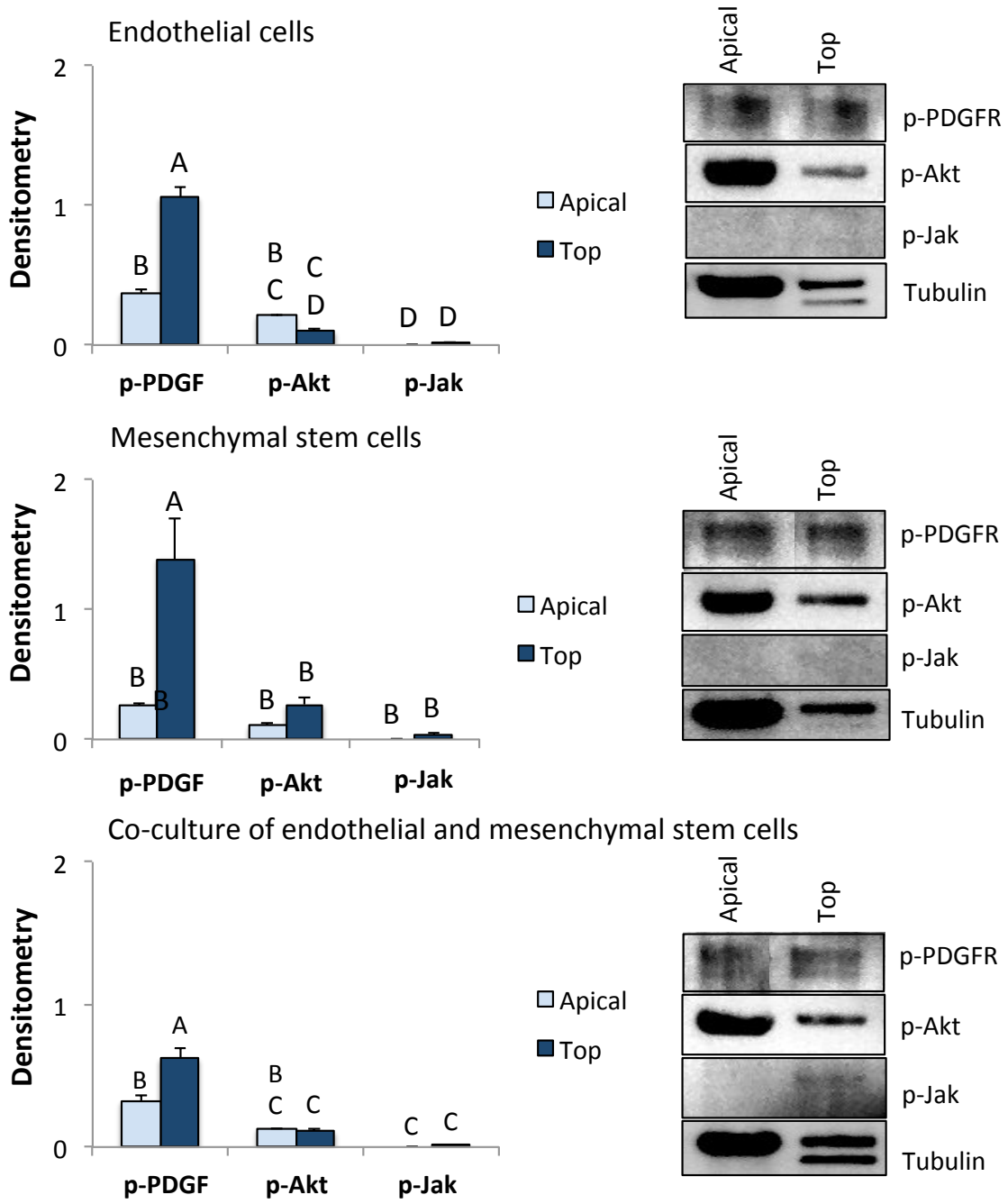

Figure B.9: Western blot analysis of migratory and non-migratory cells. Western blot analysis of p-PDGFR, p-Akt, p-Jak, and Grb2 signaling in cells collected from the top of the membrane and the apical chamber after SDF-1 exposure. Densitometry analysis was calculated for apical and membrane top samples, relative to alpha-tubulin. Top, cells collected from the top of the membrane; Apical, cells collected from the apical chamber. Data not connected by the same letter are significantly different. $p \leq 0.05$ was considered significant.

Transmigration Assay with Inhibitors

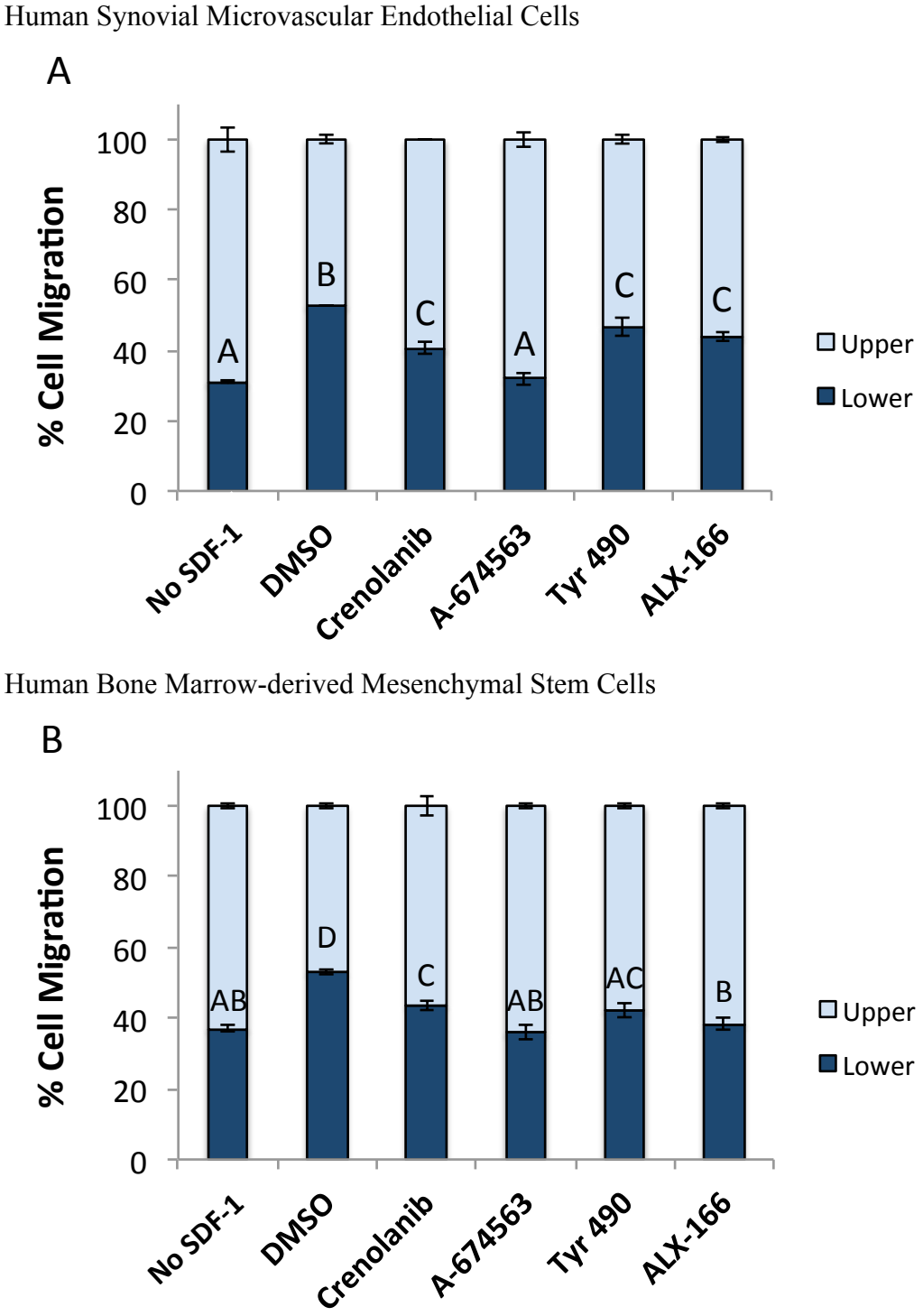

Figure B.10: Transmigration assay with inhibitors. Transmigration of human MSCs through human synovial microvascular endothelium in response to SDF-1 and inhibitors. Cell number was quantified for the apical chamber, membrane, and basal chamber with SDF-1 and inhibitor treatment for endothelial cells only (A) and MSCs only (B). Upper,

nonmigrated MSCs from the apical and membrane top; lower, migrated MSCs from the membrane bottom and basal chamber. Crenolanib, PDGFR inhibitor; A-674563, Akt inhibitor; Tyr 490, Jak inhibitor; ALX-166, Grb2 inhibitor. Error bars represent SEM. Data not connected by the same letter are significantly different. p value ≤ 0.05 was considered significant.